NTMS New Trends in Medicine Sciences

Volume 1
Issue 2
September
2020

New Trends in Medicine Sciences

Peer-Reviewed Academic Journal

ISSN: 2717- 8161
https://dergipark.org.tr/tr/pub/ntms

2020 September

New Trends In Medicine Sciences (NTMS) is an internationally recognized, referred, double-blind peer-reviewed, academic, electronic journal and published twice per year. It is aimed to contribute to scientific knowledge of medical sciences by publishing studies in the fields of basic, internal and surgical medical sciences.

ISSN: 2717-8161

Journal Abbreviation: New Trend Med Sci

Web Page: https://dergipark.org.tr/tr/pub/ntms

Correspondence Address: ntms.editor@gmail.com

New Trends in Medicine Sciences **Volume 1**

Issue 2

CONTENTS

2020 September

ISSN: 2717-8161 RESEARCH ARTICLE

New Trend Med Sci 2020; 1(2): 53-58. https://dergipark.org.tr/tr/pub/ntms

Effect of Curcumin on Testis in Mice with Ehrlich Ascites Tumor

Seher Yılmaz[1*], Ayşe Yeşim Göçmen[2], Adem Tokpınar[1], Şükrü Ateş[1], Mustafa Nisari[3], Ayşen Caniklioğlu[2], Ünal Öztekin[4]

[1]Department of Anatomy, Faculty of Medicine, Yozgat Bozok University, Yozgat, Turkey
[2]Department of Biochemistry, Faculty of Medicine, Yozgat Bozok University, Yozgat, Turkey
[3]Department of Nutrition and Dietetics, Faculty of Health Sciences, Nuh Naci Yazgan University, Kayseri, Turkey
[4]Department of Urology, Faculty of Medicine, Yozgat Bozok University, Yozgat, Turkey

Article History
Received 03 July 2020
Accepted 29 Aug 2020
Published Online 30 Sep 2020

[*]***Corresponding Author***
Dr Seher Yılmaz
Department of Anatomy,
Faculty of Medicine,
Yozgat Bozok University,
Yozgat, 66100, Turkey,
Phone: +903542126201-2686,
Fax: +90 354 4375285
E-mail:seher.yilmaz@bozok.edu.tr
ORCID:http://orcid.org/0000-0003-4551-995X

Abstract: In the current work, the effects of curcumin on testicular tissues in Ehrlich Ascites Tumor (EAT) model developed in Balb/C mice. EAT cells ($1x10^6$) received from stock of animals were injected intraperitoneally to animals. 25 mg/kg and 50 mg/kg of curcumin were administered intraperitoneally. Testicular tissues obtained after all the experiment were evaluated for histopathological and biochemical parameters. Histopathological results showed that 50 mg/kg curcumin group had less EAT cells around testicular tissues than tumor control group. Superoxide dismutase (SOD), catalase (CAT), glutathione peroxidase (GPx) activities and reduced glutathione (GSH), oxide glutathione (GSSG), total antioxidant status (TAS), total oxidant status (TOS), interleukin-1beta (IL-1β), interleukin-6, interleukin-17, tumor necrosis factor-alpha (TNF-α) levels were measured in testis tissues. Oxidative stress index (OSI) and GSH/GSSG ratio were calculated. Findings clearly suggested that antioxidant parameters (except CAT and GPx) had higher value in animal models treated with 25 and 50 mg/kg curcumin groups associated to tumor control group. There was a statistically noteworthy variance between the groups in all parameters. Antitumor effect of curcumin on ascites tumor cells produced by EAT cells evidenced with histopathological while antioxidant and anti-inflammatory biochemical parameters evidenced with biochemical parameters.
Keywords: Testis, EAT, Mice, Curcumin, Antioxidant.

1. Introduction

Testicular cancer is a common case in young people and is increasing day by day. As a common tumor, testis cancer is influenced by genetic and epigenetic factors. Additionally, oxidative stress played central role in development and progression of cancer. In addition to chemotherapy and radiotherapy, complementary medicine is also used in cancer treatment and the use of plant extracts is increasing gradually (1, 2).

One of these plant extracts is curcumin. It is a yellow herbal product with anti-inflammatory, anti-carcinogenic and anti-oxidant properties, used as spice, food coloring and preservative among the public. Curcumin, also called Curcuma longa, is a perennial plant native to South Asia (3, 4). There are many articles in the literature that demonstrate the antineoplastic mechanism of curcumin. It is stated that

Cite this article as: Yılmaz S, Göçmen AY, Tokpınar A, Ateş N, Nisari M, Caniklioğlu A and Öztekin Ü. Effect of Curcumin on Testis in Mice with Ehrlich Ascites Tumor, *New Trend Med Sci* **2020**; 1(2): 53-58.

curcumin has anticarcinogenic effects on various tumors with a variety of mechanisms.

Many studies show that curcumin suppresses many tumor genesis types including skin, mammary gland, mouth, esophagus, stomach, intestine, colon, lung and liver (5). Curcumin has captured appreciation because of its extra-ordinary pharmacological properties and experimentally verified ability to inhibit and/or prevent cancer. Wealth of information has highlighted potential of curcumin as an effective antioxidant, anti-inflammatory and an antidiabetic agent. Curcumin has been reported to exert inhibitory effects on interleukin-1β, TNF-α, superoxide ion and hydrogen peroxide production (6). It has been reported that curcumin significantly enhanced apoptosis in drug-resistant cancer types (7). Plant extracts have been tested on many cancer models while, one of which is the EAT model. EAT first appeared as a spontaneous breast adenocarcinoma in a female mouse, and tumor fragments were transplanted subcutaneously from mouse to mouse into an experimental tumor. After obtaining the liquid growing form in the peritoneum of mice, ascitic fluid was formed in addition to cells in the peritoneum, therefore the tumor was named as EAT (8, 9). In the current literature, the efficacy of curcumin on EAT tumor model was examined histologically but not in terms of biochemical parameters.

Copper, zinc-superoxide dismutase (Cu, Zn-SOD), Catalase (CAT) and Selenium-dependent glutathione peroxidase (Se-GSH-Px) are the main antioxidant enzymes of all aerobic cells (10). Cu, Zn-SOD (EC 1.15.1.1) catalyzes the dismutation of superoxide anions to hydrogen peroxide (11). CAT (EC 1.11.1.6) catalyzes the degradation of H_2O_2 to H_2O and O_2 (11). Se-GSH-Px (EC 1.11.1.9) is a biocatalyst that metabolizes H_2O_2 and lipid hydroperoxides (12). During this reaction, glutathione (GSH) is used as hydrogen donor and GSH is oxidized (GSSG) (13). Glutathione is the most important nonenzymatic antioxidant molecule inside the cell (14). GSH is also a hydroxyl radical and singlet oxygen scrounger (15). GSH (reduced glutathione)/GSSG (oxidized glutathione) ratio is one of the important determinants of oxidative stress in the body (10). The amounts of total antioxidant status (TAS) and total oxidant status (TOS) were useful for calculation of oxidative status (16). IL-1β, IL-6, IL-17 and TNF-α are among the pro-inflammatory cytokines (17, 18).

In this study we hypothesized that curcumin could play critical role on normalizing oxidative and inflammatory parameters which upregulated by EAT cells. Therefore, we aimed to evaluate the effect of low and high dosages of curcumin on testis tissue after investigated with EAT cells.

2. Material and Methods

2.1. Animals, management and experimental design

Studies with experimental animals were carried out in accordance with the decision of Ethics Committee of Animal Ethics Local in Erciyes University (2014 HADYEK-29). 25-30 grams and 8-10 weeks old Male Balb/C type mice were used for each group. The number of groups was 4, with 7 mice in each group. 4 animals were also used to create stock animals outside the groups. Mice were maintained in specially prepared, automatically air-conditioned rooms with constant temperatures of 21 °C and 12 hours of light/dark periods during the study. Before the groups were formed in the study, we first created the stock mouse to obtain enough EAT cells. The ascitic fluid from the stock animal was suspended in 0.1 ml PBS and counted on the thoma slide and $1x10^6$ EAT cells were injected intraperitoneally to form a liquid tumor in mice.

2.2. Dissolution and sterilization of curcumin extract

Curcumin was supplied as powder from Sigma Aldrich and curcumin was dissolved in different volumes to provide the desired concentrations for the experimental groups and sterilized by filtration. Curcumin was freshly prepared on each injection day to being dissolved completely.

2.3. Formation of Experimental Groups

Group 1/Negative control group: Cancer formation and animals were fed with normal diet for 10 days. 0.1 ml of physiological saline solution (PSS) was administered intraperitoneally for 10 days.

Group 2/Positive control group: In this group, 0.1 ml of ascitic fluid containing $1x10^6$ EAT cells was administered intraperitoneally to the abdomen on day 0. Mice were injected intraperitoneally with 0.5 ml of physiological saline solution (PSS) for 10 days from day 0.

Group 3/Treatment group (25 mg/kg curcumin): In this group, 0.1 ml ascitic fluid containing $1x10^6$ EAT cells was administered intraperitoneally to the abdomen on day 0. Mice were injected with curcumin 25 mg/kg; day intraperitoneally for 10 days from day 0

Group 4/Treatment group (50 mg/kg curcumin): In this group, 0.1 ml ascitic fluid containing $1x10^6$ EAT cells was administered intraperitoneally to the abdomen on day 0. From day 0, the mice were injected with Curcumin 50 mg/kg per each day intraperitoneally during 10 days.

2.4. Sample collection and preparations

All animals were sacrificed on day 10 under general anesthesia by ketamine and xylazine with concentrations of 75 mg/kg and 15 mg/kg respectively. One testis from each subject was fixed in 10% cold formaldehyde for routine histopathological examination, the other was transferred to sterile plastic bags and immediately transferred to the laboratory in cold conditions and stored at -80 °C temperature until biochemical experiments.

2.5. Preparation of testis homogenates

Testis tissue of each mouse were arranged and studied distinctly. Tissues were homogenized in 2 mL +4 °C

temperature phosphate-buffer saline in ice. At the end of the homogenization process, the mixture was centrifuged at 3000 g for 10 min and the supernatant was composed. Supernatant was deposited at -80 ºC until analysis.

2.6. Biochemical Analysis

The protein content of each tissue was determined in each sample with Bio-Rad reagents (Bio-Rad laboratories GmbH, München, Germany) using bovine serum albumin as the standard. Activities of CAT and Se-GSH-Px and the levels of GSH and GSSG were measured in tissues by the modified methods of Ozturk et al." (18). TOS, TAS levels and SOD activity were measured using commercially available kits (Relassay, Turkey). OSI was defined as TOS to TAS ratio was calculated as follows: OSI (arbitrary unit) = [(TOS, μmol H_2O_2 equivalent/mg protein)/(TAS, μmol Trolox equivalent/mg protein] × 100). The levels of IL-1β, IL-6, IL-17, TNF-α were studied from the blood samples collected with enzyme linked immunosorbent assays (ELISA) method (Elabscience, Wuhan, China) as specified in the protocol by the manufacturer.

2.7. Statistical analysis

Data were analyzed using the statistical package program SPSS for Windows® 23.0 (SPSS, Chicago, IL, USA). Normality of the all data was analyzed with Kolmogorov-Smirnov D test to determine a test type from both the parametric and non-parametric tests. Distribution of OSI, GPx and IL-1β were non-parametric. Data have a normal distribution (Kolmogorov–Smirnov D test, p≥0.05), parametric test ANOVA (post-hoc: Tukey's HSD and Tamhane) was used for multiple comparisons. Kruskall-Wallis test was used for non-parametric distribution data and pairwise comparisons of groups were made. Experimental data were expressed as the Mean±SD. The P <0.05 were considered statistically significant.

3. Results

3.1. Histopathological Findings

According to histopathological experiments, control groups' tissues showed normal histological properties. In the EAT cell groups positive control groups which has no treatment has more EAT cells as compared to the 25 and 50 mg/kg curcumin treated groups (Figure 1). Around the testicular capsule dispersed EAT cell assemblies were observed.

3.2. *Biochemical Results*

The results of oxidative stress parameters of all groups are represented in figure 2-4. SOD activity, GSH level, GSH/GSSG ratio and TAS levels, which are among the antioxidant markers, were meaningfully lower in the tumor group compared to group 1 (p<0.05). In groups 3 and 4 there was a significant dose-dependent increase compared to the tumor group. However, the increase in antioxidant activity in groups 3 and 4 did not reach the control group (p<0.05). GPx activity was expressively higher in group 2 and 3 compared to group 1 and pointedly lower in group 4 than group 2 (p<0.05). CAT activity and GSSG and TOS levels were significantly higher in the tumor group compared to group 1, and dose-dependent significantly lower in group 3 and 4 compared to the tumor group (p <0.05). While the same parameters were found to be significantly higher in group 3 than in group 1, CAT activity was lower in group 4 and GSSG and TOS levels were higher in group 4 (p<0.05). OSI values were significantly higher in group 2 and 3 than in group 1 and meaningfully lower in group 4 than in tumor group (p<0.05) (Figure 2,3).

IL-17 and TNF-α levels were suggestively lower in the treatment groups compared to the tumor group (p<0.05) The values of group 3 were lower than group 4 (p<0.05). IL-6 and IL-1β levels were lower in the treatment groups than in the tumor group (p<0.05). There was no statistically significant difference between the treatment groups (Figure 4).

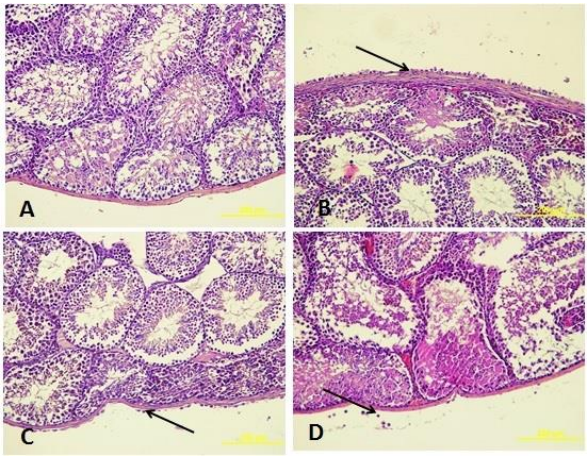

Figure 1: Histopathological findings (H&E, 20X) of the negative control, treatment and positive control groups in testicular tissue. A) Healthy control group. B) Tumor control group C) Tumor and 25 mg/kg curcumin treated group D) Tumor and 50 mg/kg curcumin treated group.

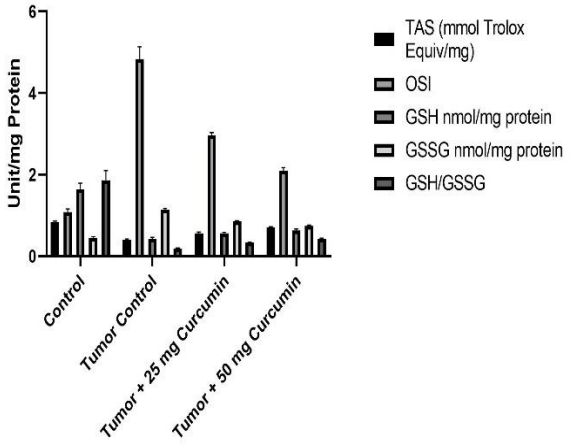

Figure 2: Measurements of oxidative stress and inflammatory markers in the testis.

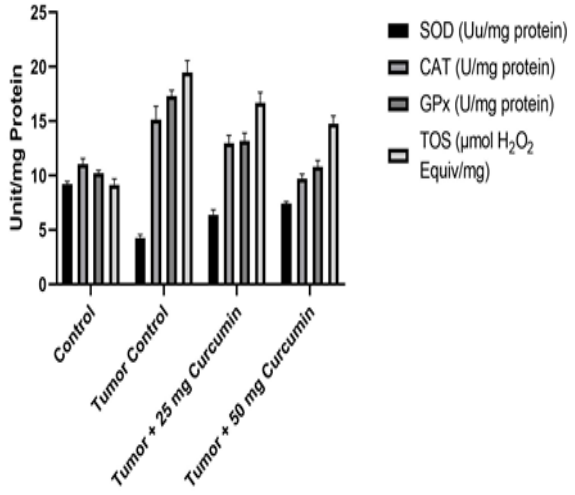

Figure 3: The results of oxidative stress parameters of all groups.

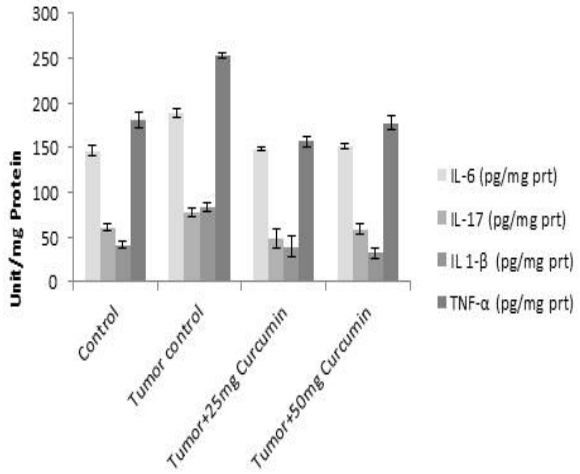

Figure 4: Assessment of IL-6, IL-17, IL1β and TNF-α levels of three groups.

4. Discussion

The prevalence of cancer types causing deaths in men and women varies. Testicular cancer has an increasing rate in young men aged 15-35 years. Drug resistance and metastatic spread have been recognized as major stumbling blocks in decreasing the quality of clinical outcome of wide ranging therapeutics. The presence of frequent metastases in other organs has accelerated the search for treatment in testicular cancer. In recent years, complementary medicine has been used in addition to medical treatments for cancer treatment. Some plants have been shown to be useful in cancer treatment. Bioactive molecules present in different Plants and vegetables used by the people in various countries have documented health promoting effects. More importantly, certain high-quality bioactive constituents have been shown to induce regression of tumors in xenografted mice (19, 20). It has been shown that the natural chemicals contained in some of these plants (resveratrol in red grapes, genistein in soybean and curcumin in turmeric) have anti-cancer properties (21). Curcumin has been reported to reduce toxicity caused by anti-cancer agents, sensitize resistant cancer cells, suppress proliferation, and induce apoptosis in tumor cells (22-24). In the current study, anti-inflammatory and antioxidant effects of curcumin in EAT model mice were investigated histopathological and biochemically on testicular tissue. Kanter et al. (25) investigated the protecting properties of curcumin and amifostine against gamma radiation-induced jejunal mucosal damage and reported that curcumin's efficacy diminished in high-dose radiation. Lopez (26) showed that curcumin at a dose of 20 µg / mL stopped growth of 50% in human chronic myelogenous leukemia cells. Pan et al. (27) examined the therapeutic effect of curcumin by forming an Alzheimer's model in mice. They reported that Bax levels did not change in hippocampal mice. Facchini et al. investigated the effects of Pleurotus ostreatus (fungus) polysaccharide fractions intraperitoneally in $5x10^6$ EAT cells and gave high tumor inhibition (28). Yilmaz et. al. (2019) studied the antioxidant properties of curcumin and Cornus mas L in mice forming EAT model and showed antioxidant properties in tissues such as kidney and liver in vivo and in vitro (29,30).

Activated monocytes/macrophages allow pro-inflammatory cytokines, such as TNF-α, IL-1, and IL-6 that play an important role in inflammatory reaction. Ketanserin has been shown BY Yank et al. (2019) in literature to inhibit TNF-α and IL-1 production in endotoxic shock (31). Ueki et al. examined the therapeutic effect of curcumin in mice with cisplatin-induced renal inflammation (32). They indicated that serum TNF-α concentration decreased by 30% in the group which has been given cisplatin (100 mg/kg) and curcumin (100 mg/kg); decreased as well as healed renal dysfunction. Cho (2007) found that curcumin inhibited the expression of TNF-α-induced IL-1β, IL-6, and TNF-α in TNF-α treated keratinocytes (33).

In this study, IL-1β, IL-6, TNF-α and as a pro-inflammatory cytokine IL-17 decreased in curcumin treated groups compared to tumor control group. The decrease in IL-17 and TNF-α was found to be lower in the dose-dependent group compared to the 25 mg administered group. IL-6 and IL-1β levels have been found lower independent of dose. These findings suggest that curcumin may have dose-dependent anti-inflammatory effects in mouse testes with EAT. Additionally, curcumin has been exposed to prevent the production of superoxide and nitric oxide by inflammatory cells, which could also donate to its anti-inflammatory motion because of the significant role of free radicals in inflammatory processes (34, 35). In literature, we could not confirm a detailed study investigating the effect of curcumin on oxidant and antioxidant system in testicular tissues with EAT

tumor. Khopde *et al.* (1999) showed that curcumin is a more effective antioxidant than α-tocopherol and inhibits lipid peroxidation (36). While Venkatesan *et al*. (1997) investigated the effects of curcumin on bleomycin-induced lung injury (BILI) in rats, they showed that curcumin had anti-inflammatory and antioxidant effects in BILI in the curcumin treated group (37). Kuhad *et al.* (2008) found that curcumin antioxidant parameters such as SOD, GSH and CAT increased compared to diabetic rats in their study (38).

5. Conclusions

In this study, TAS and GSH levels, which are antioxidant parameters, decreased in the testicular tissues of the mice, while dose-dependent increase was detected in the curcumin-treated groups likened to the tumor group. Likewise, the oxidant parameters TOS and GSSG levels increased in the testicular tissues of the mice, while dose dependent decrease was detected in the curcumin groups in proportion to the tumor group. When the enzyme activities responsible for oxidant defense were evaluated, it was evaluated that as the cancer was formed, SOD enzyme activity, which removes superoxide in the environment, decreased. We observed that CAT and GPx activities, which are responsible for the neutralization of H_2O_2 to water and oxygen, were increased in the next step. Dose-dependent SOD activity increased while CAT and GPX activity decreased with curcumin effect. The resulting high amount of H_2O_2 inhibits product inhibition on SOD, while CAT and GPx may have shown more activity to remove accumulated H_2O_2. Each tissue has diverse volume against stress response for each oxidant or antioxidant parameter (38). As a result of increased GPx activity in cancer, GSH reserve in the environment decreased and GSSG amount increased. In the curcumin group, this was vice versa. These findings support the antioxidant effects of curcumin in mouse testicular tumor tissue in accordance with the literature.

Conflict of interest statement

There is no conflict of interest.

References

1. Kayaalp SO. Tıbbi Farmakoloji, Hacettepe Taş Kitapçılık. Ankara. **1996**, pp. 731-779.
2. Weiss RB, Henney JE, DeVita VT. Multimodal treatment of primary breast carcinoma. analiysis of accomplishments and problem areas. *Am J Med* **1981**; 70: 844-851.
3. Pei Y, Ai T, Deng Z, et al. Impact of plant extract on the gastrointestinal fate of nutraceutical-loaded nanoemulsions: phytic acid inhibits lipid digestion but enhances curcumin bioaccessibility. *Food Funct* **2019**; 106: 3344-3355.
4. Toraya S, Uehara O, Daichi H, et al. Curcumin inhibits the expression of proinfammatory mediators and MMP-9 in gingival epithelial cells stimulated for a prolonged period with lipopolysaccharides derived from Porphyromonas gingivalis. *Odontology* **2020**; 108(1); 16-24.
5. Bhaumik S, Anjum R, Rangaraj N, et al. Curcumin mediated apoptosis in AK-5 tumor cells involves the production of reactive oxygen intermediates. *FEBS Lett* **1999**; 456: 311-314.
6. Basham SA, Hunter S. W, Ben M. K, et al. Effect of Curcumin Supplementation on ExerciseInduced Oxidative Stress, Inflammation, Muscle Damage, and Muscle Soreness. *J Diet Suppl* **2019**; 26: 1-14.
7. Kocaadam B, Şanlıer N. Curcumin, an active component of turmeric (curcuma longa), and Its effects on health. *Crit Rev Food Sci Nutr* **2015**; 3: 123-127.
8. Hatcher H, Planalp R, Cho J, et al. Curcumin from ancient medicie to current clinical trials. *Cell Moll Life* **2008**; 65: 1631-1652.
9. Gevorkyan L, Gambashidze K. Anticancer efficacy of hydroxyethylthiamine diphosphate in vivo. *Exp Oncol* **2014**; 36: 48-49
10. Birben E, Sahiner UM, Sackesen C, et al. Oxidative Stress and Antioxidant Defense. *WAO J* **2012**; 5: 9–19.
11. Limon-Pacheco J, Gonsebatt ME. The role of antioxidants and antioxidant related enzymes in protective responses to environmentally induced oxidative stress. *Mutat Res* **2009**; 674(1-2): 137-147.
12. Young IS, Woodside JV. Antioxidants in Health and Disease. *J Clin Pathol* **2001**; 54(3): 176-186.
13. Reiter RJ, Melchiorri D, Sewerynek E, et al. A review of the evidence supporting melatonin‘s role as an antioxidant. *J Pineal Res* **1995**; 18(1): 1-11.
14. Gürdöl F. Tıbbi biyokimya. 3. Baskı. 2018, pp. 644.
15. Joanisse DR, Storey KB. Oxidative damage and antioxidants in Rana syvatica, the freeze-tolerant wood frog. *Am J Physiol* **1996**; 271: 545-553.
16. Erel O. A novel automated direct measurement method for total antioxidant capacity using a new generation, more stable ABTS radical cation. *Clin Biochem* **2004**; 37: 277–285.
17. Mohan ML, Vasudevan NT, Naga Prasad SV. Proinflammatory Cytokines Mediate GPCR Dysfunction. *J Cardiovasc Pharmacol* **2017**; 70(2): 61-73.
18. Oztürk O, Gümüşlü S. Changes in glucose-6-phosphate dehydrogenase, copper, zinc-superoxide dismutase and catalase activities, glutathione and its metabolizing enzymes, and lipid peroxidation in rat erythrocytes with age. *Exp Gerontol* **2004**; 39(2): 211-216.
19. Scott MS, William T. Epidemiology and Diagnosis of Testis Cancer. *Urol Clin North Am* **2015**; 42(3): 269-275.
20. Raju A, Christina MJA, Murali A. Antitumor activity of ethanol and aqueous extracts of Drosera Burmannii vahl. İn EAC Bearing Mice. *Spatula DD* **2012**; 2: 83-88.
21. Azab ME, Hishe H, Moustapha Y, et al. Anti-angiogenic effect of resveratrol or curcumin in

ehrlich ascites carcinoma-bearing mice. *Eur J Pharmacol* **2011**; 652: 7-14.
22. Maheshwari RK, Singh AK, Gaddipati J, et al. Multiple biological activities of curcumin: A short review. *Life Sci* **2006**; 78: 2081-2087.
23. Kohli K, Ali J, Ansari MJ, et al. Curcumin a antiinflammatory agent. *Indian J Pharmacol* **2005**; 37: 141-147.
24. Chainoglou E, Hadjipavlou-Litina D. Curcumin analogues and derivatives with anti-proliferative and anti-inflammatory activity: Structural characteristics and molecular targets. *Expert Opin Drug Discov* **2019**; 16: 1-22.
25. Kanter P, Tarladaçalışır YT, Akpolat M, et al. Gamma radyasyona bağlı oluşan jejenum mukoza hasarına karşı curcumin ve amifostinin koruyucu etkilerinin incelenmesi. *Tıp araştırmaları dergisi* **2008**; 6(3): 128-135.
26. Lopez LM. Anticancer and carcinogenic properties of curcumin. Considerations for its clinical development as a cancer chemopreventive and chemotherapeutic agent. *Mol Nutr Food Res* **2008**; 52: 103-127.
27. Pan HM, Huang TM, Lın JK. Biotransformation of curcumin through reduction and glucuronidation in mice. *Am Soc Pharmacol Exp Ther* **1998**; 27:486-493.
28. Facchini JM, Alves EP, Aguilera C, et al. Antitumor activity of pleurotus ostreatus polysaccharide fractions on ehrlich tumor and sarcoma. *Int J Biol Macromol* **2014**; 68: 72-77.
29. Yılmaz S, Ülger H, Ertekin T, et al. Investigating the anti-tumoral effect of curcumin on the mice in which Ehrlich ascites and solid tumor is created. *Iran J Basic Med Sci* **2019**; 22: 418-425.
30. Yılmaz S, Alpa Ş, Nisari M, et al. Examining the Antitumoral Effect of Cornelian Cherry (Cornus mas) in Ehrlich Ascites Tumor-induced Mice. *J Anat Soc India* **2019**; 68: 16-22.
31. Yang W, Zhang J, Zhang B. The role of ketanserin in maintaining cırculatıon stability in endotoxic shock rats. *Acta Medica Mediterr* **2019**; 35: 2871.
32. Ueki M, Ueno M, Morishita J, et al. Curcumin ameliorates cisplatin-induced nephrotoxicity by inhibiting renal inflammation in mice. *J Biosci Bioeng* **2013**; 115: 547-551.
33. Cho JW, Lee KS, Kim CW. Curcumin attenuates the expression of IL-1beta, IL-6, and TNF-alpha as well as cyclin E in TNF-alpha-treated HaCaT cells; NF-kappaB and MAPKs as potential upstream targets. *Int J Mol Med* **2007**; 19(3): 469-474.
34. Bhaumik S, Jyothi MD, Khar A. Differential modulation of nitric oxide production by curcumin in host macrophages and NK cells. *FEBS Lett* **2000**; 483: 78-82.
35. Brouetand I, Ohshima H. Curcumin, an anti-tumour promoter and anti-inflammatory agent, inhibits induction of nitric oxide synthase in activated macrophages. *Biochem Biophys Res Commun* **1995**; 206: 533-540.
36. Khopde M S, Priyadarsini KI, Venkatesan P, et al. Free radical scavenging ability and antioxidant efficiency of curcumin and its substituted analogue. *Biophys Chem* **1999**; 80(2): 85-91.
37. Venkatesan N, Punithavathi V, Chandrakasan G. Curcumın protects bleomycın-ınduced lung ınjury ın rats. *Life Sci* **1997**; (61): 5l-58.
38. Kuhad A, Chopra K. Curcumin attenuates diabetic encephalopathy in rats: behavioral and biochemical evidences. *Eur J Pharmacol* **2008**; 576: 34-42.

Authors' ORCID
Seher Yılmaz
http://orcid.org/0000-0003-4551-995X
Ayşe Yeşi Göçmen
http://orcid.org/ 0000-0002-8511-639X
Adem Tokpınar
http://orcid.org/0000-0001-7661-9588
Şükrü Ateş
http://orcid.org/0000-0001-7096-2481
Mustafa Nisari
http://orcid.org/0000-0001-7469-8921
Ayşen Caniklioğlu
http://orcid.org/0000-0001-8128-6044
Ünal Öztekin
http://orcid.org/0000-0001-9568-9442

https://dergipark.org.tr/tr/pub/ntms

ISSN: 2717-8161 RESEARCH ARTICLE

New Trend Med Sci 2020; 1(2): 59-64. https://dergipark.org.tr/tr/pub/ntms

The Role of Chlorogenic Acid in Alleviating Intestinal Ischemia/Reperfusion-Induced Lung Injury

Ayhan Tanyeli[1], Derya Güzel Erdoğan[2], Fazile Nur Ekinci Akdemir[3], Ersen Eraslan[4], Mustafa Can Güler[1*]

[1]Department of Physiology, Faculty of Medicine, Atatürk University, Erzurum, Turkey
[2]Department of Physiology, Faculty of Medicine, Sakarya University, Sakarya, Turkey
[3]Department of Nutrition and Dietetics, High School of Health, Ağrı İbrahim Çeçen University, Ağrı, Turkey
[4]Department of Physiology, Faculty of Medicine, Yozgat Bozok University, Yozgat, Turkey

Article History
Received 24 May 2020
Accepted 10 July 2020
Published Online 30 Sep 2020

[*]***Corresponding Author***
Dr Mustafa Can Güler
Department of Physiology,
Faculty of Medicine,
Atatürk University,
Erzurum, 25240, Turkey,
Phone: +905074690369,
E-mail: mcanguler@yahoo.com
ORCID: https://orcid.org/0000-0001-8588-1035

Abstract: Here, Chlorogenic acid (CA) was examined in intestinal ischemia reperfusion (I/R)-induced lung injury. 4 experimental rat groups were created (n=8): sham, I/R, I/R+CA 5 mg/kg and I/R+10 mg/kg groups. At the end of the experimental process, rats were immolated and lung tissues were excised. Oxidant parameters increased and antioxidant activity declined in I/R group compared to sham group. CA treatments reversed these parameters. Different doses of the CA prevented intestinal I/R-induced lung injury in experimental animals. © 2020 NTMS.

Keywords: Intestinal Ischemia/Reperfusion, Lung, Chlorogenic Acid, Oxidative Stress, Inflammation, Rat.

1. Introduction

Ischemia is based on the disruption in tissue blood flow which results in cell injury (1). Even though the recovery of blood flow ameliorates the ischemic tissues, reperfusion damages cells through reactive oxygen species (ROS) (2). Ischemia reperfusion (I/R)-induced intestinal injury is a life-threatening health condition which occurs in case of various situations (3). Intestinal I/R injury causes proinflammatory cytokine release, ROS production and oxidative stress (4, 5). Intestinal I/R plays role in distal organ dysfunction development, especially in lungs. Acute lung injury (ALI) is the wide inflammation of lungs and it is a several intestinal I/R injury complication (6-9). ROS induce inflammatory response and inflammation causes more ROS and inflammatory cytokine generation which enhance intestinal injury (10-12). Neutrophils are the main sources for ROS and they play role in reperfusion injury. ROS lead to release of inflammatory cytokines (13, 14) including tumor necrosis factor-alpha (TNF-α) and interleukin-1 beta (IL-1β) (15). IL-1β enhances the production of other inflammatory cytokines and the neutrophil infiltration (16). Total oxidant status (TOS) and total antioxidant status (TAS) act on evaluation of oxidative stress. TAS is the potential of suppressing free radicals (17).

Different agents have been examined to alleviate or eliminate I/R-induced oxidative injuries in various organs (18-22). But the role of Chlorogenic acid (CA) against intestinal I/R injury has not been investigated yet. CA, isolated from Coffea arabica L., performs antioxidant (23) and anti-inflammatory activities (24). CA also demonstrates neuroprotective activity (25, 26).

Cite this article as: Tanyeli A, Güzel Erdoğan D, Ekinci Akdemir FN, Eraslan E and Güler MC. The Role of Chlorogenic Acid in Alleviating Intestinal Ischemia/Reperfusion-Induced Lung Injury, *New Trend Med Sci* **2020**; 1(2): 59-64.

Here, it was aimed to find out the effects of CA against intestinal I/R-induced lung injury.

2. Material and Methods

2.1. Ethical Approval, Animals, and Drugs

Atatürk University Experimental Animal Ethics Committee confirmed the study (Protocol No:27.04.2018/102). It was carried out at Experimental Animals Research and Application Center of Atatürk University. The animals were acquired from same center. They were caged with appropriate laboratory conditions and subjected to standard rat feed with tap water. They were deprived of food 12 hours before the experiment, but were free to reach water. Thiopental sodium (Ulagay, İstanbul, Turkey) was preferred for anesthesia. 10% povidone-iodine was used for disinfection and CA was provided by Sigma-Aldrich Co.

2.2. Surgical Procedures and Treatment Groups

32 Wistar Albino male rats, each weighing 230-250 g were used for experimental process. They were held in supine position, shaved, cleaned and applied anesthesia prior to surgical process. They were weighed and divided into 4 groups, including 8 rats in each group (n=8).

Sham group: 1-2 cm size of incision was performed as median laparotomy to abdominal region and then, repaired via 3/0 silk suture.

I/R group: Same steps with sham group were followed. Before suturation, 1-hour ischemia to superior mesenteric artery was carried out through clamping and then, 2 hours reperfusion was carried out as described before (27).

CA 5 mg/kg group: Procedures were done as described in I/R group. 5 mg/kg CA was administered intraperitoneally (i.p.) 30 minutes before the reperfusion.

CA 10 mg/kg group: All steps of CA 5 mg/kg group were carried out but 10 mg/kg CA was administered. CA doses were determined due to a previous I/R study (28). Following the experiment, rats were sacrificed, lung tissue samples were excised and cleaned with normal cold saline.

2.3. Biochemical Examination

Lung tissue samples were homogenized and centrifuged to obtain the supernatants. They were analyzed to determine malondialdehyde (MDA), superoxide dismutase (SOD), myeloperoxidase (MPO), TAS, TOS, TNF-α and IL-1β levels. MDA value was gauged as described previously (29). TAS and TOS levels were determined with appropriate kits (Rel Assay Diagnostics).

Oxidative stress index (OSI) is the ratio of TOS to TAS and measurement MPO activity was measured due to kinetic absorbance as in a former research (31). SOD measurement depends on formazan dye level (32). TNF-α and IL-1β levels were analyzed via appropriate kits (Elabscience, Wuhan, China).

2.4. Statistical Analyses

All data were evaluated through SPSS (version 20.0, for windows). One-way ANOVA test was chosen for data and Tukey HSD test was used for multiple comparisons. Biochemical data results were presented as Mean±Standard Deviation (SD). Statistical significance level was considered when p value below 0.05.

3. Results

Table 1 represents the oxidant and antioxidant biochemical parameters. TAS, SOD values declined significantly in I/R group when compared to sham group, besides TOS, OSI, MDA, MPO levels elevated significantly. CA 5 mg/kg group did not perform a significant change in TAS and SOD values while TOS, OSI, MDA and MPO levels increased. CA 10 mg/kg group was compared with I/R group, all parameters had significant changes except SOD.

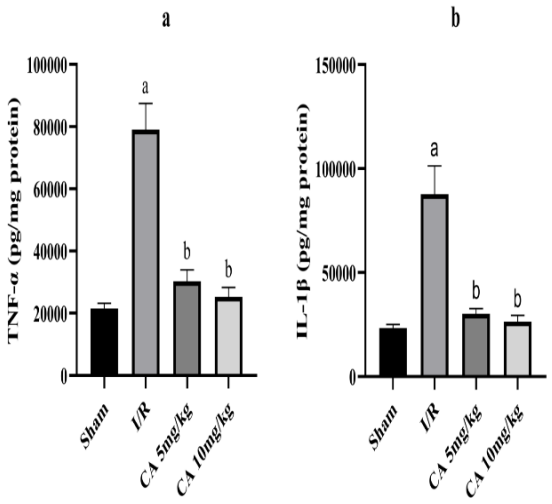

Figure 1: The results of TNF-α and IL-1β levels in intestinal I/R-induced lung injury.

Pro-inflammatory cytokine levels were shown in figure 1a, b. TNF-α and IL-1β levels were found to increase in I/R group compared to sham group. However, it was determined that these levels decreased significantly in CA 5 mg/kg and CA 10 mg/kg groups. In addition, when CA 5 mg/kg and CA 10 mg/kg groups were compared between themselves, TNF-α and IL-1β levels more decreased in CA 10 mg/kg group, but this difference was not statistically significant.

Table 1. The Mean±SD results of biochemical parameters in intestinal I/R-induced lung injury.

Groups (n=8)	TAS (mmol/L)	TOS (µmol/L)	OSI	SOD (U/mg protein)	MPO (U/g protein)	MDA (µmol/g tissue)
Sham	1.16±0.21	8.56±1.28	0.76±0.22	180.66±31.56	326543.23±37695.22	69.27±2.71
I/R	0.79±0.07[a]	12.10±1.62[a]	1.51±0.18[a]	125.88±32.84[c]	475788.57±62770.03[a]	108.46±30.99[a]
CA 5 mg/kg	0.95±0.17	9.30±0.85[b]	1.00±0.24[b]	163.09±27.16	335486.44±23297.06[b]	77.81±13.37[b]
CA10 mg/kg	1.19±0.21[b]	8.70±0.65[b]	0.74±0.08[b]	176.53±54.17	331418.75±68529.04[b]	75.26±8.90[b]

[a]$p<0.001$, [c]$p<0.05$ compared to sham group. [b]$p<0.05$ compared to I/R group.

4. Discussion

I/R is typically composed of blockage in blood flow and following a recovery phase (33). Intestinal mucosa is a vulnerable structure against I/R injury (34). Mesenteric ischemia is an emergency situation characterized with insufficient blood flow resulting from various conditions such as septic shock and surgical interventions (35). Reperfusion is the recovery of blood supply following ischemia. It is required to avoid cell injury and maintain organ functions. Despite all, reperfusion may lead to more damage than ischemia (2, 36). Several health conditions including thrombosis, sepsis, embolism and vasospasm lead to I/R and oxidative stress (37). High morbidity and mortality rates accompany to I/R because it is hard to diagnose and treat (38, 39). I/R may lead to lung injury which enhances morbidity and mortality (40). I/R may lead to ALI in which neutrophil infiltration and proinflammatory cytokine production are typically observed. Even more, ALI may result in acute respiratory distress syndrome (ARDS) and even death. ARDS treatment achieves important improvements but the mortality rate still remains at high levels which creates need to a profound research for underlying mechanisms (41, 42). Ischemia is characterized via decrease or block in blood flow and thus tissues are lack of oxygen and other nutrients. This condition complicates detrimental substance scavenging, particularly ROS (43, 44). ROS proceed from xanthine oxidase activation and play a crucial role in acute intestinal I/R injury (45, 46). ROS production raises in damaged tissues. ROS activate several signaling pathways, induce inflammatory response and injure intestinal during intestinal I/R injury (47, 48).

Intestinal I/R injury is strongly related with oxidative stress. An unbalance between oxygen input and output enhances ROS generation (49) and lipid peroxidation (50). MDA reacts with DNA and proteins resulting damage in intestinal tissues (51). Increase in TNF-α level and neutrophil adhesion capacity accompany I/R injury (52). Proinflammatory mediators including TNF-α and IL-1β play role in neutrophil activation. They also act on enhancing vascular permeability and interstitial edema during I/R injury (53). Active neutrophils secrete MPO which generate free radicals and thus trigger lipid peroxidation (54).

TOS, OSI and TAS values act as oxidative stress indicators and have been used for this purpose in various studies (42, 43). TAS and TOS demonstrate oxidant and antioxidant equilibrium. TAS is an indicator for all antioxidant activity while TOS is limited with ROS (44, 45). SOD catalyzes superoxide free radical conversion into molecular oxygen and superoxide free radical. SOD protects tissues through neutralizing free radicals (46).

Different agents with anti-inflammatory, antioxidant feature and also radical scavengers with beneficial effects have been reported in alleviation or elimination of I/R injuries in various tissues (55-60). In the current study, CA was used for this purpose. CA is a phenol molecule and obtained from various herbs. It performs several properties including antimicrobial activity (61). It is found abundantly in human diet, especially in coffee (62, 63). CA includes R-OH radicals which can inhibit free radical activity through antioxidant activity and thus prevent oxidative cell damage (64). Here, antioxidant and anti-inflammatory effects of CA have been demonstrated in intestinal I/R rat model. SOD activity and TAS value declined while MPO activity, MDA, IL-1β, OSI, TNF-α and TOS levels were elevated in I/R group compared to sham group. CA administration raised antioxidant capacity and diminished oxidant activity by reversing these parameters. Current results enrich the potential CA as to be used in the treatment of I/R related pathologies.

It is necessary to investigate the cellular injury mechanisms to able to improve I/R treatment. Coping with inflammation and oxidative stress contribute to I/R treatment. In this study, oxidative stress and inflammation were diminished via CA.

5. Conclusions

In current research, it has been demonstrated that CA administration declined lung injury caused by intestinal I/R model in experimental rats. Therefore, CA may be a new agent as to be examined against diseases associated with I/R.

Conflict of interest statement

All authors declared that there is no conflict of interest.

Financial Support

None

Compliance with ethical standards

The study was carried out in accordance with ethical standards in all aspects.

References

1. Tullis MJ, Brown S, Gewertz BL. Hepatic influence on pulmonary neutrophil sequestration following intestinal ischemia-reperfusion. *J Surg Res* **1996**; 66: 143-146.
2. Mallick IH, Yang W, Winslet MC, Seifalian AM. Ischemia-reperfusion injury of the intestine and protective strategies against injury. *Diges Dis Sci* **2004**; 49:1359-1377.
3. Stallion A, Kou TD, Latifi SQ, et al. Ischemia/reperfusion: a clinically relevant model of intestinal injury yielding systemic inflammation. *J Pediatr Surg* **2005**; 40: 470-477.
4. Li Y, Xu B, Xu M, et al. 6-Gingerol protects intestinal barrier from ischemia/reperfusion-induced damage via inhibition of p38 MAPK to NF-kappaB signalling. *Pharmacol Res* **2017**; 119: 137-148.
5. Meszaros AT, Buki T, Fazekas B, et al. Inhalation of methane preserves the epithelial barrier during ischemia and reperfusion in the rat small intestine. *Surgery* **2017**; 161: 1696-1709.
6. Moore FA. The role of the gastrointestinal tract in postinjury multiple organ failure. Am J Surg 1999; 178:449-453.
7. Thomas S, Karnik S, Balasubramanian KA. Surgical manipulation of the small intestine and its effect on the lung. *J Surg Res* **2002**; 106:145-156.
8. Ito K, Ozasa H, Horikawa S. Edaravone protects against lung injury induced by intestinal ischemia/reperfusion in rat. *Free Radic Biol Med* **2005**; 38: 369-374.
9. Aytekin FO, Tekin K, Kabay B, et al. Antithrombin III attenuates pulmonary tissue injury caused by mesenteric ischemia-reperfusion. *Am J Surg* **2005**; 189:161-166.
10. Ozacmak VH, Sayan H, Igdem AA, Cetin A, Ozacmak ID. Attenuation of contractile dysfunction by atorvastatin after intestinal ischemia reperfusion injury in rats. *Eur J Pharmaco* **2007**; 562:138-47.
11. Borges SC, da Silva de Souza AC, Beraldi EJ, Schneider LC, Buttow NC. Resveratrol promotes myenteric neuroprotection in the ileum of rats after ischemia-reperfusion injury. *Life Sci* **2016**; 166: 54-59.
12. Zu G, Guo J, Che N, et al. Protective effects of ginsenoside Rg1 on intestinal ischemia/reperfusion injury-induced oxidative stress and apoptosis via activation of the Wnt/beta-catenin pathway. *Sci Rep* **2016**; 6: 38480.
13. Carden DL, Granger DN. Pathophysiology of ischaemia-reperfusion injury. J Pathol 2000; 190:255-266.
14. Tapuria N, Kumar Y, Habib MM, Abu Amara M, Seifalian AM, Davidson BR. Remote ischemic preconditioning: a novel protective method from ischemia reperfusion injury--a review. *J Surg Res* **2008**; 150: 304-330.
15. Tao T, Chen F, Bo L, et al. Ginsenoside Rg1 protects mouse liver against ischemia-reperfusion injury through anti-inflammatory and anti-apoptosis properties. *J Surg Res* **2014**; 191: 231-238.
16. Vivo V, Zini I, Cantoni AM, et al. Protection by the Eph-Ephrin System Against Mesenteric Ischemia-Reperfusion Injury. *Shock (Augusta, Ga.)* **2017**; 48: 681-689.
17. Baysal Z, Cengiz M, Ozgonul A, Cakir M, Celik H, Kocyigit A. Oxidative status and DNA damage in operating room personnel. *Clin Biochem* **2009**; 42: 189-193.
18. Eraslan E, Tanyeli A, Polat E, Polat E. 8-Br-cADPR, a TRPM2 ion channel antagonist, inhibits renal ischemia-reperfusion injury. *J Cell Physiol* **2019**; 234: 4572-4581.
19. Eraslan E, Tanyeli A, Polat E, Yetim Z. 2019. Evodiamine alleviates kidney ischemia reperfusion injury in rats: A biochemical and histopathological study. *J Cell Biochem* **2019**; 120: 17159-17166.
20. Ozturk D, Erdogan DG, Tanyeli A, Çomaklı S, Baylan H, Polat E. The protective effects of urapidil on lung tissue after intestinal ischemia-reperfusion injury. *Turk J Biochem* **2019**; 44: 539.
21. Topdağı Ö, Tanyeli A, Ekinci Akdemir FN, Eraslan E, Guler MC. Barbaloin attenuates ischemia reperfusion-induced oxidative renal injury via antioxidant and anti-inflammatory effects. Turk J Sci 2020; 9: 246.
22. Dogan C, Halici Z, Topcu A, et al. Effects of amlodipine on ischaemia/reperfusion injury in the rat testis. *Andrologia* **2016**; 48: 441-452.
23. Yang L, Wang N, Zheng G. Enhanced Effect of Combining Chlorogenic Acid on Selenium Nanoparticles in Inhibiting Amyloid beta Aggregation and Reactive Oxygen Species Formation In Vitro. *Nanoscale Res Lett* **2018**; 13: 303.
24. Tsang MS, Jiao D, Chan BC, et al. nti-Inflammatory Activities of Pentaherbs Formula, Berberine, Gallic Acid and Chlorogenic Acid in Atopic Dermatitis-Like Skin Inflammation. *Molecules* **2016**; 21: 519
25. Nabavi SF, Tejada S, Setzer WN, et al. Chlorogenic Acid and Mental Diseases: From Chemistry to Medicine. *Curr Neuropharmacol* **2017**; 15: 471-9.
26. Heitman E, Ingram DK. Cognitive and neuroprotective effects of chlorogenic acid. *Nutr Neurosci* **2017**; 20: 32-39.
27. Tanyeli A, Ekinci Akdemir FN, Eraslan E, Güler MC, Topdağı Ö. Evodiamine Against Intestinal Tissue Injury Induced By Mesenteric Ischemia-Reperfusion: Role of Oxidative Stress. *Bozok Med J* **2019**; 9: 113-118.
28. Tanyeli A and Güzel Erdoğan D. Renal İskemi-Reperfüzyon Hasarında Antioksidan Olarak

Klorojenik Asit (CGA) Kullanımının İncelenmesi: Deneysel Çalışma. *Sakarya Med Sci* **2018**; 8: 410-415.

29. Ohkawa H, Ohishi N, Yagi K. Assay for lipid peroxides in animal tissues by thiobarbituric acid reaction. *Anal Biochem* **1979**; 95: 351-358

30. Erel O. A new automated colorimetric method for measuring total oxidant status. *Clin Biochem* **2005**; 38: 1103-1111.

31. Bradley PP, Priebat DA, Christensen RD, Rothstein G. Measurement of cutaneous inflammation: estimation of neutrophil content with an enzyme marker. *J Invest Dermatol* **1982**; 78: 206-209.

32. Sun Y, Oberley LW, Li Y. A simple method for clinical assay of superoxide dismutase. *Clin Chem* **1988**; 34: 497-500.

33. Eltzschig HK, Eckle T. 2011. Ischemia and reperfusion--from mechanism to translation. *Nat Med* **2011**; 17: 1391-401.

34. Guan Y, Worrell RT, Pritts TA, Montrose MH. Intestinal ischemia-reperfusion injury: reversible and irreversible damage imaged in vivo. *Am J Physiol Gastrointest Liver Physiol* **2009**; 297:187-196.

35. Vollmar B, Menger MD. Intestinal ischemia/reperfusion: microcirculatory pathology and functional consequences. *Langenbeck's Arch Surg* **2011**; 396: 13-29.

36. Collard CD, Gelman S. Pathophysiology, clinical manifestations, and prevention of ischemia-reperfusion injury. *Anesthesiol* **2001**; 94: 1133-1138.

37. Weil MH, Becker L, Budinger T, et al. Workshop Executive Summary Report: Post-resuscitative and initial Utility in Life Saving Efforts (PULSE): June 29-30, 2000; Lansdowne Resort and Conference Center; Leesburg, VA. *Circulation* **2001**; 103:1182-4.

38. Grootjans J, Lenaerts K, Buurman WA, Dejong CH, Derikx JP. Life and death at the mucosal-luminal interface: New perspectives on human intestinal ischemia-reperfusion. *World J Gastroentero* **2016**; 22: 2760-2770.

39. Schellekens DH, Grootjans J, Dello SA, et al. Plasma intestinal fatty acid-binding protein levels correlate with morphologic epithelial intestinal damage in a human translational ischemia-reperfusion model. *J Clin Gastroenterol* **2017**; 48: 253-260.

40. Teke Z, Sacar M, Yenisey C, Atalay AO, Bicakci T, Erdem E. Activated protein C attenuates intestinal reperfusion-induced acute lung injury: an experimental study in a rat model. *Am J Surg* **2008**; 195: 861-873.

41. Villar J, Blanco J, Anon JM, et al. The ALIEN study: incidence and outcome of acute respiratory distress syndrome in the era of lung protective ventilation. *Intens Care Med* **2011**; 37: 1932-1941.

42. Gregova K, Cikos S, Bilecova-Rabajdova M, et al. Intestinal ischemia-reperfusion injury mediates expression of inflammatory cytokines in rats. *Gen Physiol Biophys* **2015**; 34: 95-99.

43. Abu-Elmagd K, Bond G. Gut failure and abdominal visceral transplantation. *P Nutr Soc* **2015**; 62: 727-737.

44. Komatsu H, Koo A, Ghadishah E, et al. Neutrophil accumulation in ischemic reperfused rat liver: evidence for a role for superoxide free radicals. Am J Physiol **1992**; 262: 669-676

45. Parks DA, Bulkley GB, Granger DN, Hamilton SR, McCord JM. Ischemic injury in the cat small intestine: role of superoxide radicals. *Gastroenterol* **1982**; 82: 9-15.

46. Saugstad OD. Mechanisms of tissue injury by oxygen radicals: implications for neonatal disease. *Acta Pediatr* **1996**; 85: 1-4.

47. Wen SH, Ling YH, Li et al. Ischemic postconditioning during reperfusion attenuates oxidative stress and intestinal mucosal apoptosis induced by intestinal ischemia/reperfusion via aldose reductase. *Surgery* **2013**; 153: 555-64.

48. Bhattacharyya A, Chattopadhyay R, Mitra S, Crowe SE. Oxidative stress: an essential factor in the pathogenesis of gastrointestinal mucosal diseases. *Physiol Rev* **2014**; 94: 329-354.

49. Wang G, Yao J, Li Z, et al. miR-34a-5p Inhibition Alleviates Intestinal Ischemia/Reperfusion-Induced Reactive Oxygen Species Accumulation and Apoptosis via Activation of SIRT1 Signaling. *Antioxid Red Sign* **2016**; 24: 961-973

50. Cerqueira NF, Hussni CA, Yoshida WB. Pathophysiology of mesenteric ischemia/reperfusion: a review. Acta Cir Bras 2005; 20: 336-343.

51. Horton JW, Walker PB. Oxygen radicals, lipid peroxidation, and permeability changes after intestinal ischemia and reperfusion. *J App Physiol* **1993**; 74: 1515-1520.

52. Mayer AM, Pittner RA, Lipscomb GE, Spitzer JA. Effect of in vivo TNF administration on superoxide production and PKC activity of rat alveolar macrophages. *Am J Physiol* **1993**; 264: 43-52

53. Bertoni S, Arcaro V, Vivo V, et al. Suppression of inflammatory events associated to intestinal ischemia-reperfusion by 5-HT1A blockade in mice. *Pharmacol Res* **2014**; 81: 17-25.

54. Dirjomuljono M, Kristyono I, Tjandrawinata RR, Nofiarny D. Symptomatic treatment of acute tonsillo-pharyngitis patients with a combination of Nigella sativa and Phyllanthus niruri extract. *Int J Clin Pharma Th* **2008**; 46: 295-306.

55. Tanyeli A, Ekinci Akdemir F, Eraslan E, Guler M, Sebin S, Gülçin I. Role of p-Coumaric acid in Alleviating of the Intestinal Ischemia/Reperfusion Injury. *Kocaeli Med J* **2020**; 9: 166-73.

56. Topdagi O, Tanyeli A, Ekinci Akdemir FN, Eraslan E, Guler MC, Comakli S. Preventive effects of fraxin on ischemia/reperfusion-induced acute kidney injury in rats. *Life Sci* **2020**; 242: 117217.

57. Güzel Erdoğan D, Tanyeli A. Investigation of Chlorogenic Acid (Cga) as An Antioxidant in Renal Ischemia-Reperfusion Injury: An Experimental Study. *Sakarya Med Sci* **2018**; 8: 410-415.
58. Güzel Erdoğan D, Tanyeli A. Investigation of Oxidative Damage of Lung Tissue in Experimental Renal Ischemia Reperfusion Model and The Protective Effects of Chlorogenic Acid (CGA). *Sakarya Med Sci* **2018**; 8: 260-265.
59. Topdağı Ö, Tanyeli A, Ekinci Akdemir FN, Güzel Erdoğan D, Güler MC, Eraslan E. Higenamine decreases testicular damage injured by ischemia reperfusion: A biochemical study, *Turk J Sci* **2019**; 4(2): 92-99.
60. Tanyeli A, Ekinci Akdemir FN, Eraslan E, Güler MC, Özbek Şebin S, Gülçin İ. Role of p-Coumaric acid in Alleviating of the Intestinal Ischemia/Reperfusion Injury. *Kocaeli Med J* **2020**; 9: 166-173.
61. Almeida AA, Farah A, Silva DA, Nunan EA, Gloria MB. Antibacterial activity of coffee extracts and selected coffee chemical compounds against enterobacteria. *J Agric Food Chem* **2006**; 54: 8738-8743.
62. Olthof MR, Hollman PC, Katan MB. Chlorogenic acid and caffeic acid are absorbed in humans. *J Nutr* **2001**; 131: 66-71.
63. Bonita JS, Mandarano M, Shuta D, Vinson J. Coffee and cardiovascular disease: in vitro, cellular, animal, and human studies. *Pharmacol Res* **2007**; 55: 187-98.
64. Zhang J, Chen M, Ju W, et al. Liquid chromatograph/tandem mass spectrometry assay for the simultaneous determination of chlorogenic acid and cinnamic acid in plasma and its application to a pharmacokinetic study. *J Pharm Biomed Anal* **2010**; 51: 685-690.

Authors' ORCID
Ayhan Tanyeli
http://orcid.org/0000-0002-0095-0917
Derya Güzel Erdoğan
https://orcid.org/0000-002-7618-5043
Fazile Nur Ekinci Akdemir
https://orcid.org/0000-0001-9585-3169
Ersen Eraslan
https://orcid.org/0000-0003-2424-2269
Mustafa Can Güler
http://orcid.org/0000-0001-8588-1035

https://dergipark.org.tr/tr/pub/ntms

ISSN: 2717-8161 RESEARCH ARTICLE

New Trend Med Sci 2020; 1(2): 65-83. https://dergipark.org.tr/tr/pub/ntms

Ethnomedicinal Profile of Flora of District Sialkot, Punjab, Pakistan

Fozia Noreen[1]*, Mishal Choudri[2], Shazia Noureen[3], Muhammad Adil[4], Madeeha Yaqoob[4], Asma Kiran[4], Fizza Cheema[4], Faiza Sajjad[4], Usman Muhaq[4]

[1]Department of Chemistry, Faculty of Natural Sciences, University of Sialkot, Punjab, Pakistan
[2]Department of Statistics, Faculty of Natural Sciences, University of Sialkot, Punjab, Pakistan
[3]Government Degree College for Women, Malakwal, District Mandi Bahauddin, Punjab, Pakistan
[4]Department of Chemistry, Faculty of Natural Sciences, University of Gujrat Sialkot Subcampus, Punjab, Pakistan

Article History
Received 30 May 2020
Accepted 01 June 2020
Published Online 30 Sep 2020

****Corresponding Author***
Fozia Noreen
Department of Chemistry,
Faculty of Natural Sciences,
University of Sialkot,
Punjab, Pakistan
E-mail: Fozia.noreen@uskt.edu.pk
ORCID:http://orcid.org/0000-0001-6096-2568

Abstract: An ethnomedicinal profile of 112 species of remedial herbs, shrubs, and trees of 61 families with significant gastrointestinal, antimicrobial, cardiovascular, herpetological, renal, dermatological, hormonal, analgesic and antipyretic applications have been explored systematically by circulating semi-structured and unstructured questionnaires and open ended interviews from 40-74 years old mature local medicine men having considerable professional experience of 10-50 years in all the four geographically diversified subdivisions i.e. Sialkot, Daska, Sambrial and Pasrur of district Sialkot with a total area of 3106 square kilometres with population density of 1259/km^2, in order to unveil botanical flora for world. Family *Fabaceae* is found to be the most frequent and dominant family of the region. © 2020 NTMS.

Keywords: Analgesic, Antipyretic, Renal, Gastrointestinal, Dermatological.

1. Introduction

Study of green extracts as therapeutic agencies have emerged as a major field of science. Plants are effective less cost biological repositories of medicinal compounds witnessed for a large series of ailments by traditional medicine men in geographically diversified District, Sialkot in province of Punjab in Pakistan (1). About 50% of plants of worldwide flora (2), is presenting valuable potentials, prior to high-throughput screening and the post-genomic era of scientific research for curing a list of acute and chronic disorders since times of ancient civilizations (3), with technically nil drawbacks (4), both for human and animals entitled as unani, folk, eastern, or indigenous medicine (5). Despite of a rapid economic race riding over the horse of science and technology, almost over three-fourth of the total world population is facing a drastic rundown of allopathic medicines.

Herbal medicines are reported as curative agents for 80% of this population by World Health Organization (WHO) (6). WHO has ultimately reiterated the usage of traditional herbal medicines for primary health care for these parts of world (7). Pakistan being the 10th most populated country (8) is categorized under low income countries (9). Poor sanitary system of rural area is triggering the pathogenic bacteria for causing serious infectious diseases like gastro-intestinal, pneumonia, pulmonary, renal, antimicrobial, and dermatological disorders at rapid pace (10). About 61.6% of the total of rural population of Pakistan is supposed to rely on readily available herbal bank (11).

About 6000 medicinal plants are reported in Pakistan under various surveys (12), with 600/6000 flowering plants which are executing medicinal properties. Pharmaceutical industry is indulged with more than

Cite this article as: Noreen F, Choudri M, Noureen S, Adil M, Yaqoob M, Kiran A. Cheema F. Sajjad F and Mushaq U. Ethnomedicinal Profile of Flora of District Sialkot, Punjab, Pakistan, *New Trend Med Sci* 2020; 1(2): 65-83.

half from natural origin even in this modern world of pharmaceutical drug development.

It has been identified that more than 88/119 plant based drugs were discovered as a result of research on medicinal plants. Pakistan is trading about 2500 species in the international market of organic medicine (13). Although Pakistan is an agricultural country chiefly (14), but unluckily with less emphasis to systematic cultivation of medicinal plants like Russia, Lucknow, European Union (EU) and China, where the total output earning of pharmaceutical industry largely depends upon the cultivation of such medicinal plant (15). For promotion of this hidden and less studied green bank of Pakistan, various areas have been searched out, but some are still hidden and demanding attention for their discovery. A well-planned systemization of botanical knowledge of the regions with higher consumption of these natural green agents can open a new market raise it not only for population of Pakistan, but also for international market at reasonable prices. Following this source of inspiration, we have selected District Sialkot as our test city to recover a new word of natural medicines. Sialkot is in the north-east of the Punjab province running along the Chenab River, in the north. It is a climatic heaven which dramatically lies partly in Forest (less humid) zone, while remaining large part of country is lying in Arid (dry) zone (16). The mentioned area is characterized by its humid subtropical climate. From one side it resides at the foothills of the snow-covered peaks of Kashmir, at an elevation of 256 meters above the sea level between 32°30' North latitude and 74°31' East longitude. Sialkot is just a few kilometers from Indian-occupied Jammu Kashmir in north, Gujrat by the North-West, Gujranwala by the West and Narowal by the south shown in Figure 1.

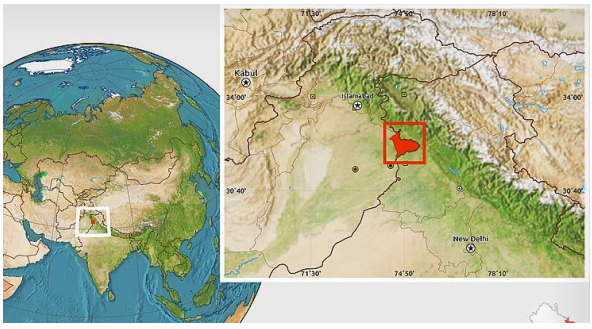

Figure 1: Satellite Location Map of Sialkot.

Three small seasonal streams viz. Aik, Behr and Palkhu are also provoking hands of natural growth of biodiversity of plants. The total area of the district is approximately 3.106 sq. kilometers comprising of four subdivisions with green ethnomedicinal floor. Average temperature of 23.64 ºC has been recorded, minimum of 5.7ºC in January that rises up to a maximum value of 40.7 ºC in June. Sialkot is among the regions with highest rainfall in Pakistan. Highest precipitation rate of 252 mm is recorded in August, and minimum in November. It is spitting, drizzling and heaven opening weather here often.

Previously an ethnomedicinal study of District Sialkot has been conducted by Zareen et. al. Medicinal package of about 48 plant species with 35 shrubs species belonging to 22 angiosperm families was documented. Indigenous people reported the use of medicinal shrubs for the treatment of human ailments of digestive tract, rheumatic pains, dermatological, cardiac and pulmonary problems etc. from a long period for generations to generations, with positive results (17).

An extended survey of Sialkot including all its sub-divisions has been carried out in order to explore hidden ethnomedicinal significance (18) of area in front of the world, which can provide a social and economic back to the inhabitants in the regard of their natural raw factories and establishment of an international market for the almost all countries of all sub continents existing at this time and space.

Figure 2: Plantation along famous Nala Aik of Sialkot

2. Material and Methods

Methodology was conducted in following rounds:

Round 1: To collect systemic facts and figures of ethnomedicinal flora of four subdivisions of District Sialkot, Punjab, Pakistan, four teams of well-trained members were designed to conduct a survey of all subdivisions. Random sampling of major medicinal plants used by all mature and experienced medicine men and individuals availing herbal medicines for health care in the selected regions is made. The conduction of the task was made by a survey through interview method. The interview consisted of unstructured open-ended questions to collect almost all possible basic information regarding following major questions.

1.Names of medicine men, along with their age and institute of training.
2. From how many years you are working in this field?
3.What are the local names of plants used as herbal remedies?
4.Which part (roots, shoots, stems, leaves, fruits or whole plant) is used for particular disease?
5.For which medical issue the mentioned plant is used?
Details of reporting individuals are given in Table 1:
Round 2: After collection of detailed raw information regarding above mentioned seven questions, a feedback of patients availing mentioned herbal medicines of the medicine men was recorded by circulating another questionnaire among sample of population consisting of ten questions and consequences regarding various herbal medicines
Based on statistical results of above feedback, a list of plants of with the most positive feedback was prepared. Short listed data of plants was searched out for the English names through search engine named under Google Urdu, because the raw data collected from local medicine men was in local national language Urdu and regional language Punjabi. English and Punjabi names were searched for their characteristic botanical information regarding habitats. A systematic table was designed containing botanical names of plants, local names, English names and families, parts of plants that are under use and mode of administration. The chemical constituents and medical significance of enlisted highest rated plants was investigated following literature review of those plants, that is get verified by a Doctor of Botany named Sadaf Honey Ghauri affiliated with Govt. Postgraduate College for Women at Mandi Bahauddin in Province Punjab of Pakistan. The data was correlated with the statements of medicine men for creating a valid report of credibility of plants and medicine men of four subdivisions of District. Sialkot, Punjab, Pakistan.
Round 3: Markets of whole District Sialkot was visited for collecting data regarding presence or cultivation of those plants in test city to check their market value. Then a complete result was drawn to attract the world towards ethnomedicinal flora, its medical significance supported with modern literature and a market of green medicinal chemicals in District Sialkot.

3. Results

In response of steps after first round, conduction of study tours, surveys, structured, semi-structured and unstructured interviews data of 112 plants of 61 families have collected and systematically arranged is given in following Table 2.
Data of Table exhibits wider variety of fertile ethnomedicinal flora of four subdivisions of District Sialkot. An overall contribution of four subdivisions fertile ethnomedical in total division flora of Sialkot district among its four subdivisions is given as followed in Figure 3.

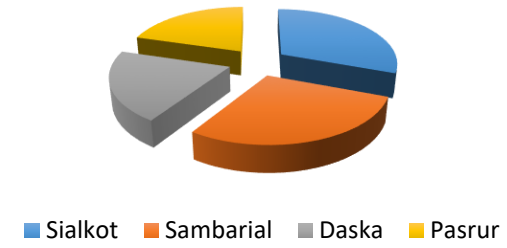

Figure 3: Comparative fraction of ethnomedicinal species of four subdivisions of Sialkot District.

Figure 3 depicts a relative ratio of ethno botanical species in Sialkot District with highest of 31% contribution with herbarium of 51 species constituting 26 herbs, 8 shrubs and 17 trees of Sialkot Subdivision itself, including Achyranthesaspera L., Adhatodavasica, Aegle marmelos L., Aloe Indica L., Asteracantha Longifolia, Azadirachtaindica, Cannabis Sativa, Centaureabehen. L, Citrus tangerina, Cercissiliquastrum, Convulvulusarvense, Cucumismelo var. agrestis Naudin, Cuscutareflexa Roxb, Cydonia oblonga, Cyperusrotundus L., Embeliaribes, Euphorbia hirta L., Euphorbia hypericifolia, Glycyrrhizaglabra L., Hibiscus rosasinensis L., Hyoscyamusniger, Ipomoea Eriocarpa, Indigoferatinctoria, Lavandula Officinalis Chaix, Leucasaspera (Jacq.) Ait., Malva sylvestris L., Melia azedarach L., Menthaviridis L., Mesua ferrea L., Murdanniapauciflora, Murraya exotica, Myristicafragrans Houtt, Myristicafragrans , Papaver somniferumL., Pipernigrum L., Pistacia Lentiscus, Phyllanthusemblica L., Plantago Ovata L., Polygonum Viviparum, Psoraleacorylifolia L., Pyrus communis, Rhyncosia minima, Ricinuscommunis L., Solanum nigrum L., Sphaeranthusindicus, Strychnos Nux-vomica L., Terminalia arjuna, Terminalia chebula, Terminalia Reticulata, Trigonellafoenum-graecum, Withaniacoagulans Dunal and Ziziphus jujuba Mill are the major medicinal species of Sialkot subdivision belonging to 26 families majorly Fabaceae, Lamiaceae, Euphorbiaceae, Malvaceae, Solanaceae and Rutaceae under higher frequencies but Amranthaceae, Liliaceae, Meliaceae, Calophyllaceae, Commelinaceae, Papaveraceae, Piperaceae, Cactaceae, Phyllanthaceae, Plantaginaceae, Polygonaceae, Convulvulaceae, Cucurbitaceae, Cuscutaceae, Cyperaceae, Myrsinaceae and Rhamnaceae, found with useful applications for gastric, hepatic, nerves, cardiovascular problems, gastrointestinal problems and viral infections and have earned confidence of people in these treatments while introduced in body as analgesic, antipyretic and nervonic tonics in particular.

Sambrial is second highly populated sub-division in this race with total of 38 botanical species including 22 herbs, 4 shrubs and 12 trees. Acacianilotica (L.) Delile, Achyranthusaspera Linn, Alliumcepa, Allium sativum, Aloe vera L, Bacopamonnieri (L.) Penn. Syn., Bambuseae, Calotropisprocera, Cassia Fistula, Catharanthusroseus, Cichoriumintybus, Cinnamomum Tamala, Cupressussempervirens L., Cinnamomumzeylanicum , Cymbopogoncitratus, Cyrillaracemiflora, Ficus Benghalensis L., Foeniculum vulgare, Fumariaofficinail L., Loliumperenne L., Malva sylvestris L., Menthapulegium, Nymphaea L., Onosmabracteatum, Piper nigrum L. , Plantago ovata, Santalum album L., Senna Alexandria, ShpaerathusIndicus, Solanum Nigrum, Solanum Pseudocapsicum, Sphaeranthusindicus, Syzygium Aromaticum, Syzygiumcumini, Terminalia arjuna, Tribulusterrestris, Xanthium strumarium L., Ziziphus jujuba, Zingiber officinale are the major ethnomedicinal species in sambrial subdivision under the umbrella of botanical families Amaranthaceae, Apiaceae, Apocynaceae, Asciepiadaceae, Asteraceae, Boraginaaceae, Caesalpiniaceae, Combretaceae, Cupressaceae, Cyrillaceae, Fabaceae, Fumariaceae, Liliaceae, Lamiaceae, Lauraceae, Malvaceae, Moraceae, Myrtaceae, Nymphaeaceae, Piperaceae, Plantaginaceae, Poaceae, Rhamnaceae, Santalaceae, Scrophulariaceae, Solanaceae, Zingiberaceae, and Zygophyllaceae, with frequent results as effective analgesics, antipyretics, anti-diabetic, purgative, gastric diseases, cardiovascular diseases, blood purifying agents, constituting 29% of total pie , with Asteraceae as the most dominent family of the mentioned subdivision. However, Daska and Pasrur contributes almost equally with 29 and 25 herbaceous species.

20 major botanical families Apiaceae, Apocynaceae, Araceae, Berberidaceae, Brassicaceae, Burseraceae, Combretaceae, Fabaceae, Liliaceae, Mimosaceae, Myristica, Myrtaceae, Nitrariaceae, Phyllanthaceae, Piperaceae, Rutaceae, Scrophulariaceae, Solanaceae, Zingiberaceaen and Zygophyllaceae consists of 31 species named Albizialebbeck, AllumSativum L, Amorphophalluspaeoniifolius, Anethumgraveolens, Berberisaristata, Brassica Compestris L., Butea monosperma, Phyllanthus Emblica., Piper longum L., Piper Nigrum L. Holarrhena Pubescens, Ciclospermum leptophyllum, Curcuma Longa L., Commiphora, Zingiber officinale, Datusa Metel L., Elettaria Cardamon, Foeniculum vulgare, Glycyrrhiza glabra, Myristica fragrans, Peganum harmala, Picrorhizakurrooa, Syzygium aromaticum, Terminalia chebula, Trachyspermumammi, Tribulusterristia, Trigonella foenum-graecum, Withaniasomnifera and Zingibir Officinale are recorded in flora of Daska subdivision.

Major botanical families of pasrur are Apiaceae, Asparagaceae, *Asteraceae,* Boraginaceae, Caesalpiniaceae, Caprifoliaceae, Cucurbitaceae, *Curculigoorchioides* Gaertn, Cyperaceae, Fabaceae, Fagaceae, Grossulariaceae, Lamiaceae, Lauraceae , Lythraceae, Malvaceae, Polygonaceae, Ranunculaceae and Tiliaceae constituting *Aconitum napellus L.,* Adiantumcapillus-veneris L., Alkannatinctoria L., *Asparagus racemosus,* Caesalpinia crista, *Chlorophytum borivilianum*, Cichoriumintybus, Cinnamomumtamala, Citrulluscolocynthis, Cordia obliqua, Corchorusolitorius , Curculigo Orchioides, Daucuscarota L., *Eleocharisdulcis,* Heliotropium strigosum, Nagar Bail, Nigella sativa L., *Ochromapyramidale, Persicariabistorta L., Polygonumbistorta* L., *Punicagranatum L.,* Quercusin fectoria, *Ribesnigrum,* Senna alexandrina and Vachellianiloticare the strengthiningpillers of the district.

3.1. Statistical Evaluation of Results:

Data shows that more than half of flora of Sialkot consists of herbs, then trees at the second peak, and finally the shrubs are in least quantity. In order to check the association of soil's fertility and growth of habits of plant chi-square test is applied. Results were found to be significant with P-value of 0.000 (P<alpha) hence concluding that soil of district of Sialkot whether from any subdivision is found to be highly fertile w.r.t the growth of different habits of plant.

Table 1: Details of local medicine men providing information.

Subdivision		Name of Medicine Men	Age	Area	Work Experience	Mother Institute
Sialkot	1	Hakim Nadar Khan Lodhi	45 Years	Chawinda Bazar Hakiman	20 Years	Tibia College Lahore
	2	Muhammad Razzaq	42 Years	Chawinda	20 Years	Tibia College Gujranwala
Sambrial	1	Muhammad Saleh	44 Years	Sambrial City	20 Years	Family occupation
	2	Akbar Ali	74 Years	-do-	50 Years	Private Source
	3	Manzoor	55 Years	-do-	10 Years	-do-
Daska	1	Hakim Khalil urRehman	40 Years		10 Years	Occupation of forefathers.
Pasrur	1	Hakim Muhammad Afzal	47 Years	Pasrur, Charwinda Phatak	18 Years	Tibia College Lahore
	2	Hakim Rana Saleem Ul Allah	72 Years	Pasrur City	37 Years	Tibiya College, Tib-e-Nabvi, Faisalabad

Table 1 depicts that data was collected by experienced and mature people in their fields from a mature age of minimum 42 to maximum 72 years, with experience of 10-50 years and 25 years on average.

Table 2: Systematic arrangement of data of ethnomedicinal flora of four subdivisions of District Sialkot Punjab Pakistan.

S. No	Botanical Name	Family Name	Habit	Local Name of Plant	Common Name of Plant	Part used	Application	Habitat
1	*Acacia nilotica (L.) Delile*	*Fabaceae*	Tree	*Kekar*	Babool, Thorn mimosa	Whole plant	For Semen Leakage, Nocturnal Ejaculation, Leucorrhea	Sambrial
2	*Aconitum napellus L.*	*Ranunculaceae*	Herb	*Meeth Talia*	Monk's-hood	Tuber	As Antibiotic	Pasrur
3	*Achyranthes aspera Linn*	*Amranthaceae*	Herb	*Puth Kanda*	Prickly Chaff	Powder	For Gastric Disorders, Pruritus, Asthma.	Sialkot, Sambrial
4	*Adiantum capillus-veneris L.*	*Pteridaceae*	Herb	*Partoshan*	Southern Maidenhair	Leaves	Control of Hormonal Secretions	Pasrur
5	*Adhatoda vasica*	*Acanthaceae*	Shrub	*Arosa*	Vasaka	Whole plant	For Jaundice, nausea.	Sialkot
6	*Aegle marmelos L*	*Rutaceae*	Tree	*Belgiri*	Bael	Fruit	For Viral Infections, Diarrhea, Flu, Purgation, Rheum, Diabetes.	Sialkot
7	*Alkanna tinctoria L.*	*Boraginaceae*	Herb	*Rattan Jot*	Alkanet	Leaves	Treatment of burned body	Pasrur
8	*Allium cepa*	*Liliaceae*/Amaryllidaceae	Herb	*Pyaz*	Onion	Stem	For treatment of Blood Pressure	Sialkot
9	*Allium sativum*	*Liliaceae*	Herb	*Lehsan*	Garlic	Stem	For treatment of Blood Pressure	Sambrial
10	*Aloe Indica L.*	*Liliaceae/ Xanthorrhoeaceae Liliaceae*	Herb	*Kanwar Gandal, Aluva*	Aloe vera	Leaves	As Analgesic, Antipyretic, Appetitive, for *removal of Intestinal Parasites, Relieve from*	Sialkot, Sambrial

							Dysmenorrhea pain.	
11	*Amorphophallus paeoniifolius*	*Araceae*	Herb	*Surana*	Elephant Foot	Corn of Rhizome	For Haemorrhoids	Daska
12	*Anethum graveolens*	*Apiaceae*	Herb	*Shatpushpa*	Dill	Dried Rippen Fruits	For relieve of Menstrual Pains	Daska
13	*Asparagus racemosus*	*Asparagaceae*	Herb	*Satawar*	Buttermilk root	Tubers	As male sexual tonic	Pasrur
14	*Asteracantha Longifolia*	*Acanthaceae*	Weed	*Talmakhana*	Hygrophila	Seed	As Nutritional Tonic, Exhilarant, for weight gain, a male sexual tonic, Hyper coagulability.	Sialkot
15	*Azadirachta indica*	*Meliaceae*	Tree	*Neem*	Nimba	Seed, Fruit,Flower,Bark	As Blood Purifier, Antipyretic, Sedative, Laxative, Resolvent and for Dermatological problems.	Sialkot
16	*Bacopa monnieri (L.) Penn. syn.*	*Scrophulariaceae*	Herb	*Jal Neem*	Brahmi	Whole plant	For Blood filtration	Sambarial
17	*Bambuseae*	*Poaceae*	Tree	*Tabashir Naqda*	Bamboo Silica	Stem, Pulp of fruit	As heart relaxant	Sambarial
18	Berberis aristata	*Berberidaceae*	Shrub	*Drauharidra decoction*	Indian berry	Roots, Stem	For Conjunctivitis	Daska
19	*Brassica Compestris L.*	*Brassicaceae*	Herb	*Lahuna oil*	Mustard	Seed oil	For earache	Daska
20	*Butea monosperma*	*Fabaceae/*Papilionaceae	Tree	*Plasha*	Flame of Forest	Seed	For Parasitic Infections	Daska
21	*Calotropis procera*	*Asciepiadaceae*	Weed	*Aak*	Milk Weeds/ Madar tree	Leaves, Roots, Latex	As Analgesic, Antipyretic effect	Sambrial
22	*Cassia Fistula*	*Fabaceae*	Tree	*Amal Tas*	*Golden Shower*	Fruit	As Purgative	Sambrial

23	*Catharanthus roseus*	*Apocynaceae*		*Sada Bahar*		Leaves	As Anti-diabetic	Sambrial
24	*Centaurea behen. L*	*Asteraceae*	Herb	*Bahiman*	White Behmen	Seed	For Leucoderma.	Pasrur
25	*Cercis siliquastrum*	*Fabaceae*	Tree	*Arghawan*	Judas-tree	Seed	For treatment of *hemoptysis*, component of ophthalmic medicines.	Sialkot
26	Cichorium intybus	*Asteraceae*	Herb	*Kasani*	Chicory	Seed	Gastric and Hepatic Tonic	Pasrur
27	*Cinnamomum tamala*	*Lauraceae*	Tree	*Kanwal Patta*	Bay Leaf	Fruit		Pasrur
28	*Cinnamomum zeylanicum*	*Lauraceae*	Tree	*Dar Cheeni*	Cinnamon	Bark	For stomach Treatment	Sambrial
29	*Citrullus colocynthis*	*Cucurbitaceae*	Herb	*Tuma*	Bitter Apple.	Tubers	As Anti-diabetic.	Pasrur
30	*Citrus tangerina*	*Rutaceae*	Tree	*Barhij Dandi*	*Citrus*	Dry leaves	For Febrifuge, Pruritus, Skin *abscess, Ringworms.*	Sialkot
31	*Commiphora*	*Burseraceae*	Tree	*Googgle*	Indian Badellium	Leaves	For Thyroid stimulation	Daska
32	*Corchorus olitorius*	*Tiliaceae*	Herb	*Jute*	Jew's Mallow	Seed	For Renal Disorders	Pasrur
33	*Cucumis melo var. agrestis Naudin*	*Cucurbitaceae*	Weed	*Chibbar*	Wild Water Melon	Seed, Fruit	For Dermatological and Gastric Problems	Sialkot
34	*Cupressus sempervirens L.*	*Cupressaceae*	Tree	*Jeriena*	Mediterranean Cypress	Whole plant	For Blood Purification	Sambarial
35	*Curculigo Orchioides*	*Curculigo orchioides Gaertn*	Herb	*Siyah Mosli*	Golden Eye Grass	Roots	As Muscular Tonics	Pasrur
36	*Curcuma Longa L.*	*Zingiberaceae*	Herb	*Haridra*	Turmeric	Rhizome	For Sprain, Wound Care	Daska
37	*Cuscuta reflexa Roxb*	*Cuscutaceae*	Tree	*Akash Bail*	Dodder	Stem	For Paralysis	Sialkot
38	*Cydonia oblonga*	*Rosaceae*	Tree	*Bahi Dana*	Quince	Seed	For Weight gain, Increase in Lactation.	Sialkot

39	*Cymbopogon citratus*	*Poaceae*	Shrub	*Lemon Grass*	Lemon Grass	Whole plant	For Viral Fever	Sambarial
40	*Cyperus rotundus L.*	*Cyperaceae*	Herb	*Deela*	Nut Grass	Rhizome	For Diarrhea, dysentery and Febrifuge	Sialkot
41	*Cyrilla racemiflora*	*Cyrillaceae*	Shrub	*Teeti*	Leather wood	Whole plant	For Jaundice	Sambarial
42	Daucus carota L.	*Apiaceae*	Herb	*Gajar*	Carrot	Seeds	As male sexual tonic	Pasrur
43	*Datusa Metel L.*	*Solanaceae*	Herb	*Dhattora*	Thorn Apple	Leaves, Seed	For Lice Infestation	Daska
44	*Elettaria Cardamon*	*Zingiberaceae*	Herb	*Ela Powder*	Cardamon	Seed	For Anti-peristaltic movements	Daska
45	*Eleocharis dulcis*	*Cyperaceae*	Herb	*Khushk Sangara*	Water chestnut	Leaves	For Stomach acidity and sexual dysfunction	Sialkot
46	*Embelia ribes*	*Myrsinaceae*	Shrub	*Bao Paring*	False Black Pepper	Seed	*For removal of Intestinal Parasites, Herpetological problems.*	Sialkot
47	*Euphorbia hirta L.*	*Euphorbiaceae*	Herb	*Aam dodak*	Doddak	Whole plant	As Expectorant, for Asthma and Cough	Sialkot
48	*Euphorbia hypericifolia*	*Euphorbiaceae*	Herb	*Pui Booti*	Graceful *Spurge*	Whole plant	To relieve warts	Sialkot
49	*Ficus Benghalensis L.*	*Moraceae*	Tree	*Borh*	Bayan	Latex, Stem, Fruit	For Muscular Strength	Sambarial
50	*Foeniculum vulgare*	*Apiaceae /Umbelliferae*	Herb	*Kamon-e-Aswad, Sonf*	Fennel	Seed	As Carminative, for Constipation and Stomach Disorders	Sambarial, Daska
51	*Fumaria officinail L.*	*Fumariaceae*	Shrub	*Shahtara*	Earth-Smoke	Whole plant	For Blood filtration	Sambarial
52	*Glycyrrhiza glabra*	*Fabaceae*	Shrub	*Mulathy*	Liquorice	Root	For Stomach ulcers, heartburn	Sialkot, Daska
53	*Holarrhena Pubescens*	*Apocynaceae*	Tree	*Kutaja*	Tellicherry Bark /Kurchi	Stem	For Diarrhea	Daska

54	*Heliotropium strigosum*	*Boraginaceae*	Herb	*Gorakh Pan Booti*	Bristly Heliotrope.	Leaves	As Anti-allergic and Blood Purifier	Sialkot
55	*Hyoscyamus niger*	*Solanaceae*	Herb	*Ajwaien Kharasani*	Black Henbane	Seed	For Insomnia, Hysteria, Belly Ache, Chesty Coughs Treatment	Sialkot
56	*Ipomoea Eriocarpa*	*Convolvulaceae*	Herb	*Lagaco cozinho*	Morning glory	Root, Leaves	For Headache, ulcers, fevers	Sialkot
57	*Indigofera tinctoria*	*Fabaceae*	Shrub	*Neel Kubthe*	True Indigo	Flower, Leaves	As Blood purifier, syphilis, Mosaic disease, Typhoid fever.	Sialkot
58	*Lavandula Officinalis Chaix*	*Lamiaceae*	Shrub	*Asto Khodos*	French Lavender	Leaves, Flower	For Hemicranias, Psychiatric issues, Asthma, Digestion, Flu	Sialkot
59	*Leucas aspera (Jacq.) Ait.*	*Lamiaceae*	Herb	*Jhumka booti*	Tunble weed	Leaves	For Gastritis	Sialkot
60	*Lolium perenne L.*	*Poaceae*	Weed	*Gaus Vail*	Reygrass	Stem	For Paralysis, Pain	Sambrial
61	*Malva sylvestris L.*	*Malvaceae*		*Khabazi, Khatm-e-khapazi*	*Mallow*	Seed	For Inflammatory diseases of mucous, Flu, Rheum, Cough, Urinary tract infection and Intestinal inflammation	Sialkot, Sambrial
62	*Mentha pulegium*	*Lamiaceae*	Herb	*Podeena*	Mint	Leaves	For stomach disorders and healthy digestion	Sialkot
63	*Mentha viridis L.*	*Lamiaceae*	Herb	*Podeena*	Mint	Leaves	For Stomach ache and Heartburn.	Sialkot
64	Mesua ferrea *L.*	Calophyllaceae	Tree	*Nagseer*	Medusa	Flower	As Astringent, Cardiac, Hepatic and Gastric Tonics and for Hemorrhoids.	Sialkot

65	*Murdannia pauciflora*	*Commelinaceae*	Herb	*Khosli*	Few Flowered Dewflower	Roots	For Sexual Dysfunction.	Sialkot
66	*Murraya exotica*	*Rutaceae*	Shrub	*Jasmine orange*	Jasmine orange	Leaves	As Analgesic	Sialkot
67	*Myristica fragrans Houtt*	*Myristicaceae*	Tree	*Jawatri*	Mace	Peels	As Cardiac and Gastric Tonic, Carminative.	Sialkot
68	*Myristica fragrans*	Myristica	Tree	*Javatri, Jaifal*	Nutmeg	Fruit, Seed	For Dyspepsia, Numbness of skin, Headache, Luxation , Premature Ejaculation Treatment, ,Stomach spasms and pain	Sialkot, Daska
69	*Nagar Bail*	*Caprifoliaceae*	Shrub	*Tunj*		Seed	For Male sexual tonic.	Pasrur
70	*Nigella sativa L.*	*Ranunculaceae*	Herb	*Kalvanji*	Klotrgi	Seed	For Gastric Tonic	Pasrur
71	*Nigella sativa L.*	*Ranunculaceae*	Herb	*Kalvanji*	Klotrgi	Seed	For Gastric Tonic	Pasrur
72	Nymphaea ***L.***	Nymphaeaceae	Herb	*Nelofar*	water lily	Flower	For Cardiovascular and nervous system	Sambrial
73	*Onosma bracteatum*	*Boraginaaceae*	Herb	*Gao Zuban*	Bee Plant	Leaves	For relieve of functional palpitation of heart	Sambrial
74	*Ochroma pyramidale*	Malvaceae	Tree	*Beera*	Balsa Tree	Fruit	For Gastric Tonic	Pasrur
75	Ocimum basilicum	Lamiaceae	Tree	*Rehan*	Basil Seeds	Seed	For male sexual tonic	Pasrur
76	*Papaver somniferum L.*	*Papaveraceae*	Tree	*Koknar*	Opium poppy	Seed, Fruit	For Conjunctivitis, Headache, Brain Tonic, Flu and Rheum	Sialkot
77	*Persicaria bistorta L.*	Polygonaceae	Tree	*Inj Bar*	Marsh pepper	Root		Pasrur
78	*Peganum harmala*	*Nitrariaceae*	Tree	*Harmel*	Aspand	Seed	As Carminative and diuretic	Daska
79	*Phyllanthus emblica L.*	*Phyllanthaceae*	Herb	*Amla*	Indian goose berry	Fruit	As Gastric Tonic	Sialkot

80	*Picrorhiza kurrooa*	*Scrophulariaceae*	Herb	*Kutaka*	Picrohiza	Rhizomes with Roots	For Jaundice	Daska
81	*Piper nigrum L.*	Piperaceae	Herb	*Mirch Siyah*	Black Pepper	Seed	For Gastrointestinal Improvements, As Gastric and Hepatic Tonics, Expectorant.	Sialkot, Sambrial, Daska
82	*Pistacia Lentiscus*	*Cactaceae*	Tree	*Mustalgi*	Lentisk	Gum	As Gastric and Hepatic Tonics, as solvent for drug, for Relieve of Menstrual Pains	Sialkot
83	*Plantago Ovata L.*	*Plantaginaceae*	Herb	*Isbaghol*	Ispaghula Husk	Seed	For Spermatorrhoea, Belly Ache, sore throat, Urinary tract infection	Sialkot
84	*Polygonum bistorta L.*	*Polygonaceae*	Herb	*Anj Bar*	Meadow Bistort.	Shoot	As Anti-allergic	Pasrur
85	*Polygonum Viviparum*	*Polygonaceae*	Herb	*Anjbar*	Bird Weed	Root	For Hemorrhage healer, Purgation treatment	Sialkot
86	*Psoralea corylifolia L.*	Fabaceae	Herb	*Babchi*	Bavanchi Seeds	Seed	For Leucoderma.	Sialkot
87	*Punica granatum L.*	Lythraceae	Small Tree	*Anar Dana*	Pomegranate	Seed	As Gastric Tonic	Sialkot
88	*Pyrus communis*	*Rosaceae*	Tree	*Nashpati*	Pear	Fruit	As Laxative, For obesity, Biliary obstruction	Sialkot
89	*Quercus infectoria*	*Fagaceae*	Shrub	*Maju*	Gallnut	Fruit	As Gastric Tonic	Pasrur
90	*Rhyncosia minima*	*Fabaceae*	Herb	*Jungli moath*	*Jumby-bean*	Whole plant	For Gyne care.	Sialkot
87	*Ribes nigrum*	Grossulariaceae	Shrub	*Manka*	Currant	Fruit	For Common Cold and as Pain killer	Pasrur

88	*Ricinus communis L.*	*Euphorbiaceae*	Small Tree	*Hernoli*	Castor oil	Seed	For Gastric problem and Constipation.	Sialkot
89	*Senna alexandrina*	Fabaceae	Herb	*Tanamki*	Senna	Leaves	As Purgative	Pasrur
90	*Santalum album L.*	*Santalaceae*	Tree	*Sandal*	Sandal wood	Stem	As Heart relaxant	Sambrial
91	*Senna Alexandria*	*Caesalpiniaceae*	Tree	*Barg-e-sarna*	Seena Plant	Leaves	Used for Gastric Problems	Sambrial
92	*Shpaerathus Indicus*	*Asteraceae*	Herb	*Mundi Booti, Gorak Mundi*	Sphaerathus	Flower, Fruit	For Somatic Pain	Sambrial
93	*Solanum Nigrum*	*Solanaceae*	Herb	*Makoh*	European *blac k nightshade*	Whole plant	For Internal Injury	Sambrial
94	*Solanum Pseudocapsicum*	*Solanaceae*	Shrub	*Aksan/ Asgandh*	Winter Cherry	Roots	As Brain tonic, for pain relieving	Sambrial
95	*Syzygium Aromaticum*	*Myrtaceae*	Tree	*Long*	Clove	Fruit, Flower, buds	For Hypertension and Toothache	Sambrial, Daska
96	*Strychnos Nux-vomica L.*	*Loganiaceae*	Tree	*Azraki*	Kuchla	Seed	As poison, Brain Tonic and Pain killer	Sialkot
97	Syzygium cumini	*Myrtaceae*	Tree	*Jaman*	Black plum	Fruit	As Anti-diabetic, Anti- jubilance	Sambrial
98	*Terminalia arjuna*	*Combretaceae*	Tree	*Arjan*	Arjun Tree	Leaves	For Cough, Cardiovascular disorders and mucus	Sambrial
99	*Terminalia chebula*	*Combretaceae*	Tree	*Har Har*	Black Myrobalan	Fruit	For Antibacterial and anti-inflammatory applications	Daska
100	*Trachyspermum ammi*	*Apiaceae*	Herb	*Ajwaien Desi*	Ajwaien	Fruit	For Atonic dyspepsia, diarrhea, abdominal tumors	Daska
101	*Tribulus terristia*	*Zygophyllaceae*	Shrub	*Gokshura*	Land Caltrops	Fruit	For Sexual disorders	Daska
102	*Trigonella foenumgraecum*	*Fabxaceae*	Tree	*Maithray*	Fenugreek	Seed	For Anorexia nervosa	Daska

103	*Vachellia nilotica*	Fabaceae	Tree	*Gond Babol*	Kekar	Gum	As Gastric Tonic	Daska, Sialkot, Sambrial
104	*Withania somnifera*	*Solanaceae*	Herb	*Ashvagandha*	Winter Cherry	Root	For Malaise	Daska
105	*Xanthium strumarium L.*	*Asteraceae*	Herb	*Chhota Dhatura*	Cocklebur	Seed, Fruit, Leaves	As Gastric Tonics	Sambrial
106	*Zingiber officinale*	*Zingiberaceae*	Herb	*Adrak*	Ginger	Stem	For Hypertension	Sambrial
107	*Ziziphus jujuba*	*Rhamnaceae*	Tree	*Anab*	Jujubes	Fruit	For Hyperthermia, Blood Clarification, Neuron Tonic.	Sambrial
108	*Zingibir Officinale*	*Zingiberaceae*	Herb	*Sunth*	Dry Ginger	Rhizomes	As Stomach settler	Daska
109				*Taram Hindi*		Seed		Pasrur
110				*Indian Mosli*		Stem	For male sexual tonic	Pasrur
111				*Sundash*		Leaves, Stem, Flower	As Brain Tonic	Pasrur
112				*Sumandri Suk*		Seed	For Leucorrhea and Sun Stroke.	Pasrur

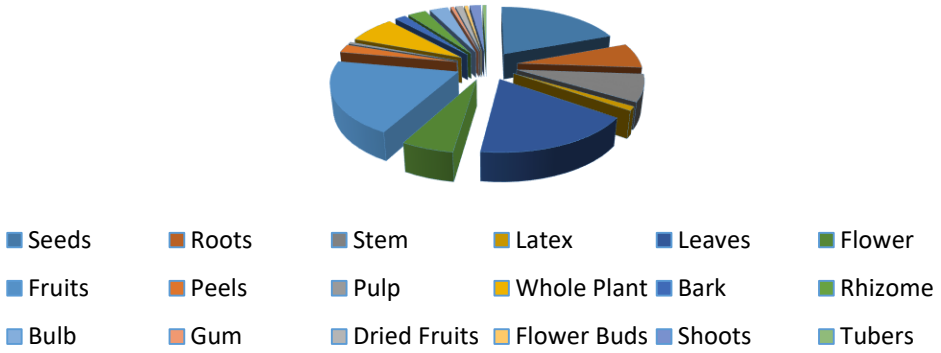

Figure 4: Comparison of various parts of Plants used for preparation of local herbal medicines.

Figure 4 shows that Seeds, roots, stems, latex, leaves, flowers, fruits, peels, pulp, bark, rhizomes, bulbs, gums, dried fruits, flower buds, shoots, tubers and whole plants of all these species are effective in gastric, hepatic, cardiovascular, respiratory, inflammatory, dermatological, neurological, sexual dysfunctions and water borne diseases.

Statistical data of frequencies of all the 61 botanical families in all the subdivisions of district represents *Fabaceae* familyas the most abundant family with a frequency of 12 in whole data, alongwith *Solanaceae, Lythraceae, Lamiaceae, Apiaceae, Asteraceae and Rutaceae*in considerable fraction.
Individual dominance of various families in individual subdivision is given in Figure 5(a-d).

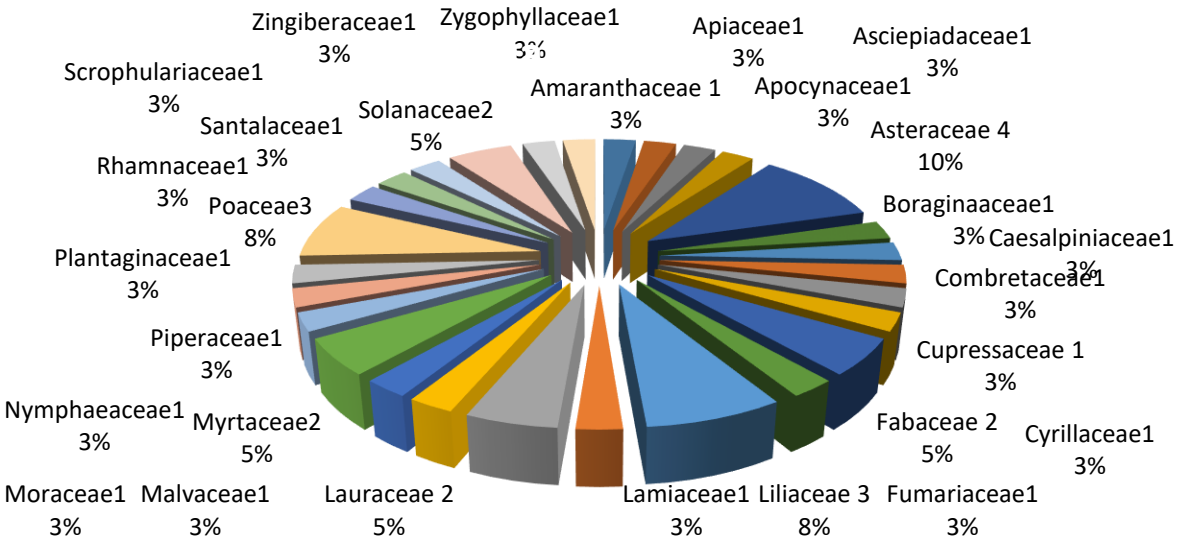

Figure 5(a): Population of botanical families in Sialkot Subdivision.

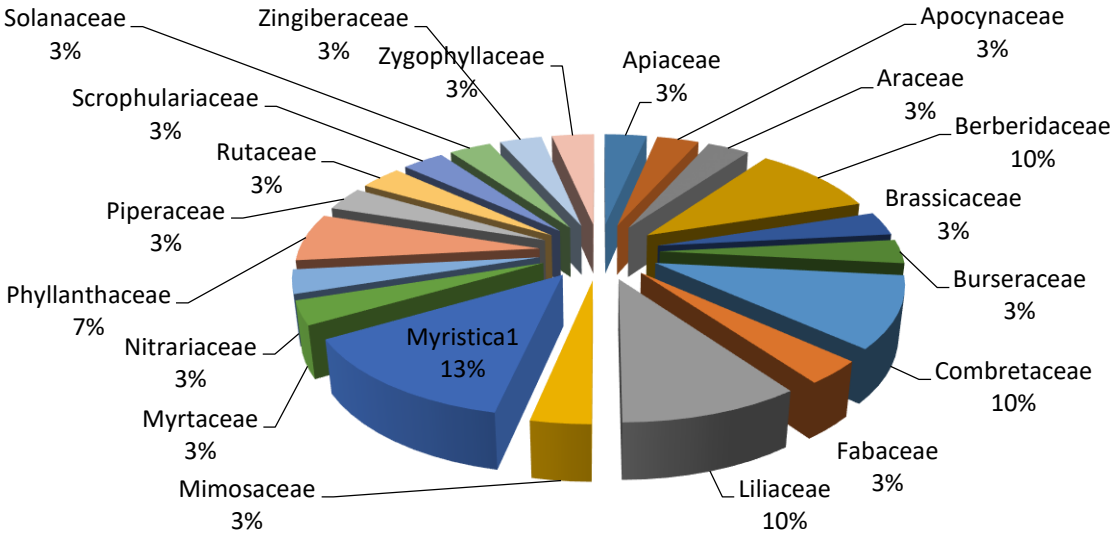

Figure 5(b): Population of botanical families in Sambrial Subdivision.

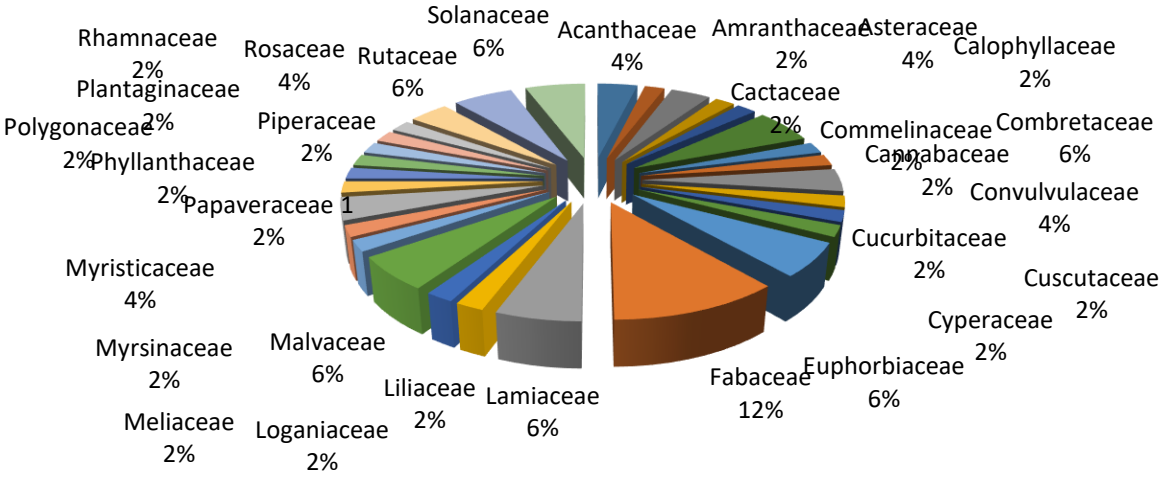

Figure 5(c): Population of botanical families in Daska Subdivision.

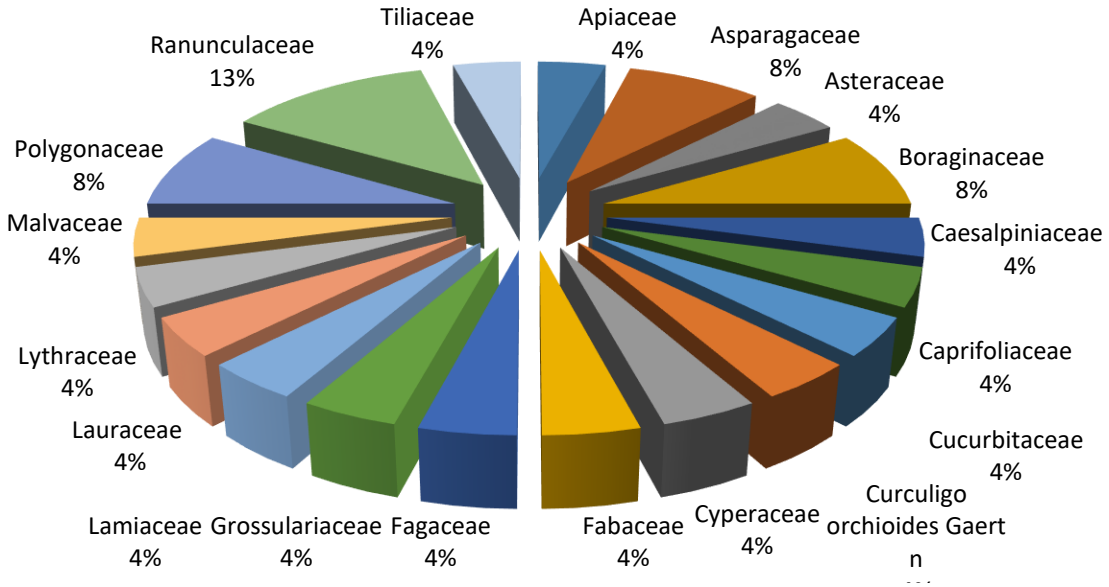

Figure 5(d): Population of botanical families in Pasrur Subdivision. Population density of different botanical species and families is shown in Table 2.

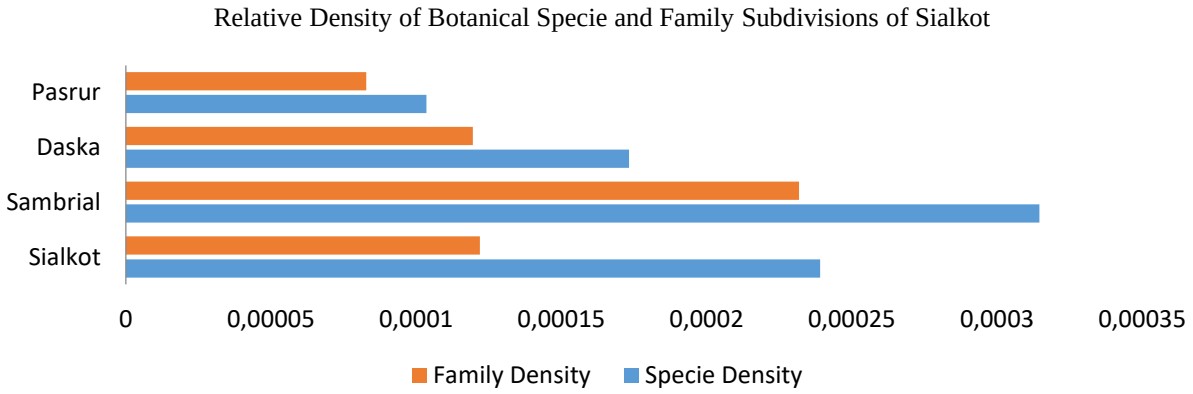

Figure 6: Comparative ethnomedicinal data of district Sialkot.
Figure 6 shows highest botanical density of specie as well as family in subdivision Sambrial in comparison with all others.

Table 3: Relative average density of various botanical species and and families in Dist. Sialkot

S. No	Name of Subdivision	Area (sq.acres^2)	Species density/ sq.acres^2	Family density/ sq.acres^2
1	Sialkot	213.255	2.39×10^{-4}	1.21×10^{-4}
2	Sambrial	120.791	3.24×10^{-4}	2.31×10^{-4}
3	Daska	167.288	1.73×10^{-4}	1.19×10^{-4}
4	Pasrur	241.531	1.03×10^{-4}	8.28051×10^{-5}
5	Sialkot District	742.885	1.57×10^{-4}	8.21123×10^{-5}

4. Discussion

A wider survey of medicinal men and local flora in order to construct a systematic data sheet of district Sialkot exploded the treasures of highly dense racks of natural resources hidden from the world eye. Now world can have a look at this ethnomedicinal heaven to diversify their market with green medicines to highlight the fertility of green pharmaceutical industry. The leaves, stem, bark and fruits of Aegle marmelos (L.) Correa (A. marmelos) has medicinal value accepted by researchers (19). These leaves are widely used to treat diarrhoea, dysentery, skin and eye diseases (20). They contain terpenoids which act as antifungal agent. Allium cepa has been used as an efficient model organism in genetic tests for chromosome aberration assays. Genotoxicity of many food dyes have been evaluated using Allum cepa as indicator. Aloe Vera is found primarily in the arid regions of Americas, Africa,

Europe, and Asia that is used for medicinal purposes (21). In India, Andhra Pradesh, Rajasthan, Maharashtra, Gujarat, and Tamil Nadu are the main Aloe vera cultivating states. For centuries, the gel of Aloe vera has been used for healing and therapeutic purposes, and more than 75 biologically active constituents have been discovered in the inner gel. Aloe vera is a rich source of bioactive compounds (22). It has been widely used in alternative medicine as health and nutritional supplements in addition to its cosmetic applications. Polyphenol-rich A. vera extracts possess various pharmacological activities. The plant has about 99-99.5% water and only 0.5-1.0% solid matter which contains more than 75 diverse compounds. Cassia fistula seeds are well defined for producing activated carbon through physical and chemical treatment for the extrusion of Ni(II) ion contaminated aqueous solution (23). The readily prepared sorbents were characterized using SEM-EDX and FTIR and explored for further studies. Solanum nigrum is a species in Solanum genus, characterized by its white flowers and purple-black berries. It contains many steroidal glycosides, steroidal alkaloids, steroidal oligoglycosides, including solamargine, solasonine, solavilline, solasdamine and solanine, steroidal saponins and glycoprotein, many polyphenolic compounds such as gallic acid, protocatechuic acid, catechin, caffeic acid, epicatechin, rutin, and naringenin (24), which possess strong anticancer and antioxidant activity with IC50 value of isolated compounds ranging from 0.25-4.49 micro metre. Each part of Terminalia arjuna, i.e. stem bark, fruit, leaves and roots is bestowed with healing properties. Particularly, Terminalia arjuna bark extract has a long antiquity of its role as a cardiac stimulant for its beneficial effects in angina.

It was identified that 74% of the 119 plant derived drugs were discovered as a result of isolation of active substances from medicinal plants (25).

5. Conclusions

Sialkot is found a densely loaded area with heave population density of ethnomedicinal herbarium. About 112 species of 61 families are found to be accommodated in fertile land of the all of the four subdivisions on behalf of its surrounding and geographical location. These species are found effective in herbal medicines of about 170 categories of gastric, hepatic, sexual, urinary, respiratory, and inflammatory and water borne diseases including analgesic and anti-pyretic activities. This data explores the unique and fertile territory of District Sialkot, executing its dynamic biological resources and promoting its pharmaceutical market in international grounds. Sialkot can be an economic company of raw materials of each and every type of pharmaceutical stuff. Any proposal of setup of safe and healthy herbal resource center would be appreciably successful here to harvest big deals of national and international business shares. It could be a ready source of green medicines introduced at least cost pharmaceutical open ground worldwide.

Conflict of interest statement

None

Financial Support

There is no financial support organization.

References

1. Arshad M., Nisar MF., Majeed A., Ismail S., Ahmad M. Ethnomedicinal flora in distirct sialkot Punjab Pakistan. *Middle East J Sci Res* **2011**; 9(2): 209-214.
2. Hawkins KG., Casolaro C., Brown JA., Edwards D. A., Wikswo JP. The Microbiome and the Gut-Liver-Brain Axis for CNS Clinical Pharmacology: Challenges in Specifying and Integrating In Vitro and In Silico Models. *Clin Pharmacol Ther* **2020**.
3. Sureshbabu P., Siddalingamurthy E., Shashidhara NL., Sooryanarayanarao B., Bhavya DC. A Review on Electrohomeopathic Medicinal Practice: Origin, Principles, Medicinal Plants Used and Its Current Status in India. *Eur J Med Plants* **2020**; published online (May 11): 31-47.
4. Stenberg K., Hanssen O., Edejer TTT., et al. Financing transformative health systems towards achievement of the health Sustainable Development Goals: a model for projected resource needs in 67 low-income and middle-income countries. *Lancet Glob Health* **2017**; 5(9): 875-887.
5. Kumar S., Maurya VK., Saxena SK. Emerging and Re-emerging Water-Associated Infectious Diseases.In Water-Associated Infectious Diseases.Springer, Singapore. **2020;** p. 27-51.
6. Xu J., Gorsky M., Mills A. A path dependence analysis of hospital dominance in China (1949–2018): lessons for primary care strengthening. *Health Policy Plan* **2020**; 35(2): 167-179.
7. Doolan A., Carne G. Evalution and complementarity? Traditional and complemantary medicine as part of the international human right law to health. *Bond Law Review* **2020**; 32: 63-89.
8. Zaman W., Ahmad M., Zafar M., et al. The quest for some novel antifertility herbals used as male contraceptives in district Shangla, Pakistan. *Acta Ecologica Sinica* **2020**; 40(1): 102-112.
9. Sheikh M. J., Khushk GM. Social Capital and Irrigation Sustainability in Pakistan.In Water Management in South Asia. Springer, Cham. **2020**; p. 93-101.
10. Zahra W., Rai SN., Birla H., Singh SS., Rathore A. S., Dilnashin H., Singh SP. Economic Importance of Medicinal Plants in Asian Countries.

In Bioeconomy for Sustainable Development. Springer, Singapore. **2020**; p. 359-377.
11. Javed N., Riaz S. Issues in urban planning and policy: the case study of lahore, Pakistan. In New Urban Agenda in Asia-Pacific. Springer, Singapore. **2020**; p. 117-162.
12. Bahadur S., Khan MS., Shah M., et al. Traditional usage of medicinal plants among the local communities of Peshawar valley, Pakistan. *Acta Ecologica Sinica*, **2020**; 40(1): 1-29.
13. Ojha SN., Tiwari D., Anand A., Sundriyal RC. Ethnomedicinal knowledge of a marginal hill community of Central Himalaya: diversity, usage pattern, and conservation concerns. *J Ethnobiol Ethnomed* **2020**; 16: 1-21.
14. Javed A., Usman M., Haider S. M., Zafar B., Iftikhar K. Potential of Indigenous Plants for Skin Healing and Care. *ASRJETS* **2019**; 51(1): 192-211.
15. Jeeva S, Kingston C, Kiruba S, Kannan D. Sacred forests-treasure trove of medicinal plants: a case study from south Travancore. In: Trivedi PC. (ed.) Indigenous medicinal plants. Jaipur: Pointer Publishers; **2007**; p. 262-74.
16. Patel DK., Patel K., Rahman M., Chaudhary S. Therapeutic Potential of "Aegeline," an Important Phytochemical of Aegle marmelos: Current Health Perspectives for the Treatment of Disease. In Nanomedicine for Bioactives. Springer, Singapore. **2020**; p. 383-392.
17. Monika D. M., Bisht PS., Chaturvedi P. Medicinal Uses of Traditionally Used Plants in Bhatwari Block, District Uttarkashi, Uttarakhand, India. *J Sci Res* **2020**; 64(1).
18. Kumari M., Jha PK. Etiology, Symptomatology and Management of Black Spot of Aloe vera (Aloe barbadensis Miller) through Botanicals and Biocontrol Agents–A Brief Review. *Curr J Appl Sci Technol* **2020**; (39): 11-20.
19. Azarfam SP., Nadian H., Moezzi A., Gholami A. Effect of sılıcon on phytochemıcal and medıcınal properties of aloe vera under cold stress. *Appl Ecol Envıron Res* **2020**; *18*(1): 561-575.
20. Hemavathy RV., Kumar PS., Kanmani K., Jahnavi N. Adsorptive separation of Cu (II) ions from aqueous medium using thermally/chemically treated Cassia fistula based biochar. *J lean Prod* **2020**; 249: 119390.
21. Ncube NS., Afolayan AJ., Okoh AI. Assessment techniques of antimicrobial properties of natural compounds of plant origin: current methods and future trends. *Afr J Biotechnol* **2008**; 7(12).
22. Borris RP. Natural products research: perspectives from a major pharmaceutical company. *J Ethnopharmacol* 1996; 51(1-3): 29-38.
23. Rates SMK. Plants as source of drugs. *Toxicon* **2001**; 39(5): 603-613.
24. Kone WM., Atindehou KK., Terreaux C., Hostettmann K., Traore D., Dosso M. Traditional medicine in North Côte-d'Ivoire: screening of 50 medicinal plants for antibacterial activity. *J Ethnopharmacol* **2004**; 93(1): 43-49.
25. Harvey AL. Natural products in drug discovery. *Drug Discov Today* **2008**; 13(19-20): 894-901.

Authors' ORCID
Fozia Noreen
http://orcid.org/0000-0001-6096-2568
Mishal Choudri
http://orcid.org/0000-0001-5978-8750
Shazia Noureen
https://orcid.org/0000-0002-9398-42363
Muhammed Adil
https://orcid.org/0000-0002-8495-8245
Madeeha Yaqoob
https://orcid.org/0000-0002-5076-3469
Asma Kiran
https://orcid.org/0000-0001-5783-4514
Fizza Cheema
https://orcid.org/0000-0002-4208-4033
Faiza Sajjad
https://orcid.org/0000-0002-2307-4323
Usman Muhaq
https://orcid.org/0000-0003-2248-044X

https://dergipark.org.tr/tr/pub/ntms

ISSN: 2717-8161 RESEARCH ARTICLE

New Trend Med Sci 2020; 1(2): 84-89. https://dergipark.org.tr/tr/pub/ntms

The Effect of Apilarnil on the Autophagia Against Lipolysaccarite-Based Sepsis in Liver

Züleyha Doğanyiğit[1*], Betül Köklü[1], Arda Üner[1], Aslı Okan[1], Emin Kaymak[1], Sibel Silici[2]

[1]Department of Histology and Embryology, Faculty of Medicine, Yozgat Bozok University, 66100 Yozgat, Turkey
[2]Department of Agricultural Biotechnology, Faculty of Agriculture, Erciyes University, Nutral Therapy Co. Erciyes Technopark, 38039 Kayseri, Turkey

Article History
Received 25 July 2020
Accepted 18 Aug 2020
Published Online 30 Sep 2020

Corresponding Author
Dr Züleyha Doğanyiğit
Department of Histology-Embryology,
Faculty of Medicine,
Yozgat Bozok University,
Yozgat, 66100, Turkey,
Phone: +90 3542126201,
Fax: +90 354 4375285
E-mail: zuleyha.doganyigit@gmail.com
ORCID:http://orcid.org/0000-0002-6980-3384

Abstract: Sepsis, triggered by highly bacterial lipopolysaccharide (LPS) endotoxins, exhibits high morbidity and mortality despite medical advances. Damage to the liver occurs due to the production of highly reactive oxygen species (ROS) and the release of various proinflammatory cytokines. It is suggested that autophagy, which regulates inflammation and selectively destroys damaged mitochondria, suppresses apoptosis and provides a possible protective mechanism in the endotoxic liver. However, apilarnil, a bee product, is known to have high antioxidant activity and positive effects against various diseases thanks to its polyphenols. In this study, it is aimed to reveal the potential protective effect of apilarnil on the autophagy mechanism in the endotoxic liver model LPS-induced. 64 male *Sprague Dawley* rats weighing 200-250 g; control, apilarnil treated groups (0.2, 0.4 and 0.8 g/kg), LPS (30 mg/kg) group and LPS+apilarnil treated groups (LPS+0.2 g/kg, LPS+0.4 g/kg and LPS+0.8 g/kg) are randomly divided into eight groups. Beclin-1, LC3 and P62 proteins were analyzed immunohistochemically in order to determine the activity level of autophagy pathway in the liver tissues taken after the completion of the experiment protocol. The data obtained showed that Beclin-1 immunoreactivity decreased while LC3 and P62 expression increased in the tissues of the LPS group compared to the control group. When apilarnil was applied with LPS, it was determined that there was an increase in Beclin-1 level ($p>0.05$) and a decrease in P62 levels ($p<0.05$) depending on the dose increase. Apilarnil increases the activity of the autophagy pathway and shows potential positive effects by providing a significant decrease on LC3 and P62 protein expression increased by LPS. However, the role of apilarnil in the autophagy pathway, which is a possible protector against LPS-induced sepsis, should be further investigated.
Keywords: Beclin-1, LC3, P62, Apilarnil, LPS, Liver.

1. Introduction

Sepsis; an uncontrolled immune response that is triggered by infection, trauma, or toxins and occurs systemically. In the following process, it can lead to death by causing septic shock and multiple organ failure (1, 2). Lipopolysaccharide (LPS) is the main structural component of the outer cell membrane of gram-negative bacteria (3). Bacterial LPS, an endotoxin, is involved as a powerful microbial agent in

Cite this article as: Doğanyiğit Z, Köklü B, Üner A, Okan A, Kaymak E and Silici S. The Effect of Apilarnil on The Autophagia Against Lipolysaccarite-Based Sepsis in Liver, *New Trend Med Sci* **2020**; 1(2): 84-89.

the pathogenesis of sepsis and septic shock. LPS delivered to the blood initiates a potentially fatal series of inflammation mediators and procoagulant factor release.

Widespread endothelial damage in tissues leads to hypoperfusion and intravascular coagulation (4). During sepsis, pro-inflammatory responses occur with activation of the complement system, coagulation system, vascular endothelium, neutrophils and platelets. However, the immune system is suppressed due to the reprogramming of antigen presenting cells and apoptosis and depletion of lymphocytes (5).

Despite the constant advances in medicine, sepsis continues to be a global problem with high morbidity and mortality rates (6, 7). However, it is known that liver dysfunction accompanying sepsis has a significant effect on mortality rates. However, the pathological mechanism of sepsis-related liver dysfunction is very complex and has not been fully elucidated yet (8).

The liver plays a key role in the regulation of a wide range of metabolic, homeostatic and host defense activities under septic conditions (9). The liver provides both the clearance of circulating pathogenic microorganisms and toxins and the release of components of the liver-induced cytokines, inflammatory mediators, and coagulation cascade (10). The irregular inflammatory response that occurs following excessive LPS stimulation can kill bacteria as well as damage the liver, which has an effective function in defense responses (11).

LPS increases hepatocyte damage and leukocyte infiltration by interacting with TLR-4, a sub-member of the Toll-like receptor (TLR) family, which is highly expressed in Kupffer cells in the liver (12). Following increased TLR-4 stimulation, chemokine from Kupffer cells, various cytokines (tumor necrosis factor-alpha (TNF-α), interleukin (IL) -1β, IL-6, IL-12 and IL-18), reactive oxygen species (ROS) and nitric oxide (NO) is secreted (13, 14). However, activation of the TLR-4 signal can interestingly contribute to the destruction of pathogens by inducing autophagy in immune cells (15, 16).

Autophagy is one of the innate and well-protected defense mechanisms against microbial attack. It controls the destruction of damaged organelles and various macro molecules, such as protein, through the formation of double membrane autophagosomes to provide cellular homeostasis (17, 18). It also plays an active role in the elimination of bacteria and pathogens in the cytoplasm (19).

Current studies in the literature reveal that in the case of sepsis, autophagy suppresses immune reactions and inhibits apoptosis by regulating inflammation and metabolism (20, 21). It also reduces cellular stress by preventing high ROS-induced LPS production and accumulation of damaged mitochondria (22). Autophagy can eliminate damaged mitochondria by selectively (23, 24). It also promotes regeneration of damaged proteins and organelles through lysosomal dependent degradation to deal with oxidative stress damage caused by ROS excess (25). Thus, autophagy has been shown to have a protective role against multiple organ failure, including liver damage (26). Various regulatory proteins such as Beclin-1, LC3 and P62, located in the autophagy pathway, allow examination of the autophagy activity in tissues.

Apilarnil is a poorly studied and little known biologically active bee product (27). It is obtained by freezing and breaking the 3-7-day old bee larvae with the nutrients they contain (28). In the analysis of the chemical composition of drones, it was observed that it contains a high rate of water, carbohydrates and lipids (29). In another analysis study conducted in 2019, similarly high protein content was determined, and 16 kinds of amino acids were detected. It has also been shown to be rich in phenolic compounds. It is suggested that it can perform its biologically beneficial activity through its antioxidant and radical inhibitory activity (30). In addition, current studies reveal that apilarnil has positive effects against gastrointestinal diseases, toothache, muscle fatigue, respiratory problems and male infertility (31).

In this study, the potential protective effect of apilarnil against LPS-induced liver sepsis will be examined. It was aimed to reveal the effect of apilarnil on the autophagy mechanism by performing immunohistochemical staining of Beclin-1, LC3 and P62 proteins in the liver tissue of the rats with sepsis model.

2. Material and Methods

2.1. Chemicals

Lipopolysaccharide was provided from Sigma Aldrich (*Escherichia coli* LPS, serotype 0127: B8) and Lyophilized Apilarnil was provided from Nutral Therapy Co Ltd (Erciyes University Technopark, Kayseri).

2.2. Experiment groups

Ethics committee approval was received from Erciyes University Animal Experiments Local Ethics Committee (HADYEK) for this study (Protokol No: 18/063). Animals were housed under controlled conditioning (on a 12-h light/12-h dark cycle at a temperature of 22-25 °C and air humidity of 55 %). Throughout the study, the animals were provided with ad libitum rat feed and drinking water. Lyophilized apilarnil distilled water was also dissolved and administered to animals by oral gavage. Sixty-four adult male *Sprague Dawley* rats (200-250 g weighing) were randomly divided into 8 groups:

- Control group: 1 ml saline (SF) (0.9% NaCl) i.p.
- LPS group: 30 mg/kg/body weight (bw) LPS single dose i.p. (32).
- 0.2 g/kg API group: 0.2 g/kg/bw oral gavage for 10 days (33),
- 0.4 g/kg API group: 0.4 g/kg/bw oral gavage for 10 days,
- 0.8 g/kg API group: 0.8 g/kg/bw gavage for 10 days,

- 0.2 g/kg API+LPS: 0.2 g/kg API for 10 days, after 60 min LPS (single-dose i.p., 30 mg/kg)
- 0.4 g/kg API+LPS: 0.4 g/kg API for 10 days, after 60 min LPS (single-dose i.p., 30 mg/kg)
- 0.8 g/kg API+LPS: 0.8 g/kg API for 10 days, after 60 min LPS (single-dose i.p., 30 mg/kg)

Experimental animals were anesthetized with Ketamine (70 mg/kg/bw) and Xylazine (10 mg/kg/bw) six hours after administration and liver tissues were removed.

2.3. Immunohistochemical analysis

Immunoreactivity of Beclin-1, LC3A/B and P62/SQSTM1 in liver tissues of the LPS-induced rat sepsis model was determined using the Avidin-Biotin peroxidase method (34). Briefly, after deparaffinization of sections taken at 5μm thickness, citrate buffer was used to open the epitopes (pH: 6.0). The slides were then taken into a 3% hydrogen peroxide solution in methanol to prevent endogenous peroxidase activity. Ultra V block solution was applied to prevent non-specific staining. Sections were then incubated overnight at 4°C with primary antibodies. Biotinylated secondary streptavidin-HRP and DAB chromogens were applied, respectively. And then sections were counterstained with Gill Hematoxylin. It was dehydrated by passing through increasing alcohol series and closed with a concealer called entellan. Sections were examined with Olympus BX53 light microscope. The evaluation of the immunoreactivity levels was done with Image J program. 10 different areas were evaluated for each slide.

2.4. Statistical analysis

Experimental data were statistically analyzed in GraphPad Prism (version 6.0, GraphPad Software Inc., San Diego, California) and presented as Mean±SEM. Data were analyzed using one-way ANOVA with Tukey's post hoc tests for multiple comparisons. $P<0.05$ was considered significant.

3. Results

As shown in Figure 1, it was observed that Beclin-1 decreased while LC3A/B and P62/SQSTM1 were increased in liver samples belonging to LPS group. In groups where LPS and apilarnil were applied together, while Beclin-1 increased with the increase of apilarnil dose ($P>0.05$), LC3A/B and P62/SQSTM1 decreased with the increase of apilarnil dose ($P<0.05$).

4. Discussion

During sepsis, cells are exposed to increased oxidative stress and metabolic demands. All of these processes can lead to cell damage and cell death (35). However, cells and tissues try to protect themselves from such stresses by activating autophagy and autophagy-like mechanisms (36).

Autophagy is critical for maintaining normal human physiology, such as cellular homeostasis, energy balance, development, and cellular defense (37). Autophagy can also play a role in the pathogenesis of cancer, neurodegenerative diseases, aging, muscle diseases, infectious diseases and immune system diseases (38, 39). In addition, the presence of autophagy in liver tissue in the case of sepsis has been reported in studies (35, 40). In this study, we aimed to determine the effects of apilarnil, a natural bee product, on the autophagy mechanism that may occur as a result of endotoxic shock caused by LPS.

In lysosomal activity during autophagy, the P62 protein is considered a biomarker of autophagy and an indicator of autophagic flow. It is also characterized as an indicator of autophagic flow prevention of P62 reduction (41). Immunohistochemical analysis of LC3A or LC3B has also been used to investigate the level of autophagy occurring in the tissue (42). In addition, in clinical and experimental studies, Beclin-1, which is one of the main proteins of autophagy, is examined as a target for the determination of the presence of autophagy (43). Accordingly, in the sepsis model created with LPS, we performed the immunohistochemical analysis of Beclin-1, LC3A/B and P62 parameters as autophagy markers in liver tissue. According to the results obtained, LC3A/B expression was significantly increased only in the groups injected with LPS compared to the control. These results confirmed the presence of autophagy in liver tissue as a result of sepsis caused by LPS endotoxicity (Figure 1C). However, it was determined that Beclin-1 expression decreased significantly and P62 expression increased as a result of LPS injection (Figure 1B and 1D).

In the study performed by Chen et al. (44), LC3A/B, Beclin-1 and P62 proteins were examined to evaluate autophagy in hepatocytes in the sepsis model created by LPS injection in C57BL/6 mice. As a result of the study, significant changes were observed in LC3 and P62, while no increase was observed in Beclin-1 (44). According to these results, it can be said that autophagy associated with LPS in liver tissue is not related to Beclin-1 and P62 molecules. Since LPS provides its effect with the TLR-4 receptor (45), more detailed studies are needed to clarify the mechanism underlying the relationship between the TLR-4 receptor and the LPS-induced autophagic pathways.

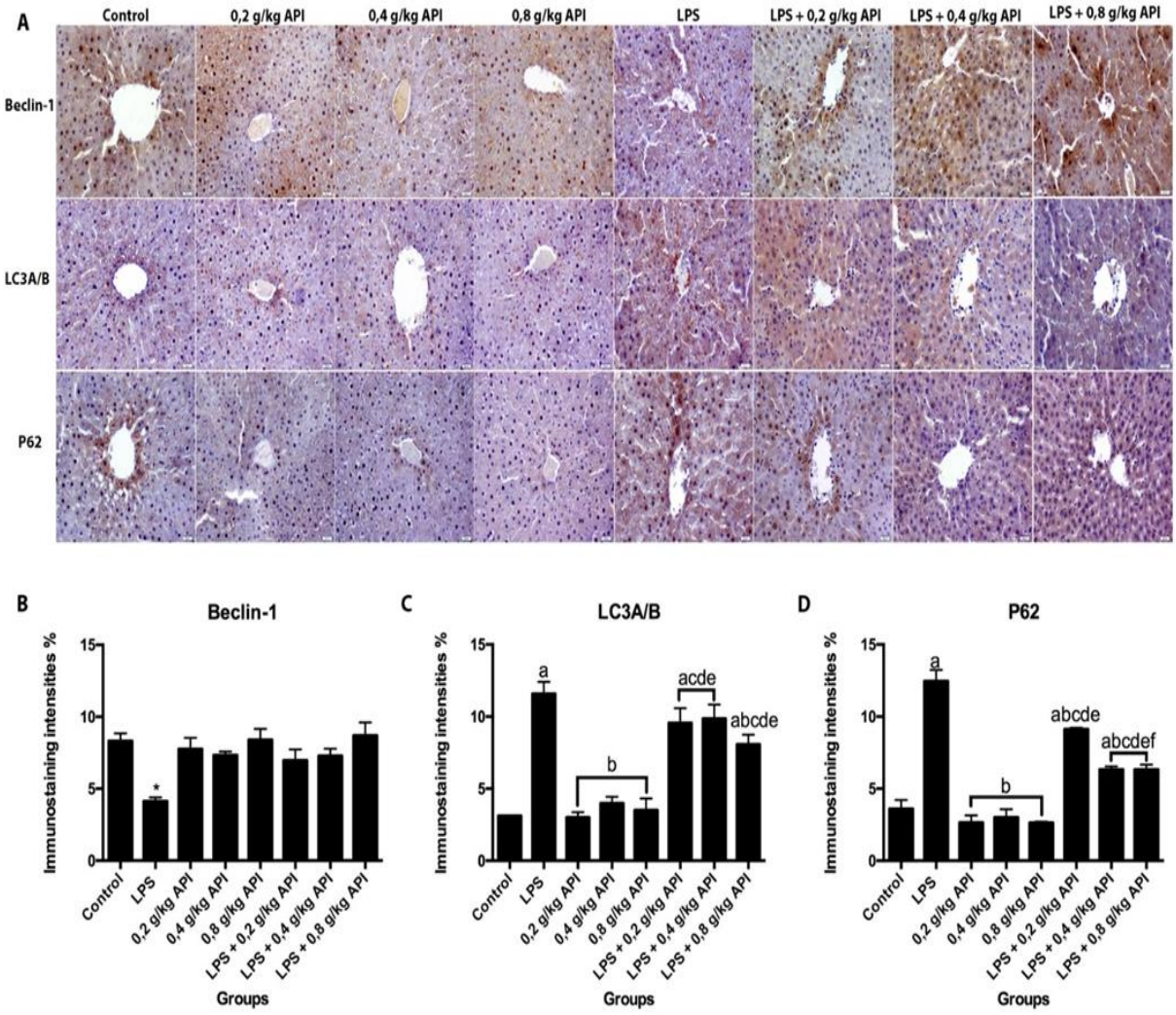

Figure 1. A. Beclin-1, LC3A/B and P62/SQSTM1 images of immunostaining in rat livers belonging to experiment groups. Histogram graphics of Beclin-1 (B), LC3A/B (C) and P62/SQSTM1 (D) represent the intensity values in percent of immunostaining obtained using Image J software. T bar graph data are expressed as mean ± SEM, and compared by one-way ANOVA and TUKEY's multiple comparisons test (a $P<0.05$ vs. control group; b $P<0.05$ vs. LPS group; c $P<0.05$ vs. 0,2 g/kg API group; d $P<0.05$ vs. 0,4 g/kg API group; e $P<0.05$ vs 0,8 g/kg API group; f $P<0.05$ vs. LPS+0,2 g/kg API group; g $P<0.05$ vs LPS+0,4 g/kg API group; * $P<0.05$ statistically different from all other groups).

In sepsis, organ damage initially progresses to dysfunction without cell death and structural damage. Therefore, it is possible to restore organ function (45). Therefore, in another study we conducted, we investigated the protective role of apilarnil in the LPS-induced sepsis model in liver tissue and observed its positive effects on TLR-4 receptor-associated inflammatory response (34). In the results obtained from the current study, P62 expression increased in the LPS group compared to the control and only apilarnil-treated groups. However, in groups in which apilarnil was administered with LPS, it showed decrease compared to the LPS group. Similarly, LC3A/B expression levels increased statistically in the LPS group compared to the control group and apilarnil-only groups (0.2, 0.4, 0.8 g/kg API). The expression amount of LC3A/B decreased in groups where apilarnil was administered with LPS, although it was not significant. No significant change was observed in Beclin-1 activity. With this result, it can be thought that apilarnil plays a role in the adaptation mechanism by acting on autophagy, LC3A/B and P62 pathways, which occur as a metabolic response to sepsis. Further research is needed to clarify the effects of this role on survival and immune response.

In another study conducted by Carchman et al. (46), adaptation metabolic responses of liver tissue to LPS sepsis model were investigated. Mitochondrial homeostasis and mitophagic pathways have been investigated in relation to the TLR-9 receptor. In the results obtained, it has been reported that TLR-9 receptor and mitophagia play an important role in the adaptation of hepatocytes to sepsis (46). Accordingly, it may be important for future studies to investigate the

effects of apilarnil on mitophagia, which is a more featured pathway of TLR-9 and autophagy, and also on mitochondrial homeostasis, one of the key players of oxidative stress.

In the literature review, there was no study evaluating the effect of apilarnil on autophagy in the LPS-induced sepsis model, and the studies evaluating the effects on autophagy in other bee products are quite limited. We believe that this study will contribute to the literature on this subject.

5. Conclusions

In the light of all this information, it is important to develop alternative therapeutic agents targeting the autophagy pathway against sepsis, which results in high mortality. In this study, we investigated the effect of apilarnil on sepsis-induced autophagy in liver tissue through Beclin-1, LC3A/B and P62 molecules. As a result, apilarnil exhibited different effects in terms of different markers on the autophagy pathway. Apilarnil increases the activity of the autophagy pathway and shows potential positive effects by providing a significant decrease on P62 protein. However, an increase in its effect was observed due to the increased dose. In the light of the findings, apilarnil, which is a natural bee product, can be targeted in further studies as an alternative treatment method by playing a which is a natural bee product, can be targeted in further studies as an alternative treatment method by playing a protective role against sepsis, especially through the LC3A/B and P62 pathways.

Conflict of interest statement

There is no conflict of interest.

Acknowledgement

This work was supported by Yozgat Bozok University Project Coordination Application and Research Center (Project Number: 6602a-TF/20-375).

References

1. Yan J, Li S, Li S. The role of the liver in sepsis. *Int Rev Immunol* **2014**; 33(6): 498-510.
2. Hotchkiss RS, Moldawer LL, Opal SM, Reinhart K, Turnbull IR, Vincent JL. Sepsis and septic shock. *Nat Rev Dis Primers* **2016**; 2: 16045.
3. Maldonado RF, Sa-Correia I, Valvano MA. Lipopolysaccharide modification in Gram-negative bacteria during chronic infection. *FEMS Microbiol Rev* **2016**; 40(4): 480-493.
4. Opal SM. Endotoxins and other sepsis triggers. *Contrib Nephrol* **2010**; 167: 14-24.
5. van der Poll T, van de Veerdonk FL, Scicluna BP, Netea MG. The immunopathology of sepsis and potential therapeutic targets. *Nat Rev Immunol* **2017**; 17(7): 407-420.
6. Cecconi M, Evans L, Levy M, Rhodes A. Sepsis and septic shock. *Lancet* **2018**; 392(10141): 75-87.
7. Sakr Y, Jaschinski U, Wittebole X, et al. Sepsis in Intensive Care Unit Patients: Worldwide Data From the Intensive Care over Nations Audit. *Open Forum Infect Dis* **2018**; 5(12): 313.
8. Woznica EA, Inglot M, Woznica RK, Lysenko L. Liver dysfunction in sepsis. *Adv Clin Exp Med* **2018**; 27(4): 547-551.
9. Nesseler N, Launey Y, Aninat C, Morel F, Malledant Y, Seguin P. Clinical review: The liver in sepsis. *Crit Care* **2012**; 16(5): 235.
10. Srivastava B, Gimson A. Hepatic changes in systemic infection. *Best Pract Res Clin Gastroenterol* **2013**; 27(4): 485-495.
11. Marshall JC. New translational research provides insights into liver dysfunction in sepsis. *PLoS Med* **2012**; 9(11): e1001341.
12. De Nardo D. Toll-like receptors: Activation, signalling and transcriptional modulation. *Cytokine* **2015**; 74(2): 181-189.
13. Kolios G, Valatas V, Manousou P, Xidakis C, Notas G, Kouroumalis E. Nitric oxide and MCP-1 regulation in LPS activated rat Kupffer cells. *Mol Cell Biochem* **2008**; 319(1-2): 91-98.
14. Wang D, Yin Y, Yao Y. Advances in sepsis-associated liver dysfunction. *Burns Trauma* **2014**; 2(3): 97-105.
15. Xu Y, Jagannath C, Liu XD, Sharafkhaneh A, Kolodziejska KE, Eissa NT. Toll-like receptor 4 is a sensor for autophagy associated with innate immunity. *Immunity* **2007**; 27(1): 135-144.
16. Fujita K, Maeda D, Xiao Q, Srinivasula SM. Nrf2-mediated induction of p62 controls Toll-like receptor-4-driven aggresome-like induced structure formation and autophagic degradation. *Proc Natl Acad Sci USA* **2011**; 108(4): 1427-132.
17. Klionsky DJ, Abdelmohsen K, Abe A, et al. Guidelines for the use and interpretation of assays for monitoring autophagy (3rd edition). *Autophagy* **2016**; 12(1): 1-222.
18. Yu L, Chen Y, Tooze SA. Autophagy pathway: Cellular and molecular mechanisms. *Autophagy* **2018**; 14(2): 207-215.
19. Hu W, Chan H, Lu L, et al. Autophagy in intracellular bacterial infection. *Semin Cell Dev Biol* **2020**; 101: 41-50.
20. Feng Y, Liu B, Zheng X, Chen L, Chen W, Fang Z. The protective role of autophagy in sepsis. *Microb Pathog* **2019**; 131: 106-111.
21. Yin X, Xin H, Mao S, Wu G, Guo L. The Role of Autophagy in Sepsis: Protection and Injury to Organs. *Front Physiol* **2019**; 10: 1071.
22. Oami T, Watanabe E, Hatano M, et al. Suppression of T Cell Autophagy Results in Decreased Viability and Function of T Cells Through Accelerated Apoptosis in a Murine Sepsis Model. *Crit Care Med* **2017**; 45(1): 77-85.

23. Ding WX, Yin XM. Mitophagy: mechanisms, pathophysiological roles, and analysis. *Biol Chem* **2012**; 393(7): 547-564.

24. Chang AL, Ulrich A, Suliman HB, Piantadosi CA. Redox regulation of mitophagy in the lung during murine Staphylococcus aureus sepsis. *Free Radic Biol Med* **2015**; 78: 179-189.

25. Baechler BL, Bloemberg D, Quadrilatero J. Mitophagy regulates mitochondrial network signaling, oxidative stress, and apoptosis during myoblast differentiation. *Autophagy* **2019**; 15(9): 1606-1619.

26. Aki T, Unuma K, Uemura K. Emerging roles of mitochondria and autophagy in liver injury during sepsis. *Cell Stress* **2017**; 1(2):79-89.

27. Akçiçek E, Yücel B, . Apiterapi'de Apilarnil. Arı Ürünleri ve Sağlık (Apiterapi). İzmir: Sidas Yayınevi; **2015**.

28. IsİdorovVA, Bakier S, Stocki M. GC-MS investigation of the chemical composition of honeybee drone and queen larva homogenate. *J Apic Res* **2016**; 60(1): 111-120.

29. Silici S. Honeybee Products and Apitherapy. *TURJAF* **2019** 7(9): 1249-1262.

30. Silici S. Chemical Content and Bioactive Properties of Drone Larvae (Apilarnil). *Mellifera* **2019** 19(2):14-22.

31. Meda A, Lamien CE, Millogo J, Romito M, Nacoulma OG. Therapeutic uses of honey and honeybee larvae in central Burkina Faso. *J Ethnopharmacol* **2004**; 95(1): 103-107.

32. Doganyigit Z, Kup FO, Silici S, Deniz K, Yakan B, Atayoglu T. Protective effects of propolis on female rats' histopathological, biochemical and genotoxic changes during LPS induced endotoxemia. *Phytomed* **2013**; 20(7): 632-639.

33. Kanbur M, Eraslan G, Beyaz L, et al. The effects of royal jelly on liver damage induced by paracetamol in mice. *Exp Toxicol Pathol* **2009**; 61(2): 123-132.

34. Doganyigit Z, Okan A, Kaymak E, Pandir D, Silici S. Investigation of protective effects of apilarnil against lipopolysaccharide induced liver injury in rats via TLR 4/HMGB-1/NF-kappaB pathway. *Biomed Pharmacother* **2020**; 125: 109967.

35. Watanabe E, Muenzer JT, Hawkins WG, et al. Sepsis induces extensive autophagic vacuolization in hepatocytes: a clinical and laboratory-based study. *Lab Invest* **2009**; 89(5): 549-561.

36. Sun Q, Gao W, Loughran P, et al. Caspase 1 activation is protective against hepatocyte cell death by up-regulating beclin 1 protein and mitochondrial autophagy in the setting of redox stress. *J Biol Chem* **2013**; 288(22): 15947-15958.

37. Kroemer G, Marino G, Levine B. Autophagy and the integrated stress response. *Mol Cell* **2010**; 40(2): 280-293.

38. Levine B, Kroemer G. Autophagy in the pathogenesis of disease. *Cell* **2008**; 132(1): 27-42.

39. Betin VM, Lane JD. Caspase cleavage of Atg4D stimulates GABARAP-L1 processing and triggers mitochondrial targeting and apoptosis. *J Cell Sci* **2009**; 122(Pt 14): 2554-66.

40. Carchman EH, Rao J, Loughran PA, Rosengart MR, Zuckerbraun BS. Heme oxygenase-1-mediated autophagy protects against hepatocyte cell death and hepatic injury from infection/sepsis in mice. *Hepatology* **2011**; 53(6): 2053-2062.

41. Puissant A, Fenouille N, Auberger P. When autophagy meets cancer through p62/SQSTM1. *Am J Cancer Res* **2012**; 2(4): 397-413.

42. Lazova R, Camp RL, Klump V, Siddiqui SF, Amaravadi RK, Pawelek JM. Punctate LC3B expression is a common feature of solid tumors and associated with proliferation, metastasis, and poor outcome. *Clin Cancer Res* **2012**; 18(2): 370-379.

43. Komatsu M, Kurokawa H, Waguri S, et al. The selective autophagy substrate p62 activates the stress responsive transcription factor Nrf2 through inactivation of Keap1. *Nat Cell Biol* **2010**; 12(3): 213-223.

44. Chen C, Deng M, Sun Q, Loughran P, Billiar TR, Scott MJ. Lipopolysaccharide stimulates p62-dependent autophagy-like aggregate clearance in hepatocytes. *Biomed Res Int* **2014**; 2014: 267350.

45. Waltz P, Carchman EH, Young AC, et al. Lipopolysaccaride induces autophagic signaling in macrophages via a TLR4, heme oxygenase-1 dependent pathway. *Autophagy* **2011**; 7(3): 315-320.

46. Carchman EH, Whelan S, Loughran P, et al. Experimental sepsis-induced mitochondrial biogenesis is dependent on autophagy, TLR4, and TLR9 signaling in liver. *FASEB J* **2013**; 27(12): 4703-4711.

Authors' ORCID

Züleyha Doğanyiğit
http://orcid.org/0000-0002-6980-3384
Betül Köklü
http://orcid.org/0000-0003-3477-3290
Arda Üner
http://orcid.org/0000-0002-9657-7757
Aslı Okan
http://orcid.org/0000-0001-8152-7338
Emin Kaymak
http://orcid.org/0000-0002-3818-2693
Sibel Silici
http://orcid.org/0000-0003-2810-2917

https://dergipark.org.tr/tr/pub/ntms

ISSN: 2717-8161 RESEARCH ARTICLE

New Trend Med Sci 2020; 1(2): 90-93. https://dergipark.org.tr/tr/pub/ntms

The Effect of COVID-19 on Autologous Cord Blood and Cord Tissue Banking in Turkey: a Cross-Sectional and Retrospective Study

Durmuş Burgucu[1*]

[1]Technopark Babylife Cord Blood Bank and Human Cell-Tissue Production Center, Akdeniz University, 07070, Antalya, Turkey

Article History
Received 17 Aug 2020
Accepted 03 Sep 2020
Published Online 30 Sep 2020

[*]***Corresponding Author***
Dr Durmuş Burgucu
Technopark Babylife Cord Blood Bank
and Human Cell-Tissue Production Center,
Akdeniz University,
07070, Antalya, Turkey,
Phone: +90 242 226 16 80
Fax: +90 242 226 16 79
E-mail: dburgucu@akdeniz.edu.tr
ORCID: https://orcid.org/0000-0003-3980-982X

Abstract: Since 1988, when cord blood was used for the first time in bone marrow transplant, over 35,000 units of cord blood have been used successfully. The collection, transfer, processing, and cryopreservation of cord blood and cord tissues have been defined by standardized protocols. There is limited data on autologous cord blood and cord tissue banking in extraordinary cases such as pandemics. Apart from the measures adopted at the global level in the fight against a pandemic, there may be varying practices at the national level. These differences are due to factors such as human behaviors, opportunities to access medical care, number of healthcare professionals, infrastructure of the healthcare institutions, and timing of the measures in different societies. The aim of this study was to retrospectively evaluate the effects of the measures adopted to fight COVID-19 pandemic on autologous cord blood and cord tissue banking in the three-month period following the first case in Turkey. The study was planned as a cross-sectional and retrospective study. The information about the cord blood collected was retrieved from the data recording software called KORDDATA and analyzed at our center. SPSS 21 software was used for statistical analysis. $P<0.05$ was considered statistically significant for the Mann–Whitney U test result. Quantities, transfer times, viability rates, and microbiological contamination rates of cord tissues and cord blood delivered to our center for storage purposes were evaluated and compared with the data from the period of 3 months during which there were no cases. Due to the measures adopted and the restrictions imposed, transfer times were prolonged, but no negative effects were observed on viability and microbiological contamination rates. This result shows that autologous cord blood and cord tissue banking can continue smoothly in Turkey during the pandemic.

Keywords: Cord Blood, COVID-19, Cord Tissue.

1. Introduction

Cord blood is the blood contained in the umbilical cord tissue, which is 10 to 50 cm long and located after the placenta, which ensures the exchange of gas and nutrients between the mother and the baby until the time of delivery (1). It can be collected from the umbilical vein in volumes of 20 to 200 ml varying from individual to individual (2). Cord blood has been a preferred source of stem cells as well as due to its other

Cite this article as: Burgucu D. The Effect of COVID-19 on Autologous Cord Blood and Cord Tissue Banking in Turkey: a Cross-Sectional and Retrospective Study, *New Trend Med Sci* **2020**; 1(2): 90-93.

uses, especially in hematopoietic stem cell transplantation and in regenerative medicine applications (3-4). Collection, transfer, processing, and cryopreservation of cord blood have been defined by standardized protocols (5). There are over 100 banks in the world. Approximately 5 million units of cord blood are preserved in these centers (6). The situation in our country has been structured such that there is one center for every 10 million people, and while one of the banks is engaged in public type banking, the others are predominantly engaged in autologous banking. In the literature, banking models have been classified into three types: public type, autologous or family-type banking model, and hybrid model (7). In the hybrid model, autologous banks also store products for allogeneic use free of charge (as in the public type). This type of banking model has been cited in the literature as the "Turkish model" (8).

Coronaviruses are enveloped RNA viruses. In general, they cause respiratory, enteric, hepatic, and neurological diseases in humans, other species of mammals, and birds. There are several members of the Coronavirus family (9). The latest type, which was first seen in China, has spread around the world and caused the pandemic and has been named as COVID-19. As per clinical presentation, COVID-19 can be asymptomatic and can also cause severe fatal manifestations in the form of septic shock and multiple organ dysfunction (10).

The measures adopted by the countries and consequent human behaviors, opportunities to access medical care, number of healthcare professionals, infrastructure of the healthcare institutions, and timing of the measures have been the key determining factors in the fight against the pandemic. The aim of this study is to retrospectively evaluate the efficacy of the measures adopted to control the COVID-19 pandemic on autologous cord blood and cord tissue banking in the period of three months following the first case in Turkey. For this purpose, quantities, transfer times, viability rates, and microbiological contamination rates of cord tissues and cord blood delivered to our center for storage purposes were evaluated and compared with the data from the period of three months during which there were no cases.

2. Material and Methods

The study was planned as a cross-sectional and retrospective study. The information about the cord blood collected was retrieved from the data recording software called KORDDATA and analyzed. Approval for the study was obtained from the Ethics Committee of Akdeniz University Faculty of Medicine (decision number: 147-date: 21.02.2018). SPSS 21 software was used for statistical analyses. $P<0.05$ was considered statistically significant for the Mann-Whitney U test result.

3. Results

There were 179 applications for cord blood and 83 applications for cord tissue to our center for autologous banking services before the pandemic and 159 applications for cord blood and 67 applications for cord tissue after the pandemic. The applications were made for 95 baby boys and 84 baby girls before the pandemic and for 78 baby boys and 81 baby girls after the pandemic. Considering the method of delivery, 40 physiological births and 139 cesarean births were found in the applications before the pandemic and 29 physiological births and 130 cesarean deliveries after the pandemic.

The transfer times of blood and tissues to the laboratory after they were collected are provided in Figure 1. After the pandemic (3-month period after the first case), the transfer time significantly increased compared to the 3-month period before the first case (before the pandemic) due to measures adopted throughout the country (mean transfer times are 23.8 hours and 31.3 hours, respectively).

It was investigated whether the increase in transfer times of blood and tissues after the pandemic had an effect on bacterial contamination rate. There was no increase in contamination rates in the period after the pandemic, as shown in Figure 2. On the contrary, even though the transfer time was prolonged, a significant decline was found in the contamination rate (1.6% and 0.6%, respectively).

Finally, when it was examined whether the increase in transfer times of blood samples had a negative effect on viability; no significant decline was detected as shown in Figure 3 (Viability: 98.2% and 97.5%, respectively).

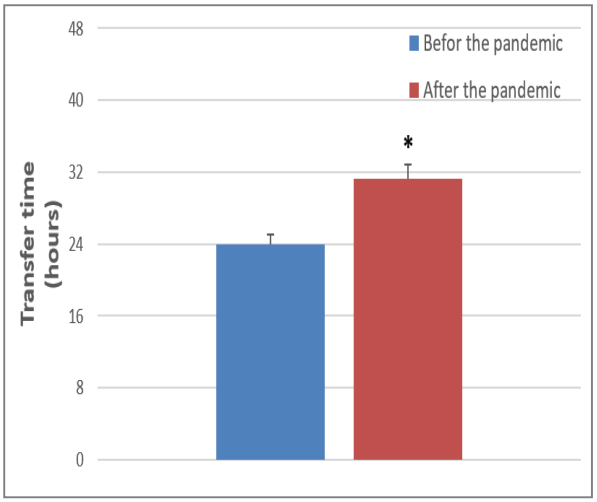

Figure 1: Transfer times of blood and tissue samples to the laboratory in the 3-month periods before and after the pandemic (cord blood n=179, cord tissue n=83 before the pandemic, cord blood n=159, cord tissue n=67 after the pandemic) (*$P<0.05$ value according to the Mann-Whitney U test).

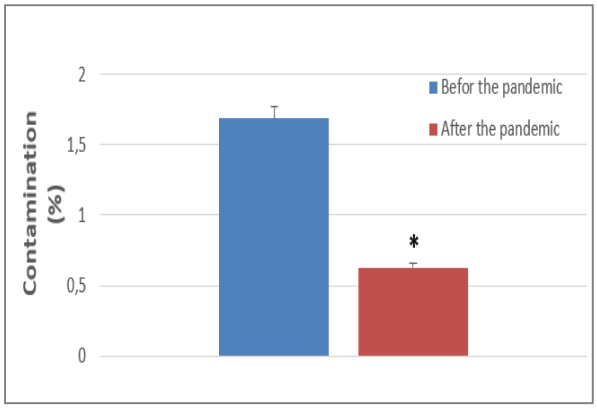

Figure 2: Microbiological contamination rates of blood and tissue samples in the 3-month periods before and after the pandemic (cord blood n=179, cord tissue n=83 before the pandemic, cord blood n=159, cord tissue n=67 after the pandemic) (*P<0.05 value according to the Mann–Whitney U test).

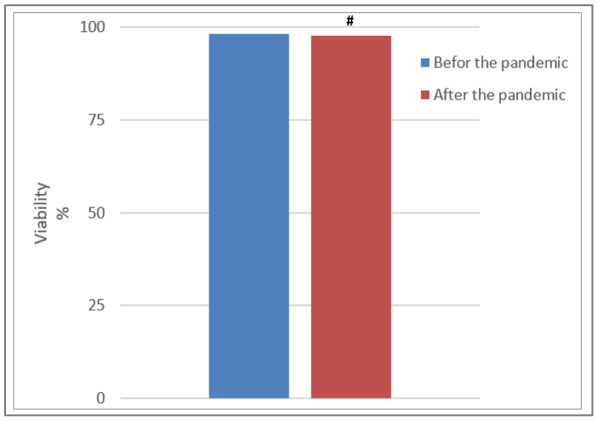

Figure 3: Viability rates of blood samples in the 3-month periods before and after the pandemic (cord blood n=179 before the pandemic, cord blood n=159 after the pandemic) (#P>0.05 value according to the Mann-Whitney U test).

4. Discussion

Although they are usually in the background, biobanks play a crucial role in the diagnosis and treatment of both infectious diseases and other diseases. The collection, transfer, and storage of biological materials are among the determining steps in the fight against important public health problems such as pandemics (11). Cord blood banks are biobanks that are particularly involved in hematopoietic stem cell transplantation. In patients infected with the COVID-19 virus, mesenchymal stem cell applications were performed at the clinical trial level. In addition, studies that accept new patients are ongoing. The aim is to ensure that especially patients who are treated with a clinical presentation of severe pneumonia benefit from the immunomodulatory effects. Data on cellular therapy in the pandemic, which began in November 2019 in China, are extremely limited. It is believed that both the number of patients and the number of clinical trials will tend to increase in the following days. In the initial mesenchymal stem cell studies, cells derived from the human umbilical cord were used (10). The important reason why mesenchymal stem cells are preferred here is that they are cryopreserved and ready to be used in case of need and the tissues are easy to reach. The measures adopted in Turkey included closure of schools, travel restrictions between cities, early initiation of treatment, contact tracing, and partial curfews (12). Transfer time is an important step in cord blood and cord tissue banking; revealing the impact of the restrictions and stringent controls imposed on land and air travel due to the pandemic can contribute to the creation of new knowledge and ideas in the field of bio banking. In the present study, transfer time was determined as an important parameter in the findings. Air transport was restricted due to the pandemic. Accordingly, the burden on the cargo companies in the supply chain and extremely restricted land transfers have been identified as important variables. The cord blood banking regulation states that the blood collected must reach the laboratory and start to be processed within 48 hours of collection (13). There are studies, although limited, related to the collection of cord blood and the time elapsed during the processing stages. The relationships between 72-hours, 96-hours cold chain, room temperature, and viability values were examined (14). However, these studies were not conducted under any pandemic conditions but during an ordinary period. In the present study, only samples that reached the laboratory within a period in accordance with the regulations were processed and those with cellular and microbiological quality control tests within limits were placed in permanent storage. Although the transfer times of the samples were prolonged, no increase was found in the microbiological contamination rate; on the contrary, a significant decrease was observed. This result may be a reflection of the emphasis placed on hand hygiene, which is an important factor in the fight against the pandemic. Apart from this, although the transfer time was prolonged, there was no significant decline in the viability values, which indicates that although there are certain limitations, these limitations

do not have a negative impact on autologous cord blood banking.

5. Conclusions

In extraordinary periods such as pandemics, autologous tissue and cell banking can be maintained smoothly in Turkey.

Conflict of interest statement

There is no conflict of interest.

Acknowledgement

I would like to thank statistician Ezgi Afşar Gür for her contributions to statistical analyses and Antalya Teknokent Babylife Özel Sağlık Yatırımları San. Tic. A.Ş. for providing the laboratory infrastructure.

References

1. Gluckman E. Umbilical cord blood biology and transplantation. *Curr Opin Hematol* **1995**; 2(6): 413-416.
2. M-Reboredo N, Diaz A, Castro A, Villaescusa RG. Collection, processing and cryopreservation of umbilical cord blood for unrelated transplantation. *Bone Marrow Transpl* **2000**; 26(12): 1263-1270.
3. Iafolla MA, Thai J, Allan DS. Transplantation of umbilical cord blood-derived cells for novel indications in regenerative therapy or immune modulation: a scoping review of polystudies. *Biol Blood Marrow Transpl* **2014**; 20(1): 20-25.
4. Broxmeyer HE. Enhancing the efficacy of engraftment of cord blood for hematopoietic cell transplantation. *Transfus Apher Sci* **2016**; 54(3): 364-372.
5. Model Criteria for Regulation of Cord Blood Banks and Cord Blood Banking: Adopted by the Cord Blood Association, Board of Directors, *Stem Cells Transl Med* **2019**; 8(4): 340-343.
6. Mayani H, Wagner JE, Broxmeyer HE. Cord blood research, banking, and transplantation: achievements, challenges, and perspectives. *Bone Marrow Transpl* **2020**; 55(1): 48-61.
7. Narayanan DL, Phadke SR. Concepts, Utility and Limitations of Cord Blood Banking: What Clinicians Need to Know. *Indian J Pediatricians* **2019**; 86(1): 44-48.
8. Dessels C, Alessandrini M, Pepper MS. Factors Influencing the Umbilical Cord Blood Stem Cell Industry: An Evolving Treatment Landscape. *Stem Cells Transl Med* **2018**; 7(9): 643-650.
9. Siddell S, Wege H, Ter Meulen V. The biology of coronaviruses. J Gen Virol 1983; 64(Pt 4): 761-776.
10. Atluri S, Manchikanti L, Hirsch JA. Expanded Umbilical Cord Mesenchymal Stem Cells (UC-MSCs) as a Therapeutic Strategy in Managing Critically Ill COVID-19 Patients: The Case for Compassionate Use. *Pain Phys* 2020; 23(2): 71-83.
11. Vaught J. Biobanking During the COVID-19 Pandemic. *Biopreserv* **2020**; 18(3).
12. Demirbilek Y, Pehlivantürk G, Özgüler ZÖ, Alp Oak E. COVID-19 outbreak control, example of ministry of health of Turkey. *Turk J Med Sci* **2020**; 50(L-1): 489-494.
13. Brand A, Rebulla P, Engelfriet CP, et al. Cord blood banking. *Vox Sang* **2008**; 95(4): 335-348.
14. Guttridge MG, Soh TG, Belfield H, Sidders C, Watt SM. Storage time affects umbilical cord blood viability. *Transfusion* **2014**; 54(5): 1278-1285

Author' ORCID

Durmuş Burgucu

http://orcid.org/0000-0003-3980-982X

https://dergipark.org.tr/tr/pub/ntms

ISSN: 2717-8161 RESEARCH ARTICLE

New Trend Med Sci 2020; 1(2): 94-99. https://dergipark.org.tr/tr/pub/ntms

Effect of Cornus Mas l. Extract on Organs in Rats Given Nicotine

Seher Yılmaz[1*], Adem Tokpınar[1], Şükrü Ateş[1], Ünal Öztekin[2], Şerife Alpa[3], Ayşe Yeşim Göçmen[4]

[1]Department of Anatomy, Faculty of Medicine, Yozgat Bozok University, Yozgat, Turkey
[2]Department of Urology, Faculty of Medicine, Yozgat Bozok University, Yozgat, Turkey
[3]Department of Anatomy, Faculty of Medicine, KTO Karatay University, Konya, Turkey
[4]Department of Biochemistry, Faculty of Medicine, Yozgat Bozok University, Yozgat, Turkey

Article History
Received 24 July 2020
Accepted 29 Aug 2020
Published Online 30 Sep 2020

****Corresponding Author***
Dr Seher Yılmaz
Department of Anatomy,
Faculty of Medicine,
Yozgat Bozok University,
Yozgat, 66100, Turkey,
Phone: +903542126201-2686,
Fax: +90 354 4375285
E-mail:seher.yilmaz@bozok.edu.tr
ORCID:http://orcid.org/0000-0003-4551-995X

Abstract: Nicotine plays an important role in oxidative stress formation. For this purpose, to reveal the antioxidant effect of cornelian cherry plant, the effects of nicotine-induced oxidative stress. 28 adult Wistar Albino (180-220 g) male rats were used in the study. Rats were divided into four groups as control group (n=6), cornelian cherry group (n=7), nicotine group (n=7) and nicotine+cornelian cherry group (n=8). While nicotine extract was applied to the experimental group, cornelian cherry extract was applied to the treatment group as well as nicotine. TBARS, SOD, GSH, GSSG, TOS, TAS, Redox potential values were measured by spectrophotometric analysis in lung, brain, kidney, heart and liver tissues. OSI and GSH/GSSG values were calculated as TOS/TAS and GSH/GSSG rates, respectively. When the experimental groups are examined, it is seen that there is a significant difference between the nicotine-treated group and the other groups ($p<0.05$). Its effects on lung, brain, kidney, heart and liver tissues are seen biochemically. Especially when the TAS value is examined, a significant difference is observed in the Nicotine group compared to other groups ($p<0.05$). Cornelian cherry is understood to be an important plant with antioxidant properties against nicotine by increasing TAS level against oxidative stress formation.

Keywords: Cornelian Cherry, Cornus Mas L., Nicotine, Oxidative Stress.

1. Introduction

Smoking is one of the biggest risk factors for the development of cancer, lung and cardiovascular diseases (1). Epidemiological studies have shown that smoking across the community is the most important risk factor for coronary heart disease and cardiovascular diseases (2). Smoking causes serious health problems by increasing the risk of thrombosis, atherosclerosis and death (3). In addition, the loss of productivity caused by it is considered as a public health problem (4).

There is usually 0.6-2 mg of nicotine in a single cigarette (5). Nicotine is one of the important chemicals in tobacco addiction (6). Tobacco consumption through smoking is known to promote a high level of free radical production in individuals. Free radicals oxidize proteins, lipids and DNA, leading to tissue damage (8). Exposure to cigarette smoke causes interleukins (IL-6) and myocardial inflammation in diabetes models through fibrosis, lipid peroxide and nitrite formation (9).

Cite this article as: Yılmaz S, Tokpınar A, Ateş Ş, Öztekin Ü, Alpa Ş and Göçmen AY. Effect of Cornus Mas l. Extract on Organs in Rats Given Nicotine, *New Trend Med Sci* **2020**; 1(2): 94-99.

Herbal extracts are widely used in complementary medicine (16). Cornelian cherry fruits are grown in some countries of Europe and West Asia (11). Fruits are usually dark or reddish, and sometimes pink and yellow. It is very beneficial nutritionally and is consumed as jam, liqueur and wine (10). *Cornus Mas L.* is rich in natural flavonoids, vitamins, phenolic acids and carotenes and is considered an antioxidant plant. It is also used in modern medicine as antimicrobial, anti-inflammatory, cardioprotective (12). Previous studies have shown that cornelian cherry plants have antioxidant and anti-carcinogenic effects (13).

Oxidative stress is one of the main causes of embryonal development disorders (15). Factors such as oxidative stress and inflammation are held responsible for the development of cardiovascular diseases (7). Oxidative stress is defined as an increase in oxidants or a decrease in functionally antioxidants. Therefore, antioxidant levels are important. In addition, oxidative stress plays an important role in cancer diseases and cancer's pathogenesis (13).

Total antioxidant status (TAS) is measured to determine overall antioxidant status. Total oxidant status is also measured (TOS). To assess the net oxidative stress in the organism, the oxidative stress index (OSI) is measured. OSI value is calculated by the ratio of TOS to TAS (13, 14).

Cornelian cherry (*Cornus mas L.*) belongs to the Umbelliferae Cornaceae family, is a type of fruit that sheds leaves in winter and can grow up to 7-8 meters (10). Turkey, many fruit species and different genotypes of these species has extremely important in terms of hosting ecology. *Cornus mas L.* is known as an herb with an effective antioxidant, antidiabetic and anti-inflammatory effects. Other studies have shown that *Cornus mas L.* is a powerful antioxidant and has an anti-carcinogenic effect (13).

2. Material and Methods

2.1. Experimental Design and Laboratory Animals Groups

28 adult Wistar Albino (180-220 g) male rats were included in the study. Rats were handled according to institutional guidelines and the Guide for Care and Use of Laboratory Animals of the National Research Council. The entire study was carried out according to 1986 Strasbourg Universal Declaration on Animal Welfare and was done with the approval of the ethics committee (2019 HADYEK-31). Free access to food and drinking water was provided for the compatibility of the animals to the laboratory 1 week before the experiment. Cages for animals' welfare were regularly ventilated and cleaned routinely. The animals were housed in a temperature control room (20-23 ºC) with a light/dark cycle of 12 hours throughout the experiment.

2.2. Experimental Groups

Control group (C) (n=6): During the experiment, 0.9% saline was applied once daily by subcutaneous (sc) injection.

Cornus Mas L. Group (CML) (n=7): 800 mg/kg *Cornus Mas L.* extract was given with gavage.

Nicotine group (N) (n=7): 4 mg/kg nicotine was given (sc).

Nicotine+Cornus Mas L. group (N+CML) (n=8): 4 mg/kg nicotine+800 mg/kg *Cornus Mas L.* extract was given.

These practices were carried out to all groups for 35 days.

2.3. Antioxidant indices and cytokines measurements

Activities of superoxide dismutase (SOD), catalase (CAT) and glutathione peroxidase (GPx) and the levels of glutathione (GSH) and glutathione disulfide (GSSG) were measured in blood and tissue samples by the modified methods (20). Colorimetric kits were used to measure the levels of total anti-oxidative status (TAS), total oxidative status (TOS) and Thiobarbituric Acid Reactive Substances/malondialdehyde (TBARS/MDA). Each sample was analyzed in duplicate. Glutathione content was calculated using the formula GSH=T-GSH-(2×GSSG).The levels of GSH was calculated by the formula: GSH=GSHt-2×GSSG. The results of GSHt, GSH, and GSSG were normalized to the total protein content and were expressed as nmol of GSH or GSSG per mg of protein (nmol GSH/mg protein or nmol GSSG/mg protein). Oxidative stress index (OSI) value was calculated using the formula: OSI=[TOS (μmol H_2O_2 equiv./l)/TAS (μmol trolox equiv./l)×100]. Commercial enzyme-linked immunosorbent (ELISA) assay kits were used to measure the serum levels of cytokines (IL-6, TNF-α (Elabscience, MD, USA)).

2.4. Statistical Analysis

The statistical analysis on the obtained data was carried out on the computer using IBM SPSS 22.0 program. In the data obtained, 5 parameters were evaluated (kurtosis, skewness, mean-standard deviation ratio, Gauss curve, Shapiro-Wilko test and normal distribution analysis). Since all 5 parameters scored 3.5 and above, it was accepted that our data was normally distributed and parametric tests were applied. In statistical analysis, $\alpha=0.05$ was taken and $p<\alpha$ was considered statistically significant, while $p>\alpha$ was considered statistically insignificant.

3. Results

The results of biochemical analysis on oxidative stress parameters and antioxidant enzymes according to groups in lung, brain, kidney, heart, liver tissues taken from rats are given in the tables below.

When we examine the biochemical values, there is a significant difference in SOD, GPx, TAS, OSI, GSH/GSSG, Redox potential values between Nicotine+Cornus Mas L. group and other groups.
There is also a significant difference between the Nicotine group and other groups when looking at TBAS, SOD, GPx, TAS, OSI, GSH, GSSG, GSH/GSSG and Redox potential values. It is observed that lung tissue is biochemically affected in groups given nicotine (Table 1).

According to the results of biochemical analysis on brain tissue, TBARS, CAT, GPx, TAS, TOS, OSI and GSSG values of the Nicotine group had a statistically significant difference from other groups. TBARS values of Control, Cornus Mas L. and Nicotine+Cornus Mas L. groups were statistically similar, while TBARS of Nicotine group was significantly different from other groups.

Table 1. Cornelian cherry effect on lung tissue in groups given nicotine.

Parameters/Groups	C	CML	N	N+CML
TBARS	4.03±0.19^{a}	3.84±0.12^{a}	5.02±0.58^{b}	3.86±0.34^{a}
SOD	9.08±0.39^{a}	9±0.28^{a}	13.43±0.34^{b}	12.6±0.3^{c}
CAT	52.9±3.47^{a}	44.97±1.37^{b}	52.15±1.6^{a}	47±1.26^{b}
GPx	6.55±0.16^{a}	6.25±0.11^{a}	10.11±0.43^{b}	8.03±0.26^{c}
TAS	0.95±0.03^{a}	0.97±0.07^{a}	0.57±0.02^{b}	0.7±0.03^{c}
TOS	3.82±0.09^{a}	4.25±0.07^{a}	5.27±0.96^{b}	4.47±0.28^{a}
OSI	0.4±0.01^{a}	0.44±0.02^{a}	0.92±0.18^{b}	0.63±0.05^{c}
GSH	5.68±0.13^{a}	5.72±0.09^{a}	4.48±0.49^{b}	5.36±0.24^{a}
GSSG	0.87±0.05^{a}	0.85±0.01^{a}	1.52±0.24^{b}	0.99±0.13^{a}
GSH/GSSG	4.5±0.26^{a}	4.71±0.05^{a}	1.02±0.72^{b}	3.5±0.77^{c}
Redox potential	-71.01±0.28^{ac}	-71.53±0.22^{a}	-57.66±3.76^{b}	-67.95±2.34^{c}

P<0.05 was considered statistically significant. Data are expressed as Mean±Standard Deviation.The same letter indicates similarity between groups, different letters indicate differences between groups (C: Control group, CML: Cornus Mas L. group, N: Nicotin group, N+CML: Nicotine+Cornus Mas L. group).

Table 2. Cornelian cherry effect on brain tissue in groups given nicotine.

Parameters/Groups	C	CML	N	N+CML
TBARS	3.36±0.17^{a}	3.25±0.26^{a}	3.88±0.11^{b}	3.24±0.16^{a}
SOD	13.84±0.83^{a}	12.4±0.46^{b}	12.61±0.86^{b}	14.4±0.98^{a}
CAT	7.88±0.87^{a}	6.5±0.33^{b}	3.79±0.86^{c}	6.14±0.89^{b}
GPx	25.34±1.73^{ac}	24.38±0.32^{a}	31.45±1.34^{b}	26.07±1.4^{c}
TAS	1.02±0.05^{a}	1.05±0.07^{a}	0.49±0.03^{b}	0.96±0.06^{a}
TOS	7.19±0.92^{a}	7.19±0.33^{a}	11.49±1^{b}	9.08±0.24^{c}
OSI	0.7±0.11^{ac}	0.68±0.04^{a}	2.34±0.3^{b}	0.94±0.05^{c}
GSH	6.68±1.59^{a}	4.93±0.56^{b}	4.01±0.72^{b}	4.71±0.2^{b}
GSSG	0.4±0.04^{a}	0.4±0.01^{a}	0.61±0.03^{b}	0.53±0.06^{c}
GSH/GSSG	14.64±4.71^{a}	10.26±1.65^{b}	4.57±1.29^{b}	6.9±1.12^{b}
Redox potential	-84.56±7.31^{a}	-77.29±3.06^{b}	-66.27±4.78^{c}	-72.6±1.63^{bc}

P<0.05 was considered statistically significant. Data are expressed as Mean±Standard Deviation.The same letter indicates similarity between groups, different letters indicate differences between groups.

Table 3. Cornelian cherry effect on kidney tissue in groups given nicotine.

Parameters/Groups	C	CML	N	N+CML
TBARS	2.91±0.26^{a}	3.21±0.27^{a}	3.62±0.25^{b}	3.03±0.28^{a}
SOD	22.26±0.2^{a}	20.06±0.73^{b}	21.87±1.58^{ac}	20.44±1.27^{bc}
CAT	23.82±0.46^{a}	20.3±0.78^{a}	33.91±5.31^{b}	33.55±5.02^{b}
GPx	70.26±2.53^{a}	66.87±1.4^{a}	87.91±9.72^{b}	73±2.96^{a}
TAS	1.38±0.05^{a}	1.41±0.12^{a}	1.1±0.15^{b}	1.08±0.06^{b}
TOS	0.57±0.06^{a}	0.6±0.06^{ab}	0.69±0.11^{b}	0.7±0.05^{b}
OSI	0.04±0^{a}	0.04±0^{a}	0.06±0.01^{b}	0.06±0^{b}
GSH	5.14±0.99^{a}	3.88±0.19^{b}	4.36±0.74^{ab}	4.38±0.3^{ab}
GSSG	1.64±0.15^{a}	1.48±0.32^{a}	1.79±0.29^{a}	1.71±0.22^{a}
GSH/GSSG	1.15±0.78^{a}	0.71±0.48^{a}	0.45±0.38^{a}	0.57±0.23^{a}
Redox potential	-59.77±5.88^{a}	-54.46±2.20^{b}	-54.58±3.44^{ab}	-55.47±1.51^{ab}

P<0.05 was considered statistically significant. Data are expressed as Mean±Standard Deviation.The same letter indicates similarity between groups, different letters indicate differences between groups.

Table 4. Cornelian cherry effect on heart tissue in groups given nicotine.

Parameters/Groups	C	CML	N	N+CML
TBARS	2.89±0.19[a]	3.09±0.25[a]	3.63±0.24[b]	31±0.24[a]
SOD	15.5±0.49[a]	14.34±0.48[b]	17.13±0.84[c]	16.2±0.87[ac]
CAT	12.6±0.66[a]	10.8±0.36[a]	18.1±2.86[b]	16.12±3.11[b]
GPx	31.36±0.98[a]	30.07±0.54[a]	39.29±4.38[b]	32.78±1.34[a]
TAS	1.53±0.03[a]	1.57±0.12[a]	1.22±0.17[b]	1.2±0.07[b]
TOS	7.35±0.46[a]	9.08±0.68[b]	10.69±1.02[c]	9.19±0.9[b]
OSI	0.48±0.03[a]	0.57±0.04[b]	0.88±0.07[c]	0.76±0.06[d]
GSH	3.81±0.13[a]	3.21±0.53[ab]	2.49±0.8[b]	3.59±0.19[a]
GSSG	0.56±0.05[a]	0.5±0.1[a]	0.69±0.05[b]	0.58±0.08[ab]
GSH/GSSG	4.79±0.44[a]	4.73±1.96[a]	1.68±1.51[b]	4.28±0.9[a]
Redox potential	-66.38±0.47[a]	-63.3±6.24[a]	-51.66±8.32[b]	-64.48±2.58[a]

P<0.05 was considered statistically significant. Data are expressed as Mean±Standard Deviation.The same letter indicates similarity between groups, different letters indicate differences between groups.

Table 5. Cornelian cherry effect on liver tissue in groups given nicotine.

Parameters/Groups	C	CML	N	N+CML
TBARS	3.07±0.13[a]	3.62±0.25[b]	4.2±0.2[c]	3.73±0.18[b]
SOD	20.77±0.15[a]	18.32±0.68[b]	14.78±0.72[c]	19.95±0.55[a]
CAT	25.19±0.29[a]	21.49±0.83[b]	11.34±0.99[c]	21.53±0.85[b]
GPx	21.06±0.65[a]	20.15±0.46[a]	20.1±1.69 [a]	19.64±0.8 [a]
TAS	1.46±0.01[a]	1.5±0.12[a]	0.51±0.07[b]	0.94±0.18[c]
TOS	8.79±0.67[a]	8.12±1.51[a]	14.84±2.46[b]	13.22±0.54[b]
OSI	0.59±0.05[a]	0.54±0.1[a]	2.94±0.7[b]	1.43±0.21[c]
GSH	10.33±0.53[a]	8.95±1.53[a]	7.02±1.04[b]	9±0.33[a]
GSSG	2.51±0.13[a]	2.29±0.5[a]	3.13±0.33[b]	2.41±0.15[a]
GSH/GSSG	2.11±0.31[a]	2.1±1.19[a]	0.29±0.6[b]	1.74±0.37[a]
Redox potential	-72.82±1.6[a]	-70.21±6.27[a]	-59.73±5.14[b]	-69.76±1.68[a]

P<0.05 was considered statistically significant. Data are expressed as Mean±Standard Deviation.The same letter indicates similarity between groups, different letters indicate differences between groups.

There was no significant difference in GSH, GSH/GSSG and Redox potential biochemical values in the brain dox between the Nicotine group and the Nicotine+Cornus Mas L. group (Table 2).

When kidney tissue was examined, there was a significant difference between the Nicotine group and other groups in terms of TBARS and GPx values. There was no statistically significant difference in SOD, CAT, TAS, TOS, OSI, GSH, GSSG, GSH/GSSG and Redox potential values between the Nicotine group and the Nicotine+Cornus Mas L group. The effect of cornelian cherry plant on the specified biochemical values in kidney tissue has not been observed (Table 3).

In heart tissue biochemical analysis, the TBARS, GPx, TOS, OSI, GSH/GSSG and Redox potential values of the Nicotine group were statistically different compared to the other groups. There is a significant difference between the Nicotine group and the Nicotine+Cornus Mas L group in TBARS, GPx, TOS, OSI, GSH, GSH/GSSG and Redox potential values (Table 4).

Except for the GPx and TOS values of the nicotine group, all values have a statistically significant difference from those of the other groups. As a result of the data obtained, the negative effect of nicotine on liver tissue is clearly seen (Table 5).

GPx (Glutathione peroxidase) is an antioxidant enzyme localized in the cytosol and mitochondria matrix. In our study, GPx level in kidney, lung, brain and heart had a significant difference between nicotine group and other groups.

4. Discussion

Nicotine is an important toxic component of cigarette smoke, has devastating and malignant consequences (19). Smoking is among the most important risk factors for diseases such as coronary diseases, chronic obstructive pulmonary disease and lung cancer.

Since the lung is the main organ exposed to cigarette smoke and is the main region of nicotine absorption, it has been accepted as a highly sensitive organ against the toxic effect and free radical formation of nicotine (20).

It is known that antioxidants taken from plants contribute to the defense system against oxidative stress. Thus, they can protect cells against oxidative damage and prevent chronic diseases (22).

The decrease in antioxidant enzyme activities (SOD, CAT and GPx) and increase in peroxidation reactions in the liver show oxidative stress in animals exposed to nicotine (23). To reduce the toxicity of nicotine, cellular antioxidant enzymes are produced for defense purposes. Thus, inhibition of enzymes, lipid peroxidation and gene expression in rats exposed to nicotine changes and leads to cell death (25).

In our study, it was investigated whether nicotine in rats caused biochemical changes on heart, brain, liver, kidney and lung tissue and whether cornelian cherry plant had any role in response to this effect. Seher et al., in their study, they investigated the effect of cornelian cherry plant in mice with ehrlich solid tumor and reached the conclusion that TAS, GSH and SOD values were lower in all tissues of the tumor group compared to the control group (13). The plant extract (curcumin 50 mg/kg) used in the study by Mustafa et al., appears to increase CAT activity in the kidney (17).

The SOD enzyme is found in excessive amounts in the liver, adrenal gland, kidney, spleen and erythrocytes, where oxygen pressure is high (18). Therefore, in our study, we examined SOD values in kidney and liver. SOD value in liver was lower in nicotine group compared to other groups and there was a significant difference between other groups. In kidney, SOD value was significantly lower in nicotine group compared to control group. In study by Dhouib et al. there is an increase in CAT and SOD values in the lung tissue in the group given nicotine (21). It shows similar results with our study.

In another study, Karafakioğlu et al. stated that there was a significant decrease in erythrocyte levels compared to the control group and that erythrocytes were vulnerable to oxidative stress (26). In their study on diabetic rats, Karabulut et al. stated that myocardial damage due to oxidative stress was caused by insufficient reactive oxygen production (27). In our study, the TBARS level in the heart tissue of the group given nicotine was calculated as 3.63±0.24. Accordingly, nicotine appears to cause oxidative stress in the heart. In another study, it was observed that oxidative stress decreased antioxidant enzyme activities in liver damage caused by Lipopolysaccharide (LPS) (28). In our study, it is seen that SOD and CAT decreased in nicotine group compared to other groups, and increased TBARS value. Thus, nicotine appears to increase oxidative stress in the liver.

Oxidative stress is an important phenomenon expressed by excessive accumulation of TBARS (24). In our study, 5.02±0.58 in TBARS lung tissue in nicotine group; 4.2±0.2 in liver tissue; 3.63±0.24 in the heart; 3.62±0.25 in kidney; and it was found to be 3.88±0.11 in the brain. Thus, the high TBARS values of nicotine groups indicate that nicotine causes oxidative stress in the organs we specify.

5. Conclusions

Oxidative stress caused by nicotine was created in rats and antioxidant properties of cornelian cherry extract were evaluated. According to the results, cornelian cherry plant has an antioxidant feature against nicotine. Based on these data, cranberries can be considered as an alternative medicinal plant for tobacco users and other conditions that cause oxidative stress.

Conflict of interest statement

There is no conflict of interest.

References

1. Rosa MB, Fernandes MDS, Bonjardim LR, Gaviao MBD, Calixto LA, Castelo PM. Evaluation of oral mechanical and gustatory sensitivities and salivary cotinine levels in adult smokers. *Acta Odontol Scand* **2020**; 78(4): 256-264.
2. Zhang P, Li Y, Fu Y, et al. Inhibition of Autophagy Signaling via 3-methyladenine Rescued Nicotine-Mediated Cardiac Pathological Effects and Heart Dysfunctions. *Int J Biol Sci* **2020**; 16(8): 1349-1362.
3. Wipfli H. The Tobacco Atlas, Fourth Edition. *Am J Epidemiol* **2012**; 176(12): 1193.
4. Baker CL, Flores NM, Zou KH, Bruno M, Harrison VJ. Benefits of quitting smoking on work productivity and activity impairment in the United States, the European Union and China. *Int J Clin Pract* **2017**; 71(1):e12900.
5. Yılmaz H, Ertekin T, Atay E, et al. Antioxidant role of melatonin against nicotine's teratogenic effects on embryonic bone development. *Iran J Basic Med Sci* **2018**;21(8):787-793.
6. Altun I, Yuksel KZ. An Experimental Study on the Effects of Smoking in the Perinatal Period and During Lactation on the Intervertebral Disks of Newborns. *World Neurosurg* **2017**; 99: 1-5.
7. Mayyas F, Aldawod H, Alzoubi KH, Khabour O, Shihadeh A, Eissenberg T. Comparison of the cardiac effects of electronic cigarette aerosol exposure with waterpipe and combustible cigarette smoke exposure in rats. *Life Sci* **2020**; 251: 117644.
8. Khabour OF, Alzoubi KH, Bani-Ahmad M, Dodin A, Eissenberg T, Shihadeh A. Acute exposure to waterpipe tobacco smoke induces changes in the oxidative and inflammatory markers in mouse lung. *Inhal Toxicol* **2012**; 24(10): 667-675.
9. Mayyas F, Alzoubi KH. Cardiac effects of cigarette tobacco smoking in rat model of diabetes. *Life Sci* **2018**; 211: 279-85.
10. Selçuk E, Özrenk K. Erzincan Yöresinde Yetiştirilen Kızılcıkların (Cornus mas L.) Fenolojik ve Pomolojik Özelliklerinin Belirlenmesi. *Iğdır Uni J Inst Sci Tech* **2011**; 1(4): 23-30.
11. Yarilgac T, Kadim H, Ozturk B. Role of maturity stages and modified-atmosphere packaging on the quality attributes of cornelian cherry fruits (Cornus mas L.) throughout shelf life. *J Sci Food Agric* **2019**; 99(1): 421-428.
12. Dinda B, Kyriakopoulos AM, Dinda S, et al. Cornus mas L. (cornelian cherry), an important European and Asian traditional food and medicine: Ethnomedicine, phytochemistry and pharmacology for its commercial utilization in drug industry. *J Ethnopharmacol* **2016**; 193: 670-690.
13. Yilmaz S, Alpa S, Gocmen AY, et al. The investigation of the antitumoral effect of Cornus

mas L in mice with ehrlich solid tumor. *Bratisl Lek Listy* **2020**; 121(1): 22-30.
14. Wu R, Feng J, Yang Y, Dai C, Lu A, Li J, et al. Significance of Serum Total Oxidant/Antioxidant Status in Patients with Colorectal Cancer. *PLoS One* **2017**; 12(1): e0170003.
15. Yılmaz S, Göçmen AY, Üner AK, Akyüz E, Tokpınar A. The protective role of melatonin against the effect of caffeine on embryonic kidney. *Turk Hij Den Biyol Derg* **2020;** 77: 51-58.
16. Yılmaz S, Ülger H, Ertekin T, Yay AH, Nisari M, Alpa Ş, Acer N. Investigating the anti-tumoral effect of curcumin on the mice in which Ehrlich ascites and solid tumor is created. *Iran J Basic Med Sci* **2019**; 22: 418-425.
17. Nisari M, Yılmaz S, Ertekin T, et al. Effects of Curcumin on Lipid Peroxidation and Antioxidant Enzymes in Kidney, Liver, Brain and Testis of Mice Bearing Ehrlich Solid Tumor. *Postepy Hig Med Dosw* **2020**; 74: 1-10
18. Kantekin ÇÜ, Çakırca M, Yaman F, Göçmen AY. Does the Application of Desflurane at The Same Concentration by Different Flows Change the Oxidative Stress? Animal Experiment. *OTJHS* **2019**: 4(4); 492-504.
19. Momi N, Ponnusamy MP, Kaur S, et al. Nicotine/cigarette smoke promotes metastasis of pancreatic cancer through a9 nAChR-mediated MUC4 upregulation. *Oncogene* **2013**; 32: 1384-1395.
20. El-Sokkary GH, Cuzzocrea S, Reiter RJ. Effect of chronic nicotine administration on the rat lung and liver: beneficial role of melatonin. *Toxicol* **2007**; 239: 60-67.
21. Dhouib H, Jallouli M, Draief M, Bouraoui S, El-Fazaa S. Oxidative damage and histopathological changes in lung of rat chronically exposed to nicotine alone or associated to ethanol. *Pathol Biol* **2015**; 63: 258-267
22. Ferrari, C.K.B., and Torres, E.A.F.S. Biochemical pharmacology of functional foods and prevention of chronic diseases of aging. *Biomed Pharmacother* **2003**; 57: 251-260.
23. Saad AB, Rjeibi I, Alimi H, Ncib S, Bouhamda T, Zouari. Protective effects of Mentha spicata against nicotine-induced toxicity in liver and erythrocytes of Wistar rats. *Appl Physiol Nutr Metab* **2018**; 43: 77-83.
24. Hritcu, L., Ionita, R., Motei, D.E., Babii, C., Stefan, M., and Mihasan, M. Nicotine versus 6-hydroxy-l-nicotine against chlorisondamine induced memory impairment and oxidative stress in the rat hippocampus. *Biomed Pharmacother* **2017**; 86: 102-108.
25. Halliwell, B. Reactive species and antioxidants. Redox biology is a fundamental theme for aerobic life. *Plant Physiol* **2006**; 141: 312-322.
26. Karafakıoglu YS, Dündar Y, Aslan R, Fidan AF, Ciğerci IH. The effects of tobacco harvesting on oxidant-antioxidants status, some biochemical and hematologic markers in women workers. *Res J Biol Sci* **2009**; 4: 691-696.
27. Khanduja KL, and Bhardwaj A. Stable free radical scavenging and antiperoxidative properties of reservetrol compared in vitro with some other bioflavonoids. *Ind J Biochem Biophys* **2003**; 40: 416-422.
28. Karabulut D, Ulusoy HB, Kaynak E, Sönmez MF. Therapeutic effects of pentoxifylline on diabetic heart tissue via NOS. *Anatol J Cardiol* **2016**; 16: 310-315.
29. Doğanyiğit Z, Okan A, Kaymak E, Pandır D, Silici S. Investigation of protective effects of apilarnil against lipopolysaccharideinduced liver injury in rats via TLR 4/ HMGB-1/ NF-κB pathway. *Biomed Pharmacother* **2020**; 125: 1099673.

Authors' ORCID
Seher Yılmaz
http://orcid.org/0000-0003-4551-995X
Adem Tokpınar
http://orcid.org/0000-0001-7661-9588
Şükrü Ateş
http://orcid.org/0000-0001-7096-2481
Ünal Öztekin
http://orcid.org/0000-0001-9568-9442
Şerife Alpa
http://orcid.org/0000-0001-8665-3632
Ayşe Yeşim Göçmen
http://orcid.org/ 0000-0002-8511-639X

https://dergipark.org.tr/tr/pub/ntms

ISSN: 2717-8161 RESEARCH ARTICLE

New Trend Med Sci 2020; 1(2): 100-105. https://dergipark.org.tr/tr/pub/ntms

Diagnosis Confirmation Rates of Desired Electroneuromyography Results with Pre-Diagnosis of Upper Extremity Entrapment Neuropathy

Özgül Ocak[1], Hamit Çelik[2*]

[1]Department of Neurology, Faculty of Medicine, Çanakkale Onsekiz Mart University, Çanakkale, Turkey
[2]Department of Neurology, Buhara Hospital, Erzurum, Turkey

Article History
Received 13 Aug 2020
Accepted 07 Sep 2020
Published Online 30 Sep 2020

[*]***Corresponding Author***
Dr Hamit Çelik
Department of Neurology,
Buhara Hospital, Erzurum, Turkey,
Phone: +90 536 5112675
E-mail: drhamitceliknrlj@gmail.com
ORCID: https://orcid.org/0000-0002-8654-2518

Abstract: Electroneuromyography (ENMG) is an examination used by clinicians to confirm the diagnosis of patients with suspicion of entrapment neuropathy. The correlation between the ENMG results and requests increases when the clinical examination and anamnesis are well evaluated. This study aims to determine the compatibility of the electroneurophysiological examinations made due to the prediagnosis of entrapment neuropathy at the ENMG Laboratory in the Neurology Clinic and determine whether there is a difference between the clinics that made the requests. The study complied with the examinations made in Çanakkale Onsekiz Mart University neurology clinic ENMG laboratory between 01/07/2019 and 21/07/2020, and these examinations were retrospectively scanned.In total, 1464 results were scanned and those who underwent ENMG examination on the entrapment neuropathy protocol (SUT code 703220) were included in the study. Patients for whom requests were made lower extremity entrapment neuropathy and those who were younger than 18 were not included. Information regarding 445 (313 women, 132 men) patients with upper extremity entrapment neuropathy were obtained. The mean age of the patients was 49.5±14.2 (18-89). The study found that among electroneurophysiological examinations made due to the prediagnosis of entrapment neuropathy, 155 (34.8%) were diagnosed with carpal tunnel syndrome, 18 (4.0%) were diagnosed with ulnar nerve entrapment neuropathy, 3 (0.7%) were diagnosed with radial nerve entrapment neuropathy and 253 (56.9%) had normal results. But there were no significant differences between the rates of normal results in terms of clinics that made the requests. While normal results were obtained on the majority of the electroneurophysiological requests due to the pre-diagnosis of upper extremity entrapment neuropathy, there were no significant differences between the clinics.

Keywords: Electroneuromyography, Upper Extremity Entrapment Neuropathy, Clinical Compatibility.

Cite this article as: Ocak Ö and Çelik H. Diagnosis Confirmation Rates of Desired Electroneuromyography Results with Pre-Diagnosis of Upper Extremity Entrapment Neuropathy, *New Trend Med Sci* **2020**; 1(2): 100-105.

1. Introduction

Entrapment neuropathies (compression neuropathies) are a type of mononeuropathy characterized with sensory, motor and autonomous symptoms that occur as a result of entrapment of peripheral nerves at certain points during their course for different reasons. While entrapment neuropathies are commonly observed between the ages of 25-40 due to professional reasons, it can be observed between the ages of 40-60 due to metabolic and hormonal reasons (1-2).

Although entrapment neuropathies can be observed both in lower and upper extremities, it is more common in upper extremities.

Upper extremity entrapment neuropathies include cervical rib syndrome, thoracic outlet syndrome, carpal tunnel syndrome (CTS), anterior interosseous syndrome, pronator teres syndrome, cubital tunnel syndrome, guyon canal syndrome, posterior interosseous nerve (PIN) syndrome, and superficial cutaneous radial nerve entrapment (keralgia paresthetica- wartenberg syndrome), and entrapment of the radial nerve in the axillary area. The most common upper extremity entrapment neuropathy is carpal tunnel syndrome. Carpal tunnel syndrome develops due to the compression of the median nerve in the carpal tunnel. Clinically, numbness, pain and tingling are observed in the first three fingers of the hand. The patients complain of numbness that increases at night (3).

Anterior interosseous syndrome is based on the compression of the anterior interosseous which is the motor branch of the median nerve while PIS is the compression of the median nerve between two ends of the pronator teres muscle. Cubital tunnel syndrome develops due to the entrapment of the ulnar nerve in elbow while guyon canal syndrome develops due to the entrapment of the ulnar nerve inside the guyon canal. PIN is induced by the entrapment of radial nerve due to various reasons such as radius head fractures at the level of radial head, tumors, etc. Superficial cutaneous radial nerve entrapment (keralgia paresthetica-wartenberg syndrome) develops when the superficial sensory branch of the radial nerve is exposed to compression during its course in the forearm. Clinical symptoms are pain and numbness on the dorsum of the hand and radial region. Compression of the radial nerve on the axillary region may develop due to using crutches, tumor or trauma. Clinically, weakness in triceps and distal muscle with radial nerve innervation are observed (4). Diagnosis is based on anamnesis and clinically in entrapment neuropathy and confirmed with ENMG. Nerve conduction is checked in electroneurophysiological studies and needle electromyography is performed. It can be detected whether the affected nerve is affected demyelination or axonal (5).

Epineural blood stream decreases in acute period after the entrapment of the nerve, and as a result, malfunctions occur in axonal transport. The severity of the pressure increases, and intraneural blood stream is affected in time and fibrosis starts. This period is the mid phase and edema starts both as epineural and intrafascicular. If the pressure continues, endoneural edema and fibrosis develop in addition to edema. Lastly, segmental demyelinating and Wallerian degeneration occur (2-6). Remyelination and demyelination develop due to chronic pressure on the nerve. No axon loss is observed for a long time. Axon loss and muscle atrophy occur in the last phases of the chronic period (7). Diabetes, obesity, thyroid diseases, excessive alcohol intake, pregnancy, systemic inflammatory diseases, chronic renal failure and diseases that cause edema in the body are reasons that catalyze the occurrence of entrapment neuropathy. The frequency of entrapment neuropathy is also increased in professions with excessive repetitive movements such as playing a musical instrument. Patients with entrapment neuropathy consult to many branch clinics. ENGM examination is requested in polyclinics to confirm the prediagnosis without making sufficient physical examination and requesting radiological imaging. Thus, there is overcrowding in laboratories and patients have to wait for a long time (9-10).

The aim of this study was to determine how compatible the patients are with their pre-diagnosis by reviewing the electroneurophysiological results of the patients who were directed to ENGM unit of our hospital with the prediagnosis of upper extremity entrapment neuropathy and whether there is a difference in terms of compatibility between the clinics that make the request.

2. Material and Methods

The patients who consulted to Çanakkale Onsekiz Mart University neurology clinic ENMG laboratory between 01/07/2019-21/07/2020 and whose examinations were made were retrospectively scanned.

In total, 1464 patients were scanned and those on whom ENMG examination was made on the entrapment neuropathy protocol (SUT code 703220) were included in the study. Patients for whom requests were made lower extremity entrapment neuropathy and those who were younger than 18 were not included. Information regarding 445 (313 women, 132 men) patients who consulted with the prediagnosis of upper extremity entrapment neuropathy were obtained. The mean age of the patients was 49-50 (18-89). The compatibility between the prediagnosis of entrapment neuropathy and electroneurophysiological diagnosis was retrospectively investigated. All ENMGs were performed using the NihonKohden ENGM device in the ENMG unit of the Neurology clinic. ENMG results were categorized as normal, carpal tunnel syndrome (CTS), ulnar entrapment neuropathy, radial nerve entrapment neuropathy, radiculopathy and polyneuropathy (PNP).

Data were transferred to digital environment and were controlled. Frequency and percentage were calculated and presented for discrete variables while mean and standard deviation were calculated and presented for continuous variables. A very small number of departments that made the requests were combined as the "other" group (Infection Diseases and Clinical Microbiology: 1, Internal Diseases: 3, Cardiology: 1, Plastic, Reconstructive and Aesthetic Surgery: 1, Medical Oncology: 1). Analyses between the departments that made the requests and ENMG results were carried out by calculating with Exact test in a multi-mesh table. Test constant and absolute p value were given for the analysis, and the general significance limit was accepted as $p<0.05$.

3. Results

Demographic characteristics of the participants were evaluated as age and sex. Of 445 patients included in the study, 313 (70.3%) were female and 132 (29.7%) were male (Figure 1). The mean age of the patients was 49.5±14.2 (youngest 18-eldest 89).

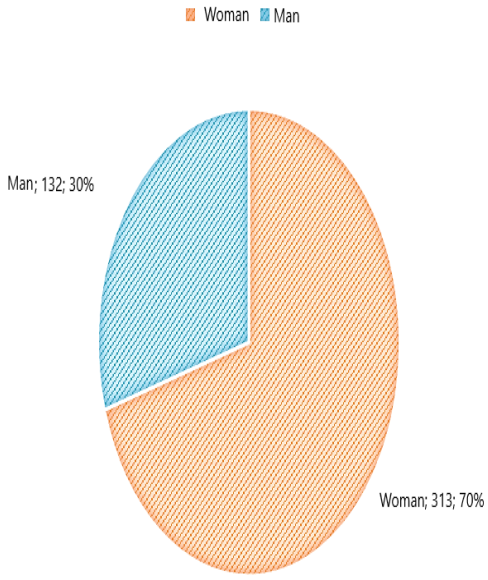

Figure 1: Gender ratio of the patients included in the study.

Considering the ENMG results, the highest number of requests were made from the neurology polyclinic (200, 44.9%).

The departments that made requests for electroneurophysiological examination and the number of requests are as follows; Neurology Clinic: 200, Orthopedics: 90, Physical Treatment and Rehabilitation (PTR) Clinic: 80, Neurosurgery Clinic: 68, other: 7 (Infection Diseases and Clinical Microbiology: 1, Internal Diseases: 3, Cardiology: 1, Plastic, Reconstructive and Aesthetic Surgery: 1, Medical Oncology: 1).

Most of the ENGMs (253, 56.9%) requested due to the prediagnosis of upper extremity entrapment neuropathy were observed to be normal. Abnormal results obtained from the ENMG results were as follows based on the frequency order; CTS (155, 34.8%), ulnar nerve entrapment neuropathy (18, 4.0%), polyneuropathy (15, 3.4%), radial nerve neuropathy (3, 0.7%) and radiculopathy (1, 0.2%).

According to the ENMG results in terms of gender, while the rates of normal results were similar between female (56.5%) and male (57.6%) patients, CTS diagnosis and other diagnoses were significantly higher in women (CTS: 37.4%, other: 13.6%) than men (CTS: 28.8%, other: 6.1%) ($X^2=8.377$; $p=0.015$).

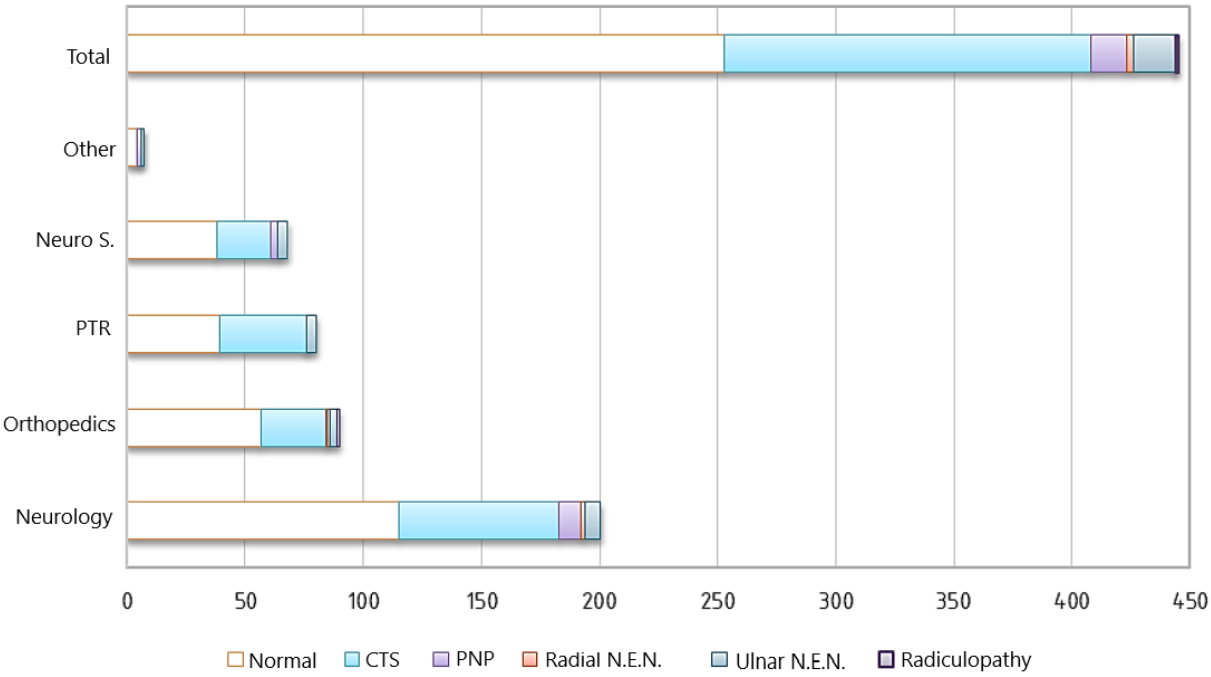

Figure 2: Distribution of diagnosis in terms of clinics.

Table 1: Distribution of diagnosis in terms of clinics (Exact X^2=32.206; p=0.023).

	Neurology	Orthopedics	PTR	Neurosurgery	Other	Total
Normal	115[a] (57.5%)	57[a] (63.3%)	39[a] (48.8%)	38[a] (55.9%)	4[a] (57.1%)	253
CTS	68 [a,b,c] (34.0%)	27[c] (30%)	37[b] (46.2%)	23 [a,b,c] (33.8%)	0 [a,c]	155
PNP	9[a] (4.5%)	1[a] (1.1%)	0[a]	3[a] (4.4%)	2[b] (28.6%)	15
Radial Nerve Entrapment Neuropathy	2 (1.0%)	1 (1.1%)	0	0	0	3
Ulnar Nerve Entrapment Neuropathy	6[a] (3%)	3[a] (3.3%)	4[a] (5%)	4[a] (5.9%)	1[a] (14.3%)	18
Radiculopathy	0[a]	1 [a] (1.1%)	0[a]	0[a]	0[a]	1
Total	200	90	80	68	7	445

*a,b,c: It defines the different subgroups that form in each row as a result of post-hoc analysis. Those who were included in more than one group were not significantly different from the groups they were included. ** Infection Diseases and Clinical Microbiology: 1, Internal Diseases: 3, Cardiology: 1, Plastic, Reconstructive and Aesthetic Surgery: 1, Medical Oncology: 1.

Table 2: Carpal tunnel syndrome results between clinics.

	Neurology	Orthopedics	PTR	Neurosurgery	Other	Total
Normal	115[a]	57[a]	39[a]	38[a]	4[a]	253
	57.5%	63.3%	48.8%	55.9%	57.1%	56.9%
CTS	68[a, b, c]	27[c]	37[b]	23[a, b, c]	0[a, c]	155
	34.0%	30.0%	46.2%	33.8%	0.0%	34.8%
Other	17[a]	6[a]	4[a]	7[a]	3[b]	37
	8.5%	6.7%	5.0%	10.3%	42.9%	8.3%
Total	200	90	80	68	7	445
	100.0%	100.0%	100.0%	100.0%	100.0%	100.0%

*a,b,c: It defines the different subgroups that form in each row as a results of post-hoc analysis. Those who were included in more than one group were not significantly different from the groups they were included.

ENMG results in terms of clinics are presented in Table 1. There were significant differences between ENMG results in terms of clinics (Exact X^2=32.206; p=0.023). While the most frequently obtained normal results rates were not significantly different between the clinics, CTS diagnoses were higher in PTR clinic and there were significant differences in Orthopedics and Traumatology. Observed values regarding all diagnoses are presented in Table 1 and Figure 2. The clinic whose prediagnosis of entrapment neuropathy was confirmed with ENMG results the most (41, 51.3%) was PTR, and the clinic with highest number of normal results were Orthopedics and Traumatology (57, 63.3%). While 4 out of 7 examinations were normal in other clinics, obtained 3 results were CTS diagnosis.

4. Discussion

Electrophysiological examinations are useful for diagnosing entrapment neuropathies and deciding on the treatment. To confirm the clinical diagnosis, other possible problems must be excluded first. False negative results can be observed in the early period of entrapment neuropathies. Various studies have shown that the number of requests for ENMG examinations has increased in recent years. The most important reason for this increase is requesting an ENMG examination to confirm the prediagnosis of entrapment neuropathy without making detailed physical examination on patients who consulted to the polyclinics (9-11).

The workload of ENMG laboratories increases due to unnecessary requests; thus, the patients have to wait a long time for the examination (12). The normal result rates of the ENMG requests were reported between 16-38% in numerous studies. The most important reason that the results turn out normal was reported to be insufficiency of neurological examination. Nikolic et al. found that there are differences even among the neurologists in terms of the compatibility between the prediagnosis and electrodiagnostic diagnosis (13).

In this study, 56.8% of the ENMG results that were performed with the prediagnosis of entrapment neuropathy were normal. This result was found to have a higher rate of normal ENMG results compared with the studies in the literature. The study compared the examinations requested for carpal tunnel syndrome between clinics and found that the clinic with the highest compatibility between pre-diagnosis and ENMG results was PTR (46.2%) (Table 2).

All requests for ENMG examination were made by specialist physicians in this study. There were no significant differences between the clinics that made requests in terms of normal results. This shows that clinics that made requests have approximately the same knowledge and clinical experience about entrapment neuropathy. ENMG requests of general practitioners and specialist physicians were compared in numerous studies in the literature, and the electroneurophysiological diagnosis compatibility was lower among general practitioners. The compatibility rate in the requests made by general practitioners was 36.5% while this rate was higher among specialist physicians. The compatibility rate in the requests made by neurology specialists was 42% (14-16).

5. Conclusions

The fact that 56.8% of the ENMG results were normal in this study and it indicates that the requests for ENMG examinations are made without performing sufficient physical examination and taking anamnesis. The fact that the results of the requests are normal more than expected can be interpreted as that the number of unnecessary requests is high, and this situation may cause additional costs for the health system, patients undergo unnecessarily painful examinations and loss of workforce among medical staff. Therefore, physicians should spare more time while examining patients with the prediagnosis of entrapment neuropathy and should perform more detailed physical examination.

Conflict of interest statement
The authors declare no conflict of interest.
Financial Support
None
Ethics Committee Approval
2011-KAEK-27/2020-E.2000111728.

References

1. Allieu Y, Mackinnon SE, editors. Nerve compression syndromes of the upper limb. London: Martin Dunitz; **2002**.
2. Lundborg G, Dahlin LB. The pathophysiology of nerve compression. *Hand Clin* **1992**; 8(2): 215-227.
3. Assmus H, Antoniadis G, Bischoff C. Carpal and cubital tunnel and other, rarer nevre compression syndromes. *Dtsch Arztebl Int.* **2015**;112(1-2):14-25.
4. Ay S, Evcik D. Tuzak nöropatiler Romatoloji e. kitap **2018**.
5. Alba C. Therapist's management of radial tunnel syndrome. In: Mackin EJ, Callahan AD, Skirven TM, Schneider LH, Osterman AL, Hunter JM, editors. Rehabilitation of the hand and upper ekstremity, 5th ed. St. Louis: Mosby; **2002** p.696-700.
6. Tunç A, Güngen B. Karpal Tünel Sendromu Hastalarında Elektrodiagnostik Evreleme ile Klinik Evre, Semptom Süresi ve Vücut Kitle İndeksi Arasındaki İlişkinin Değerlendirilmesi. *Dicle Tıp Dergisi* **2017**;44: 159-166.
7. Gupta R, Steward O. Chronic nerve compression induces concurrent apoptosis and proliferation of Schwann cells. *J Comp Neurol* **2003**; 461(2): 174-186.
8. Ettema AM, Amadio PC, Zhao C, et al. Changes in the functional structure of the tenosynovium in idiopathic carpal tunnel syndrome: a scanning electron microscope study. *Plast Reconstr Surg* **2006**; 118(6): 1413-1422.
9. Podnar S. Critical reappraisal of referralsto electromyography and nerve conduction studies. *Eur J Neurol* **2005**; 12(2): 150-155.
10. Rosenberg NR, Portegies P, de Visser M, Vermeulen M. Diagnosticinvestigation of patients with chronicpoly neuropathy: evaluation of a clinical guideline. *J Neurol Neurosurg Psychiatry* **2001**; 71(2): 205-209.
11. Chemali KR, Tsao B. Electrodiagnostictesting of nervesandmuscles: when, why, and how toorder. *Cleve Clin J Med* **2005**; 72(1): 37-48.
12. Karadag YS, Golgeleyen D, Saka M, et al. Referral Diagnosis Versus Electroneurophysiological Findings-Three Years Eksperiencefrom a Tertiary Hospital. *Eur J General Med* **2014**; 11(4): 244-247.
13. Nikolic A, Stevic Z, Peric S, et al. Evaluation of theadequacy of requests for electrodiagnostic eksamination in a tertiary referral center. *Clin Neurol Neurosurg* **2016**; 148: 130-136.
14. Johnsen B, Fuglsang-Frederiksen A, Vingtoft S, et al. Differences in the handling of the EMG eksamination at seven European laboratories. *Electroencephalogr Clin Neurophysiol* **1994**; 93(2): 155-158.
15. Mondelli M, Giacchi M, Federico A. Requests for electromyography from general practitioners and specialists: critical evaluation. *Ital J Neurol Sci* **1998**; 19(4): 195-203.
16. Cocito D, Tavella A, Ciaramitaro P, et al. A further critical evaluation of requests for electrodiagnostic examinations. *Neurol Sci* **2006**; 26(6): 419-422.

Authors' ORCID
Özgül Ocak
http://orcid.org/0000-0001-8276-0174
Hamit Çelik
https://orcid.org/0000-0002-8654-2518

https://dergipark.org.tr/tr/pub/ntms

ISSN: 2717-8161 RESEARCH ARTICLE

New Trend Med Sci 2020; 1(2): 106-117. https://dergipark.org.tr/tr/pub/ntms

Determination of Developmental Dysplasia of the Hip Using Artificial Neural Networks (ANN) on Ultrasound Viewing According to Graf's Method

Kadri Yıldız[1*], Vahit Yıldız[2]

[1]Department of Orthopaedia and Traumatology, Faculty of Medicine, Kafkas University, Kars, Turkey
[2]Department of Orthopaedia and Traumatology, Faculty of Medicine, Adnan Menderes University, Aydın, Turkey

Article History
Received 16 Aug 2020
Accepted 09 Sep 2020
Published Online 30 Sep 2020

[*]***Corresponding Author***
Dr Kadri Yıldız
Department of Orthopedia and Traumatology,
Faculty of Medicine,
Kafkas Univeristy, Kars, Turkey,
Phone: +90 538 545 0559
E-mail: drkadri1980@hotmail.com
ORCID: https://orcid.org//0000-0002-8164-7687

Abstract: Developmental dysplasia of the hip (DDH) is a preventable disorder. Hip ultrasound is the best choice for the early detection of hip deformity. But, because of the multitude of out-patient clinics, sometimes mixing may be occurred. We organize a study to determine the usable capability of Artificial Neural Networks (ANN) for follow up of hip ultrasonography according to the Graf's US method. 135 cases with hip ultrasonography evaluation have been obtained from the study group. Alpha and beta angles were measured according to the Graf's US method. Two groups were determined according to alpha and beta angles, gender, and the Graf's US classification. Measurements were done by a radiologist that 25-year experienced. The databases were loaded to the software. 18 samples for the input data and target data were selected among 135 cases. The samples were used for training the neural network. The target date was arranged for 3 types (Type I, II, and III). Resilient Backpropagation" training function as 87.4%. The coefficient of determination (R-Squared) and accuracy values were 100% in most cases. And Polak-Ribiére Conjugate Gradient training function as 83.0%. We consider that using artificial intelligence to follow these USG records may provide easier follow-up. Thus, possible mixing problems can be avoided. © 2020 NTMS.
Keywords: Developmental Dysplasia of the Hip, Graf's US Method, Artificial Neural Networks.

1. Introduction

Developmental dysplasia of the hip (DDH) is one of the common orthopedic diseases. It is seen nearly in 1/1000 born, the female/male ratio is 6/1. The DDH is a dynamic musculoskeletal disease, and the treatment is easier in the earlier months. Some musculoskeletal diseases may be risks factor for the DDH as torticollis, congenital club foot, metatarsus adductus.

Pregnancy period, type of birth, first birth, prematurity, family history, gender is etiologic factors for DDH. Ultrasound (US) viewing according to Graf's method is the one of used tool for diagnosis of the DDH because of its advantages as absent of radiation risks and early diagnosis (1-3).

The Graf's classification includes several major types

Cite this article as: Yıldız K and Yıldız V. Determination of Developmental Dysplasia of the Hip Using Artificial Neural Networks (ANN) on Ultrasound Viewing According to Graf's Method, *New Trend Med Sci* **2020**; 1(2): 106-117.

that have subdivided. The types are classified by angle measurements and morphological aspects (Table 1) (4). Neural networks can be used as a classification system to determine malformed classes where the definition of an undesirable characteristic would not change. The network would be expected to perform the same classification repeatedly (5). Receiver Operating Characteristics (ROC) graphs are useful for organizing classifiers and visualizing performance. ROC graphs are used in medical decision making commonly. In recent years it has been used increasingly in machine learning and data mining research. Although ROC graphs are considered as simple, some common misconceptions and pitfalls occur in some studies (6).
This research aims to determine the best Artificial Neural Networks (ANN) structure for classification to be used in the diagnosis of developmental dysplasia of the hip classes using alpha and beta angles obtained from US and to test the most successful network on the cases of the orthopedic clinic.

2. Material and Methods

This research has been approved by the IRB of the authors' affiliated institutions. Ethics approval was obtained for this study. The data of 135 cases have been obtained from the orthopedic clinic of our hospital by using ultrasonography. Measurement of alpha and beta angles was done according to the Graf's US method.
The data were divided into 2 groups according to which side (left or right) that have developmental dysplasia of the hip. Each group has been treated separately and has its information about alpha and beta angles, gender, and the Graf's US classification.
In the general primer care of a newborn, hip ultrasounds according to the Graf's classification were assessed. The alpha and beta angle measurements were made by a radiologist that has worked in our university hospital. The alpha angle is drawn between the acetabular roof and the vertical cortex of the ilium. It reflects the development of the bony acetabular roof. The beta angle is drawn between the vertical cortex of the ilium and the triangular labral fibrocartilage. It measures the cartilaginous coverage over the femoral head. Alpha and beta angles are continuous measurements that are determined during ultrasound hip imaging. The angles are classified for hip type (Ia, Ib, IIa, IIb, IIc, III, IV, or D) (7).
The data was organized using tabulation software. 18 samples for the input data and target data were selected among 135 cases. The samples were regarded to be determinant for training the neural network. There were not any cases in some hip dislocation classes. In some classes, there were a few cases. For this reason, the target data was arranged for 3 types (Type I, II, and III). The artificial neural network (ANN) for the classification of hip dislocation was established, trained, and tested in Mathworks Matlab R2015a software. For these purposes, a script was coded, following the steps shown in Listing 1.

The script runs 27 combinations of 3 different neuron numbers (3, 6, 10) in the hidden layer and 9 different training functions. The training functions are listed in Table 2. Half of the input values were used for training, a quarter for validation, and the rest for testing. For each combination, the script loops at most 20 times to reach the desired performance values. Among those networks, the network with the best performance value was saved to get the outputs. The coefficient of determination (R-Squared) of the network was calculated using targets across outputs.
The best network out of 27 combinations was compared to the others and the network with the highest R-Squared value was used on all of 135 cases. The confusion matrix of the network was conducted using outputs and targets using the 0.5 thresholds.
The accuracy of the networks was calculated with the formula:

$$Accuracy = \frac{TP+TN}{P+N}$$ [1].

where TP is true positives, TN is true negatives, P is several positives and N is the number of negatives. ANN diagram for classification with 10 neurons in the hidden layer is shown in Figure 1.

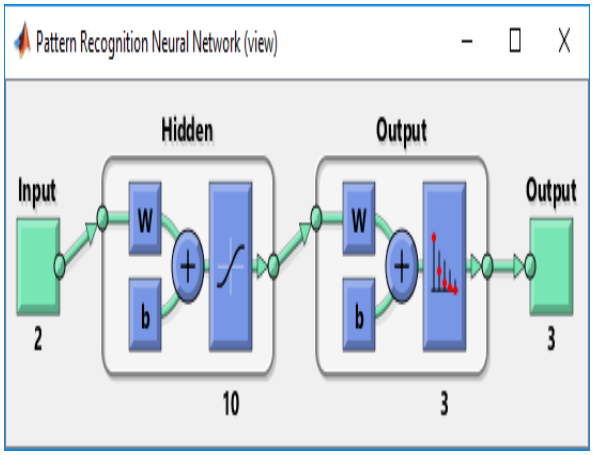

Figure 1: Demonstration of pattern recognition neural network.

3. Results

The script firstly was run for the right hip. Networks with 10 neurons in the hidden layer had the highest coefficient of determination (R-Squared) values and most of them had 100% accuracy while training. The highest R-Squared value was measured for the network with 10 neurons in the hidden layer, "One Step Secant" and "Variable Learning Rate Backpropagation" training functions. However, when the networks were tested for all the samples, the highest accuracy was found with the network with 3 neurons in the hidden layer, and the "Resilient Backpropagation" training function as 87.4% (Listing 2, Figures 2).
Lastly, the script was run for hip dislocation on the left. Most of the networks had 100% of the coefficient of

determination (R-Squared) values and most of them had 100% accuracy while training.
However, when the networks were tested for all the samples, the highest accuracy was found with the network with 10 neurons in the hidden layer and "Polak-Ribiére Conjugate Gradient" training function as 83.0% (Listing 3 and Figures 3).

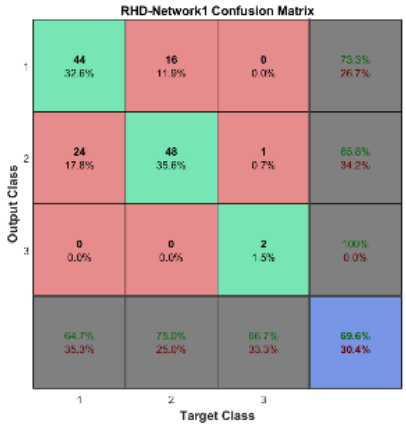

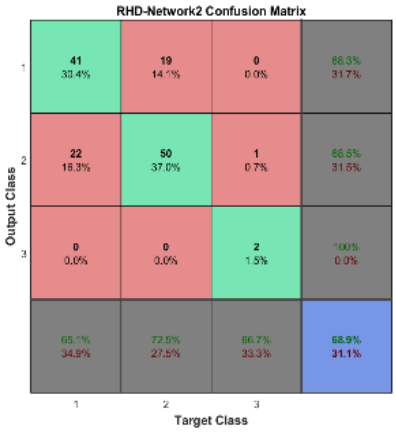

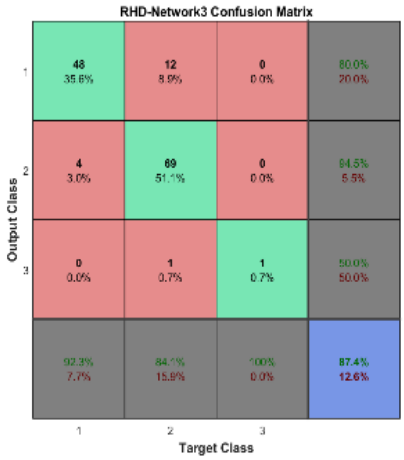

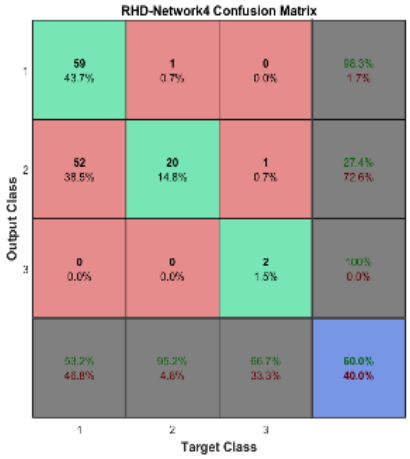

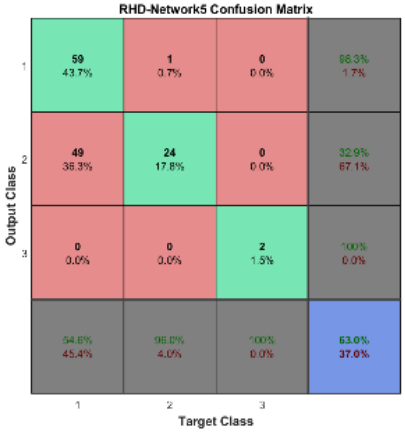

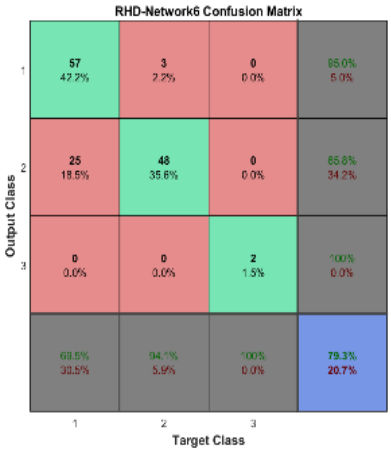

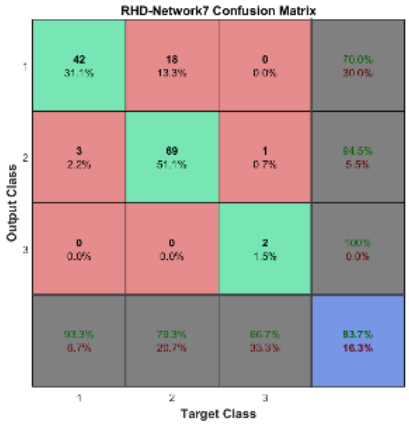
RHD-Network7 Confusion Matrix
Output Class
Target Class

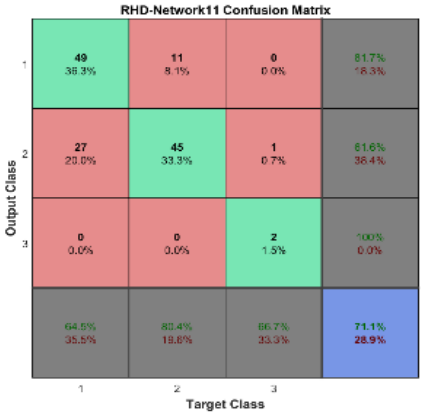
RHD-Network11 Confusion Matrix
Output Class
Target Class

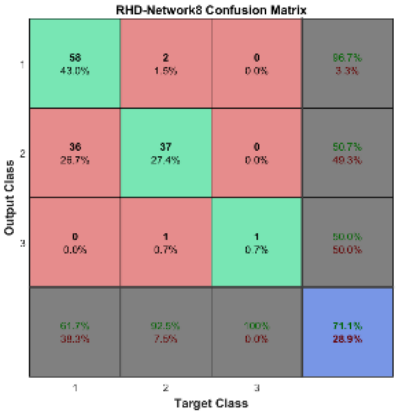
RHD-Network8 Confusion Matrix
Output Class
Target Class

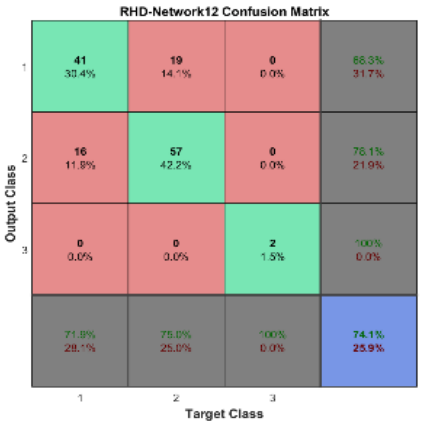
RHD-Network12 Confusion Matrix
Output Class
Target Class

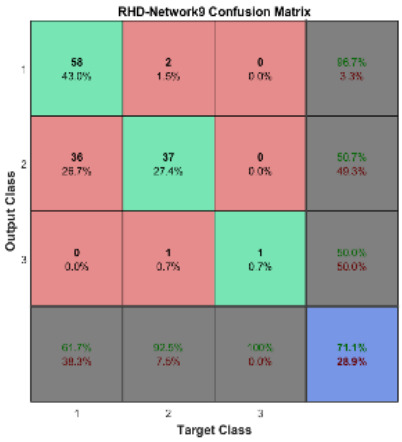
RHD-Network9 Confusion Matrix
Output Class
Target Class

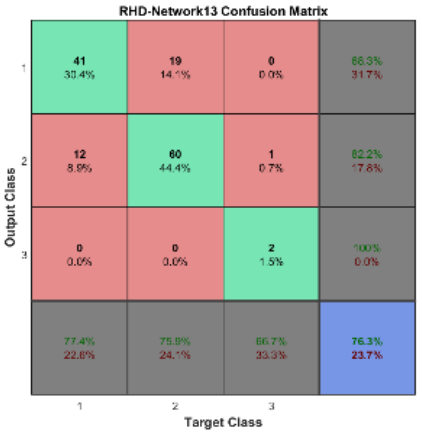
RHD-Network13 Confusion Matrix
Output Class
Target Class

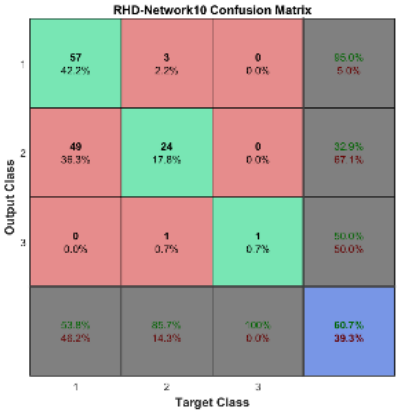
RHD-Network10 Confusion Matrix
Output Class
Target Class

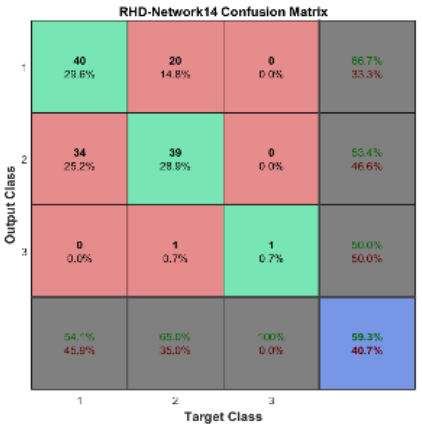
RHD-Network14 Confusion Matrix
Output Class
Target Class

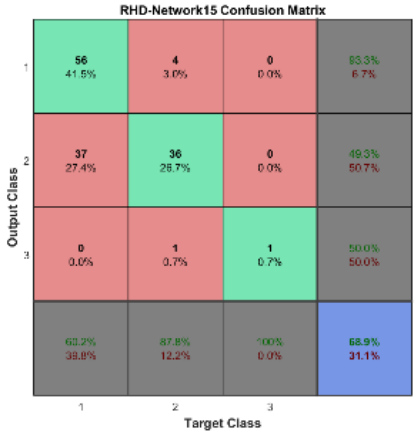
RHD-Network15 Confusion Matrix
Output Class
Target Class
56
41.5%
4
3.0%
0
0.0%
93.3%
6.7%
37
27.4%
36
26.7%
0
0.0%
49.3%
50.7%
0
0.0%
1
0.7%
1
0.7%
50.0%
50.0%
63.2%
36.8%
87.8%
12.2%
100%
0.0%
68.9%
31.1%

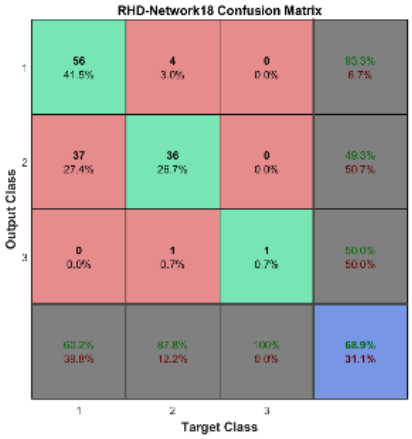
RHD-Network18 Confusion Matrix
Output Class
Target Class
56
41.5%
4
3.0%
0
0.0%
93.3%
6.7%
37
27.4%
36
26.7%
0
0.0%
49.3%
50.7%
0
0.0%
1
0.7%
1
0.7%
50.0%
50.0%
63.2%
36.8%
87.8%
12.2%
100%
0.0%
68.9%
31.1%

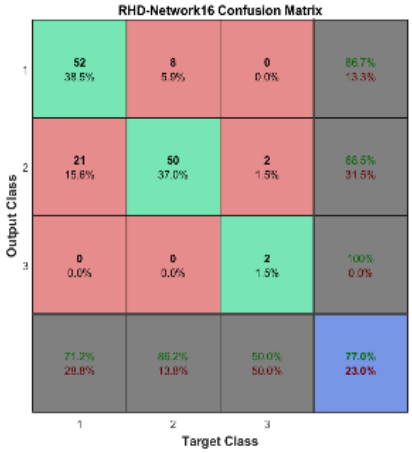
RHD-Network16 Confusion Matrix
Output Class
Target Class
52
38.5%
8
5.9%
0
0.0%
86.7%
13.3%
21
15.6%
50
37.0%
2
1.5%
66.5%
31.5%
0
0.0%
0
0.0%
2
1.5%
100%
0.0%
71.2%
28.8%
86.2%
13.8%
50.0%
50.0%
77.0%
23.0%

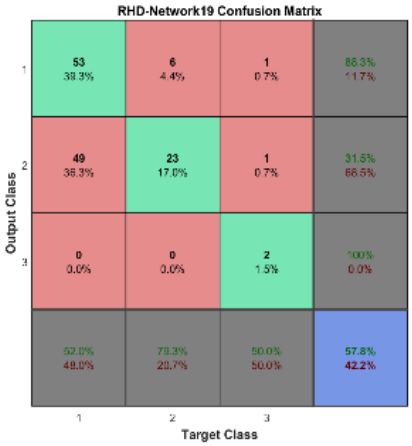
RHD-Network19 Confusion Matrix
Output Class
Target Class
53
39.3%
6
4.4%
1
0.7%
88.3%
11.7%
49
36.3%
23
17.0%
1
0.7%
31.5%
68.5%
0
0.0%
0
0.0%
2
1.5%
100%
0.0%
52.0%
48.0%
79.3%
20.7%
50.0%
50.0%
57.8%
42.2%

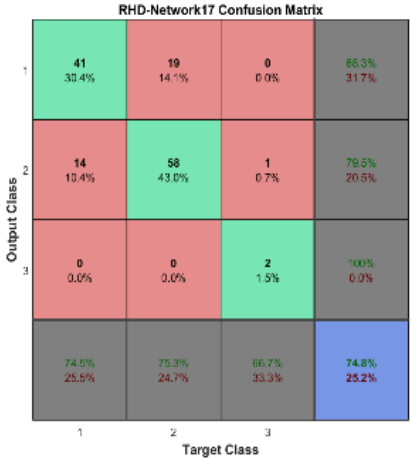
RHD-Network17 Confusion Matrix
Output Class
Target Class
41
30.4%
19
14.1%
0
0.0%
68.3%
31.7%
14
10.4%
58
43.0%
1
0.7%
79.5%
20.5%
0
0.0%
0
0.0%
2
1.5%
100%
0.0%
74.5%
25.5%
75.3%
24.7%
66.7%
33.3%
74.8%
25.2%

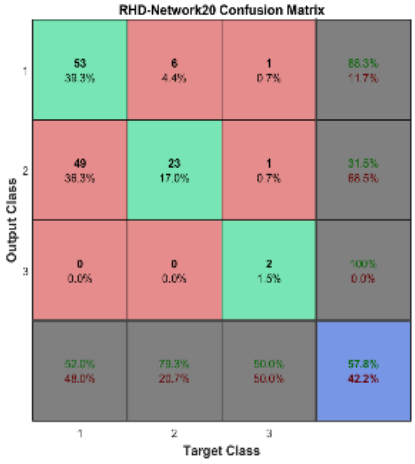
RHD-Network20 Confusion Matrix
Output Class
Target Class
53
39.3%
6
4.4%
1
0.7%
88.3%
11.7%
49
36.3%
23
17.0%
1
0.7%
31.5%
68.5%
0
0.0%
0
0.0%
2
1.5%
100%
0.0%
52.0%
48.0%
79.3%
20.7%
50.0%
50.0%
57.8%
42.2%

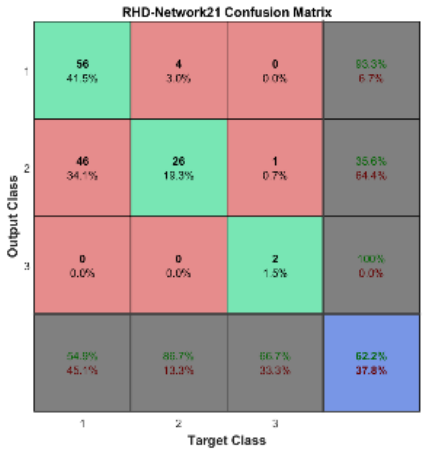
RHD-Network21 Confusion Matrix
Output Class
Target Class
56
41.5%
4
3.0%
0
0.0%
93.3%
6.7%
46
34.1%
26
19.3%
1
0.7%
35.6%
64.4%
0
0.0%
0
0.0%
2
1.5%
100%
0.0%
54.9%
45.1%
86.7%
13.3%
66.7%
33.3%
62.2%
37.8%

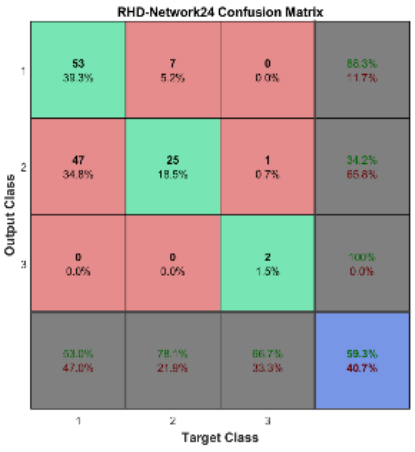
RHD-Network24 Confusion Matrix
Output Class
Target Class
53
39.3%
7
5.2%
0
0.0%
88.3%
11.7%
47
34.8%
25
18.5%
1
0.7%
34.2%
65.8%
0
0.0%
0
0.0%
2
1.5%
100%
0.0%
53.0%
47.0%
78.1%
21.9%
66.7%
33.3%
59.3%
40.7%

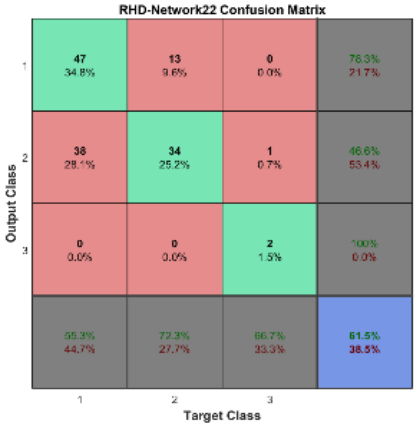
RHD-Network22 Confusion Matrix
Output Class
Target Class
47
34.8%
13
9.6%
0
0.0%
78.3%
21.7%
38
28.1%
34
25.2%
1
0.7%
46.6%
53.4%
0
0.0%
0
0.0%
2
1.5%
100%
0.0%
55.3%
44.7%
72.3%
27.7%
66.7%
33.3%
61.5%
38.5%

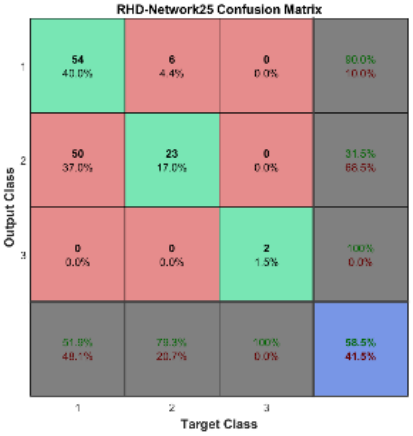
RHD-Network25 Confusion Matrix
Output Class
Target Class
54
40.0%
6
4.4%
0
0.0%
90.0%
10.0%
50
37.0%
23
17.0%
0
0.0%
31.5%
68.5%
0
0.0%
0
0.0%
2
1.5%
100%
0.0%
51.9%
48.1%
79.3%
20.7%
100%
0.0%
58.5%
41.5%

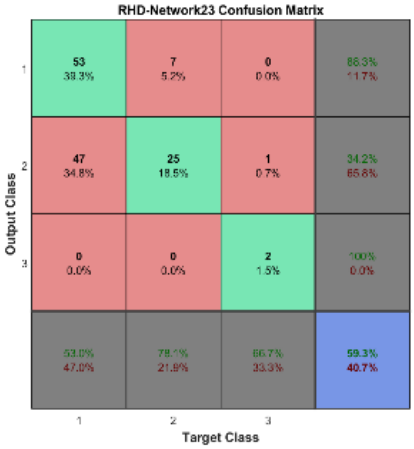
RHD-Network23 Confusion Matrix
Output Class
Target Class
53
39.3%
7
5.2%
0
0.0%
88.3%
11.7%
47
34.8%
25
18.5%
1
0.7%
34.2%
65.8%
0
0.0%
0
0.0%
2
1.5%
100%
0.0%
53.0%
47.0%
78.1%
21.9%
66.7%
33.3%
59.3%
40.7%

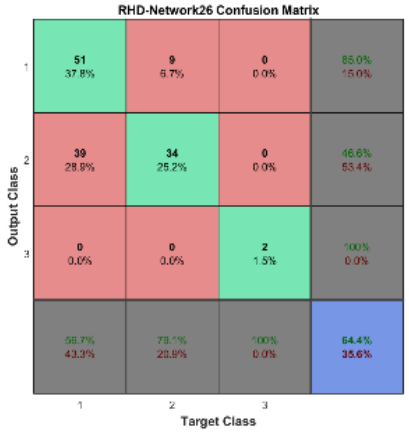

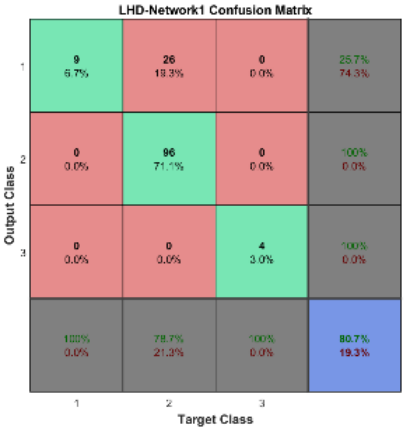

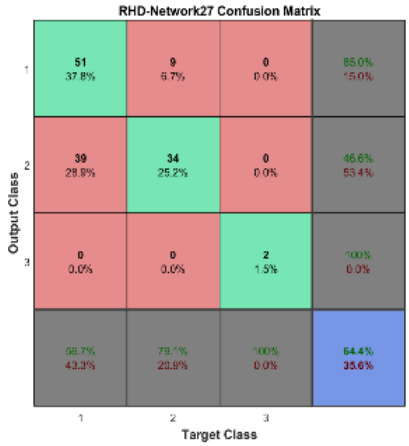

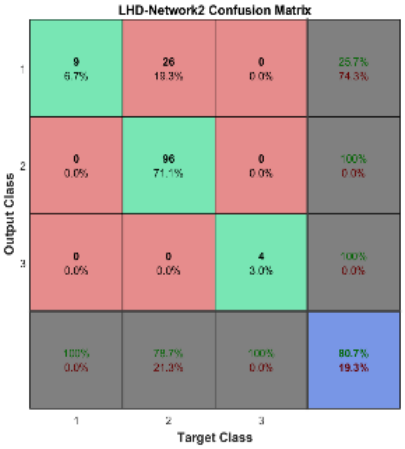

Figure 2: RHD Network Confusion Matrix (Network confusion matrix for right hip dysplasia disease.

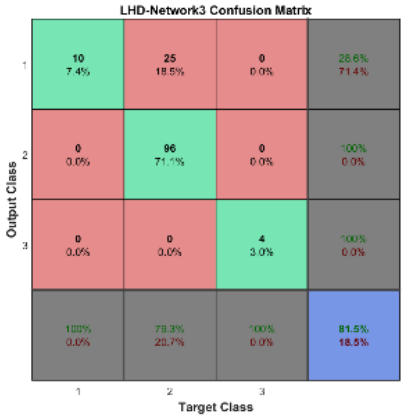

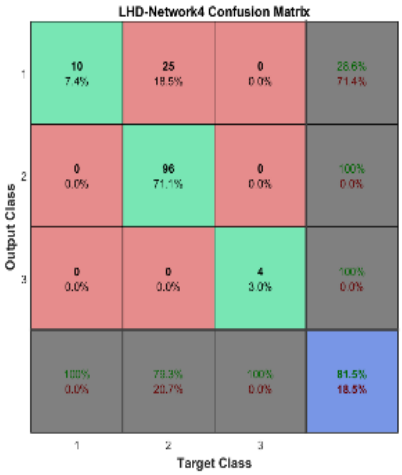
LHD-Network4 Confusion Matrix
Output Class
Target Class
10 7.4%
25 18.5%
0 0.0%
28.6% 71.4%
0 0.0%
96 71.1%
0 0.0%
100% 0.0%
0 0.0%
0 0.0%
4 3.0%
100% 0.0%
100% 0.0%
79.3% 20.7%
100% 0.0%
81.5% 18.5%

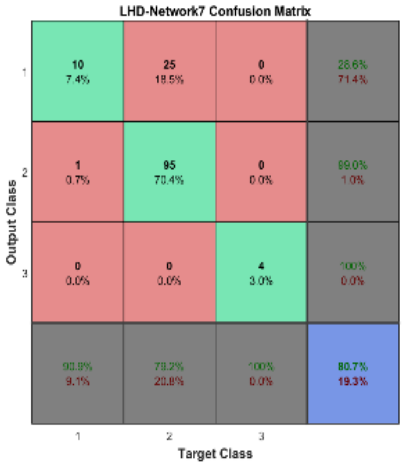
LHD-Network7 Confusion Matrix
Output Class
Target Class
10 7.4%
25 18.5%
0 0.0%
28.6% 71.4%
1 0.7%
95 70.4%
0 0.0%
99.0% 1.0%
0 0.0%
0 0.0%
4 3.0%
100% 0.0%
93.8% 6.1%
79.2% 20.8%
100% 0.0%
80.7% 19.3%

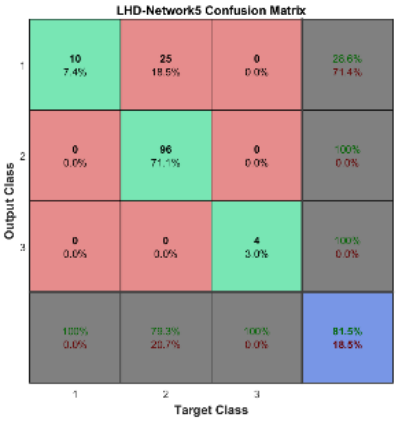
LHD-Network5 Confusion Matrix
Output Class
Target Class
10 7.4%
25 18.5%
0 0.0%
28.6% 71.4%
0 0.0%
96 71.1%
0 0.0%
100% 0.0%
0 0.0%
0 0.0%
4 3.0%
100% 0.0%
100% 0.0%
79.3% 20.7%
100% 0.0%
81.5% 18.5%

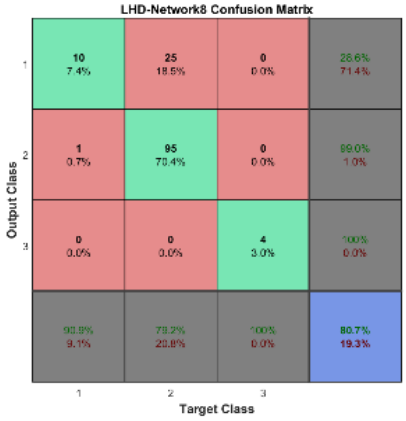
LHD-Network8 Confusion Matrix
Output Class
Target Class
10 7.4%
25 18.5%
0 0.0%
28.6% 71.4%
1 0.7%
95 70.4%
0 0.0%
99.0% 1.0%
0 0.0%
0 0.0%
4 3.0%
100% 0.0%
93.8% 6.1%
79.2% 20.8%
100% 0.0%
80.7% 19.3%

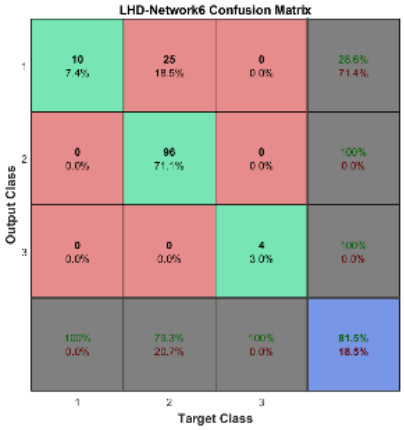
LHD-Network6 Confusion Matrix
Output Class
Target Class
10 7.4%
25 18.5%
0 0.0%
28.6% 71.4%
0 0.0%
96 71.1%
0 0.0%
100% 0.0%
0 0.0%
0 0.0%
4 3.0%
100% 0.0%
100% 0.0%
79.3% 20.7%
100% 0.0%
81.5% 18.5%

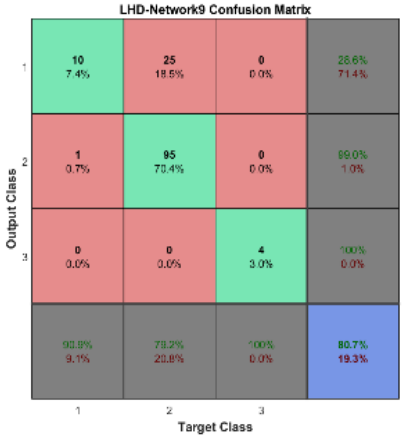
LHD-Network9 Confusion Matrix
Output Class
Target Class
10 7.4%
25 18.5%
0 0.0%
28.6% 71.4%
1 0.7%
95 70.4%
0 0.0%
99.0% 1.0%
0 0.0%
0 0.0%
4 3.0%
100% 0.0%
93.8% 6.1%
79.2% 20.8%
100% 0.0%
80.7% 19.3%

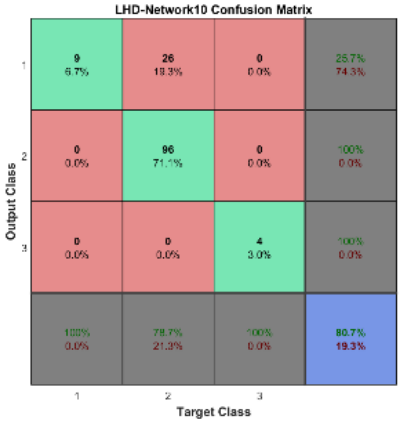
LHD-Network10 Confusion Matrix
Output Class
Target Class
9 6.7%
26 19.3%
0 0.0%
25.7% 74.3%
0 0.0%
96 71.1%
0 0.0%
100% 0.0%
0 0.0%
0 0.0%
4 3.0%
100% 0.0%
100% 0.0%
78.7% 21.3%
100% 0.0%
80.7% 19.3%

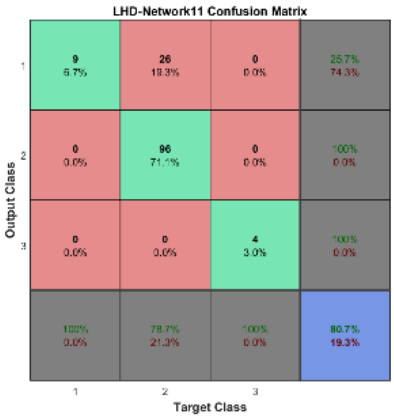
LHD-Network11 Confusion Matrix
Output Class
Target Class
9
6.7%
26
19.3%
0
0.0%
25.7%
74.3%
0
0.0%
96
71.1%
0
0.0%
100%
0.0%
0
0.0%
0
0.0%
4
3.0%
100%
0.0%
100%
0.0%
78.7%
21.3%
100%
0.0%
80.7%
19.3%

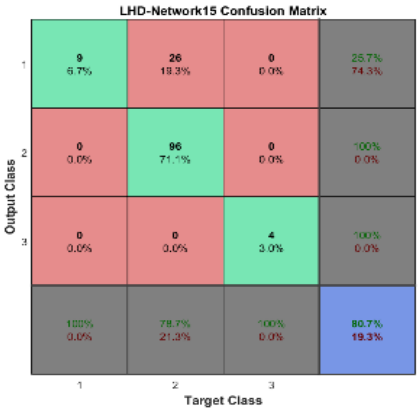
LHD-Network15 Confusion Matrix
Output Class
Target Class
9
6.7%
26
19.3%
0
0.0%
25.7%
74.3%
0
0.0%
96
71.1%
0
0.0%
100%
0.0%
0
0.0%
0
0.0%
4
3.0%
100%
0.0%
100%
0.0%
78.7%
21.3%
100%
0.0%
80.7%
19.3%

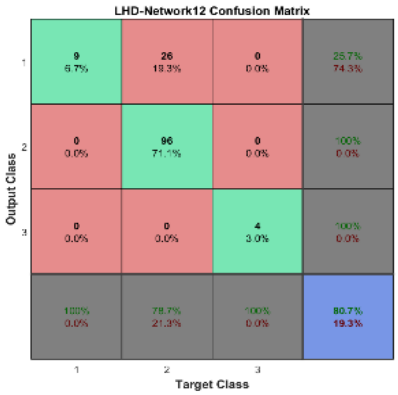
LHD-Network12 Confusion Matrix
Output Class
Target Class
9
6.7%
26
19.3%
0
0.0%
25.7%
74.3%
0
0.0%
96
71.1%
0
0.0%
100%
0.0%
0
0.0%
0
0.0%
4
3.0%
100%
0.0%
100%
0.0%
78.7%
21.3%
100%
0.0%
80.7%
19.3%

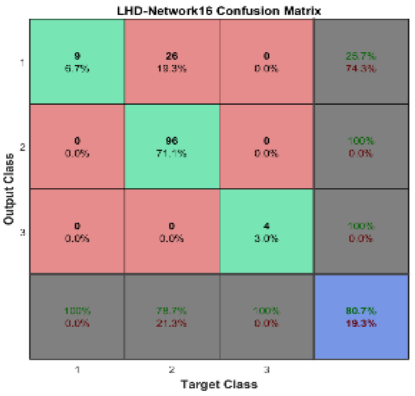
LHD-Network16 Confusion Matrix
Output Class
Target Class
9
6.7%
26
19.3%
0
0.0%
25.7%
74.3%
0
0.0%
96
71.1%
0
0.0%
100%
0.0%
0
0.0%
0
0.0%
4
3.0%
100%
0.0%
100%
0.0%
78.7%
21.3%
100%
0.0%
80.7%
19.3%

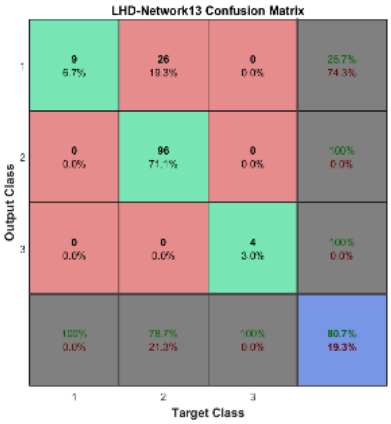
LHD-Network13 Confusion Matrix
Output Class
Target Class
9
6.7%
26
19.3%
0
0.0%
25.7%
74.3%
0
0.0%
96
71.1%
0
0.0%
100%
0.0%
0
0.0%
0
0.0%
4
3.0%
100%
0.0%
100%
0.0%
78.7%
21.3%
100%
0.0%
80.7%
19.3%

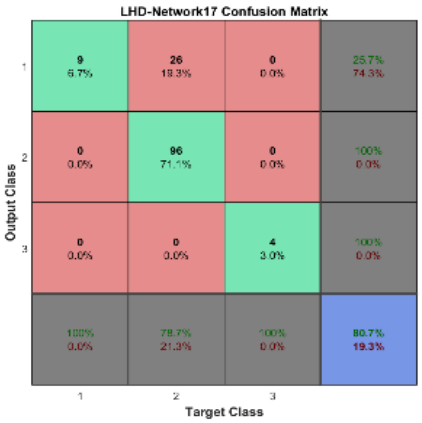
LHD-Network17 Confusion Matrix
Output Class
Target Class
9
6.7%
26
19.3%
0
0.0%
25.7%
74.3%
0
0.0%
96
71.1%
0
0.0%
100%
0.0%
0
0.0%
0
0.0%
4
3.0%
100%
0.0%
100%
0.0%
78.7%
21.3%
100%
0.0%
80.7%
19.3%

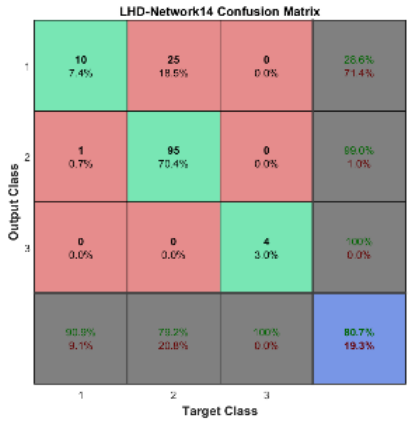
LHD-Network14 Confusion Matrix
Output Class
Target Class
10
7.4%
25
18.5%
0
0.0%
28.6%
71.4%
1
0.7%
95
70.4%
0
0.0%
99.0%
1.0%
0
0.0%
0
0.0%
4
3.0%
100%
0.0%
90.9%
9.1%
78.2%
20.8%
100%
0.0%
80.7%
19.3%

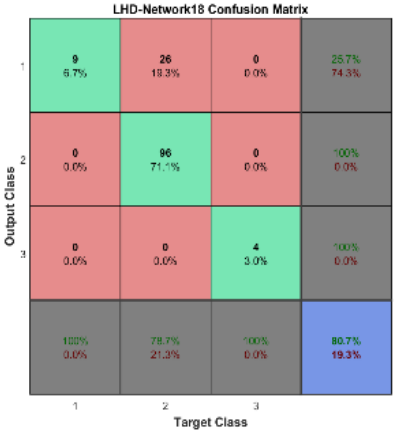
LHD-Network18 Confusion Matrix
Output Class
Target Class
9
6.7%
26
19.3%
0
0.0%
25.7%
74.3%
0
0.0%
96
71.1%
0
0.0%
100%
0.0%
0
0.0%
0
0.0%
4
3.0%
100%
0.0%
100%
0.0%
78.7%
21.3%
100%
0.0%
80.7%
19.3%

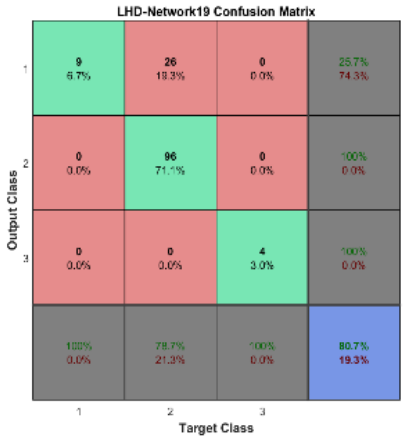
LHD-Network19 Confusion Matrix
Output Class
Target Class

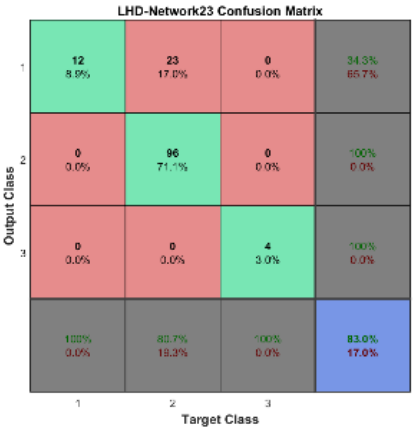
LHD-Network23 Confusion Matrix
Output Class
Target Class

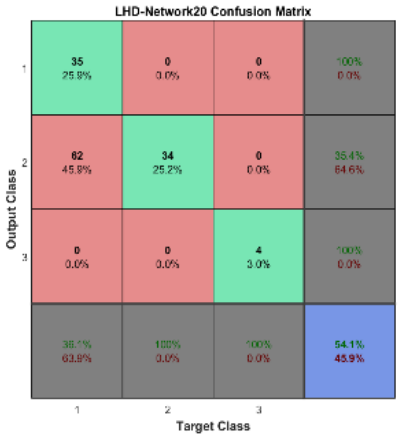
LHD-Network20 Confusion Matrix
Output Class
Target Class

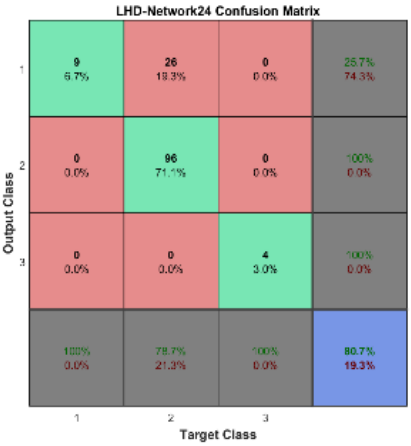
LHD-Network24 Confusion Matrix
Output Class
Target Class

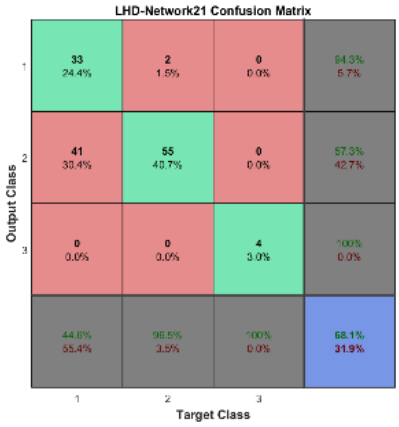
LHD-Network21 Confusion Matrix
Output Class
Target Class

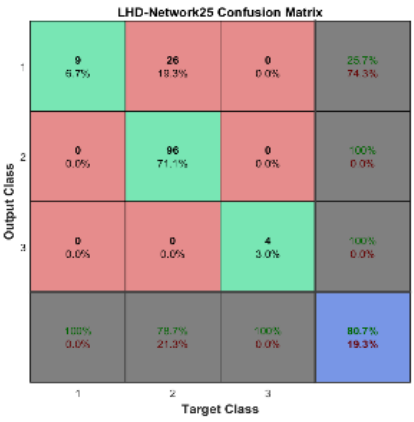
LHD-Network25 Confusion Matrix
Output Class
Target Class

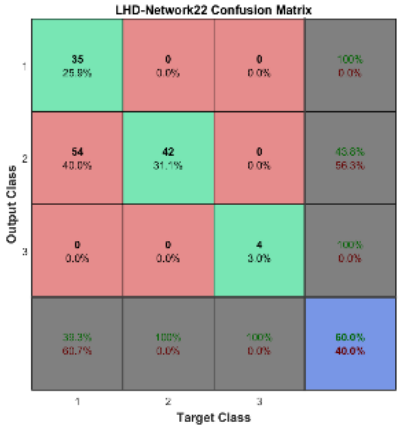
LHD-Network22 Confusion Matrix
Output Class
Target Class

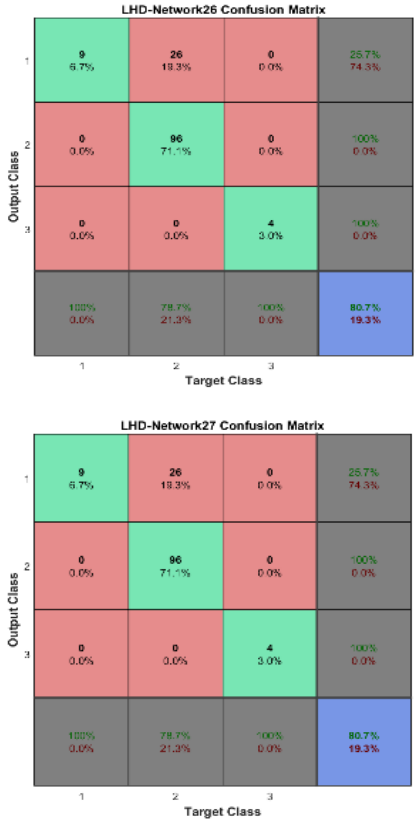

Figures 3: LHD Network Confusion Matrix (Network confusion matrix for left hip dysplasia disease.

4. Discussion

Developmental dysplasia of the hip (DDH) is a pediatric musculoskeletal disorder (8). The reported incidence of DDH is between 1 and 34 per 1000 newborns (9, 10). In Europe, it is between 3% and 13%, real dysplasia as between 1% and 3% (11, 12). In 1988, Huang reported the incidence of DDH was 2,7/1000 in Taiwan. The incidence of a one-year follow-up was 1.2/1000 (13). In our country, the rate is between 0.4/1000 and 1.7/1000 as a wide range (14-24).

Ultrasonography was introduced to orthopedic trials in the 1980s. This method has been assured to evaluate the infant's hip structure. The Graf's classification has gained popularity due to its early detection and accuracy features (7,25). Ultrasound screening for DDH is has become more effective at detecting the disease. National Health Services (NHS) from the United Kingdom's Newborn and Infant Physical Examination (NIPE) Programme advises hip ultrasound screening within 2-6 weeks.

Lusier screened 1683 newborns during their study period (25). They declared that later than 28 days after birth does not increase surgery rates and it might reduce clinical visits counts. They recommended a cut-off day like 28 days. Also, they predicted decreasing of parental stress, lesser the number of ultrasound studies, cost-sensitive screening programs. Also, this condition reduces the multitude of pediatric and orthopedic clinics, the beneficial use of medical resources.

Ultrasonographic early detection of DDH by the Graf's US method is recommended for reducing the need for surgery and comorbidities due to operations (25). Roovers found that earlier screenings could provide an early diagnosis of abnormal hips (26). However, follow-up of frequent US scans can be a problem for orthopedic surgeons and radiologists during intensive policlinic service. Especially during serial and personal follow-up of the patients for the Graf's US scans, mixing and non-tracking problems may arise. In our country, almost 100 patients are examined daily in orthopedic policlinics.

5. Conclusions

In the outpatient clinics, we emphasize that using artificial intelligence to follow these US records may provide more correct follow-up. The mixing can be avoided in this way.

Conflict of interest statement

The authors declare that they have no conflict of interest.

Financial Support

There is no funding source.

Ethical approval

Ethics approval was obtained for this study.

Informed consent

Informed consent was obtained from all individual participants included in the study.

Acknowledgment

Thank you to Sefa Altıkat for the support in this study.

References

1. Graf R. Hip Sonography. Diagnosis and management of infant hip dysplasia. Berlin, Springer **2006**. p. 1-87.
2. Omeroglu H. Ultrasonographic Graf type 2a hip needs more consideration in newborn girls. *J Chilp Orthop* **2013**; 7(2): 95-98.
3. Puhan MA, Woolacott N, Kleijinen J, Streurer J. Observational studies on ultrasound screening for developmental dysplasia of the hip in a newborns-a systematic review. *J Ultrasound Med* **2003**; 24(6): 377-82
4. Langer R. Ultrasonic investigation of the hip in newborns in the diagnosis of congenital hip dislocation: classification and results of a screening program, *Skeletal Radiol* **1987**; 16: 275-279
5. Taylor BJ. Methods and Procedures for the Verification and Validation of Artificial Neural Networks, Springer **2006**; p: 280
6. Fawcett T. An Introduction to ROC Analysis. *Pattern Recognition Letter*s **2005**; 27(8): 861-874

7. Graf R. New possibilities for the diagnosis of congenital hip joint dislocation by ultrasonography. *J Pediatr Orthop* **1983**; 3(3): 354–359
8. Storer SK, Skaggs DL. Developmental dysplasia of the hip. *Am Fam Physician* **2006**; 15; 74(8): 1310-1316.
9. Tachdjian M. Congenital dysplasia of the hip. In: Tachdjian M, editor. Pediatric Orthopaedics. Philadelphia: W.B. Saunders. **1990**; p: 247-549
10. 10. Noordin S, Umer M, Hafeez K, Nawaz H. Developmental dysplasia of the hip. *Orthop Rev (Pavia)* **2010**; 23;2(2): e19.
11. Holen KJ, Terjesen T, Tegnander A, Bredland T, Saether OD, Eik-Nes SH. Ultrasound Screening for Hip Dysplasia in Newborns. *J Pediatr Orthop* **1994**; 14(5): 667-73.]
12. Rosendahl K, Markestad T, Lie RT. Developmental dysplasia of the hip. A population-based comparison of ultrasound and clinical findings. *Acta Paediatr* **1996**; 85(1):64-9.
13. Huang SC, Liu HC, Chen CF, Chen CL, Liu TK. Incidence of congenital dislocation of the hip in Chinese. *J Orthop Surg* **1988**; 5(3): 53-65
14. Dogruel H, Atalar H, Yavuz OY, Sayli U. Clinical examination versus ultrasonography in detecting developmental dysplasia of the hip. *Int Orthop* **2008**; 32(3): 415-9.
15. Duramaz A, Peker G, Arslan L, Bilgili MG, Erçin E, Kural C. Hip Ultrasonography in the Diagnosis of Developmental Dysplasia of the Hip: Bakırköy Experience. *Med Bull Haseki* **2014**; 52(2): 262-267
16. Cakir BC, Kibar AE, Cakir HT, Arhan E, Cansu A, Yakut HI. Screening of 300 Infants for Developmental Hip Dysplasia by Ultrasonography. *Turkey Children's Hospital Journal* **2009**; 3(2): 5-9.
17. Demirhan M, Shar C, Aydinok HC, Cakmak M, Coban A. Ultrasonography in the diagnosis of congenital hip dislocation. *Acta Orthop Traumatol Turc* **1994**; 28: 8-14
18. Oguz T, Ege A, Gungor S, Toppare M, Erdemtok N. The ultrasonographic evaluation of 1099 infants by Graf method. *Arthroplasty Arthroscopic Surgery* **1996**; 7: 64-66
19. Okur A, Nakışlar F, Karsan O, Alparslan B. The value of ultrasonographic examination in diagnosis and screening of congenital hip dislocation. *Acta Orthop Traumatol Turc* **1996**; 30: 107-112
20. Kose N, Omeroglu H, Ozyurt B. Our three-year experience in the ultrasonographic hip screening program in infants of three to four weeks. *Acta Orthop Traumatol Turc* **2006**; 40(4): 285-90.
21. Akman A, Korkmaz A, Aksoy MC, Yazici M, Yurdakok M, Tekinalp G. Evaluation of risk factors in developmental dysplasia of the hip: results of infantile hip ultrasonography. *Turk J Pediatr* **2007**; 49(3): 290-4.
22. Tosun HB, Bulut M, Karakurt L, Belhan O, Serbest S. Evaluation of hip ultrasonography results for developmental hip dysplasia screening. *Firat Med J* **2010**; 15(4): 178-183
23. Cekic B, Erdem-Toslak I, Sertkaya O. Incidence and follow-up outcomes of developmental hip dysplasia of newborns in the Western Mediterranean Region. *Turk J Pediatr* **2015**; 57(4): 353-358
24. Sahin F, Akturk A, Beyazova U. Screening for developmental dysplasia of the hip: results of a 7-year follow-up study. *Pediatr Int* **2004**; 46(2): 162-6.
25. Lussier EC, Sun YT, Chen HW, Chang TY, Chang CH. Ultrasound screening for developmental dysplasia of the hip after 4 weeks increases exam accuracy and decreases follow-up visits. *Pediatr Neonatol* **2019**; 60(3): 270-277.
26. Roovers EA, Boere-Boonekamp MM, Castelein RM, Zielhuis GA, Kerkhoff TH. Effectiveness of ultrasound screening for developmental dysplasia of the hip. *Arch Dis Child Fetal Neonatal Ed* **2005**; 90(1): 25-30.

Authors' ORCID

Kadri Yıldız
http://orcid.org/0000-0002-8164-7687
Vahit Yıldız
http://orcid.org/0000-0003-3639-0912

https://dergipark.org.tr/tr/pub/ntms

ISSN: 2717-8161 RESEARCH ARTICLE

New Trend Med Sci 2020; 1(2): 118-122. https://dergipark.org.tr/tr/pub/ntms

Evaluation of 0-2 Month Old Infants Brought to the Pediatric Outpatient Clinic for Restlessness

İsmail Topal[1], Sara Salcan[2*]

[1]Department of Pediatrics, Faculty of Medicine, Erzincan Binali Yıldırım University, Erzincan, Turkey
[2]Department of Public Health, Faculty of Medicine, Erzincan Binali Yıldırım University, Erzincan, Turkey

Article History
Received 01 Sep 2020
Accepted 24 Sep 2020
Published Online 30 Sep 2020

[*]***Corresponding Author***
Dr Sara Salcan
Department of Public Health,
Faculty of Medicine,
Erzincan Binali Yıldırım University,
Erzincan, Turkey,
Phone: +90 505 295 2984
E-mail: saratas_1984@hotmail.com
ORCID: https://orcid.org/0000-0001-5049-1838

Abstract: Restlessness is one of the most frequent causes to bring a baby to a medical facility by parents. Most of the restless infants are diagnosed with infantile colic. We aimed to evaluate hypercalciuria and urinary system in 0-2 month old infants who were brought to the pediatric outpatient clinic due to restlessness**.** Only the 0-2 month old infants who were evaluated only for restlessness between January 1 and December 31, 2018 were included in the study. The data were obtained as retrospective evaluation of medical records. Complete urine analysis, urine culture, abdominal ultrasonography, calcium to creatinine ratio in spot urine and blood calcium examination was performed. The 95th percentile of the urinary calcium/creatinine ratio was accepted as the upper limit of normal. Blood calcium level above 10.8 mg/dl was considered as hypercalcemia. Of the 240 infants included in the study. The number of infants receiving breast milk alone was 146 (73.3%). Leukocyturia was detected in 24 infants. Urine culture was evaluated as positive for 59 infants. Spot urine calcium/creatinine ratio was evaluated in 201 infants. Of these, 10 patients had a high calcium/creatinine ratio. In infants receiving breast milk alone had a lower calcium/creatinine ratio. Urinary calcium/creatinine ratio was found to be significantly higher in infants with urinary tract stones and hypercalcemia**.** Not all infants brought to a medical facility due to restlessness should be considered to have infantile colic. Urine analysis should be performed and urinary tract infection and hypercalcuria should be investigated. Positive urine cultures obtained using a bladder bag should be considered hesitantly and should always be repeated.
Keywords: Baby, Restlessness, Hypercalciuria, Urinary Tract Infection.

1. Introduction

Crying is a way for babies to communicate with the environment. In most babies, crying and restlessness begin spontaneously during the first weeks of birth and spontaneously diminish towards the 3rd to 4th months (1). Babies cry to express their physiological needs such as hunger, sweating, chills and irritation from fecal soiling. If their needs are met, they stop crying and calm down in a short time. Although crying is a physiological event in infants, excessive crying and restlessness may also occur in pathological conditions such as infantile colic, otitis and urinary tract infection (UTI). Crying and restlessness are among the most common reasons to bring a healthy baby to a doctor's office in the first four

Cite this article as: Topal İ and Salcan S. Evaluation of 0-2 Month Old Infants Brought to the Pediatric Outpatient Clinic for Restlessness, *New Trend Med Sci* **2020**; 1(2): 118-122.

months of life. Infantile colic is the most common condition for those infants who present to hospitals with crying (2). Infantile colic is episodes of crying lasting more than three hours a day and more than three days a week and that lasts at least three weeks (3). It has been reported to occur in 5-30% of babies during infancy (4).

There may be an underlying organic cause in 10% of infants brought to a medical facility due to crying. Organic causes include cow and/or soy milk protein allergy, gastroesophageal reflux or lactose intolerance. All etiological causes should be evaluated in infants who present with crying. Medical reasons can often be ruled out by careful history taking and physical examination (1).

In this study, we aimed to evaluate hypercalciuria and urinary system in children with 0-2 months admitted to outpatient clinics with restlessness.

2. Material and Methods

Only the 0-2 month old babies admitted to our outpatient clinic between January 1, 2018 and December 31, 2018 due to restlessness were included in the study. Data were obtained retrospectively from patient files. Physical examinations were recorded in detail. Infants who were diagnosed with otitis media, upper respiratory tract infection, lower respiratory tract infection or infantile colic were excluded from the study. The age, gender, weight, type of feeding and the use of formula of the infants were recorded. The data of complete urine analysis, urine culture (using a sterile urinary bag), abdominal ultrasonography (USG), calcium to creatinine ratio in spot urine (Ca/Cr) and blood calcium levels were also recorded.

A 24-hours urinary Ca excretion level above 4 mg/kg or 95th percentile values of urinary Ca/Cr ratio in children was accepted to be the upper limits of normal (5,6). The 5th, 10th, 25th, 50th, 75th and 95th percentile values were calculated for the Ca/Cr ratio. The 95th percentile value of the Ca/Cr ratio was accepted as the upper limit of normal. Blood calcium levels above 10.8 mg/dl were considered as hypercalcemia. (7)

The present study was approved by the clinical ethics committee of Erzincan University Faculty of Medicine (accession number: 604.01.02-E.43283)

2.1. Statistical Analysis

Data were interpreted using SPSS statistical package program (SPSS Inc, v22.0, USA). All results were expressed as Mean±Standard Deviation (SD). Using the Kolmogorov Smirnov test, the data was determined to have a non-normal distribution. For this reason, non-parametric tests were used. Spearman correlation test and Mann Whitney U test were applied to analyse the association between variables. $P<0.05$ was considered statistically significant.

3. Results

Of the 240 babies included in the study, 114 were female (47.5%) and 126 were male (52.5%). The mean age of the infants was 29.9±15.4 days. When breast milk feeding was questioned, 180 (75%) infants were found to receive breast milk alone, 13 (5.5%) infants received formula alone and 47 (19.6%) infants received breast milk+formula. Demographic characteristics of the babies participating in the study were shown in Table 1.

Table 1: Demographic characteristics of infants.

Age	Male	31.4±15.2 days (Min-Max: 7-59)	
	Female	28.2±15.6 days (Min-Max: 6-59)	
	Total	29.9±15.4 days (Min-Max: 6-59)	
Gender	Male	126 (n)	52.5%
	Female	114	47.5%
Height		53.67±2.4 cm	Min-Max: 46-61
Weight		3917±695 g	Min-Max: 2800-6200
Head circumference		35.8±1.35 cm	Min-Max: 32-39
Nutritional status	Breast milk	180(n)	75%
	Formula	13	5.4
	Breast milk+Formula	47	19.6

Urinalysis and urine culture were requested in a total of 240 infants. Leukocyturia was detected in 24 (10%) infants. Urine microscopy was normal in 216 infants (90%). *E.coli* (76%) and *Klebsiella* (24%) was isolated in the urine of 59 infants with positive urine culture. Positive urine culture samples were repeated using a urinary catheter and 27 (45%) of them revealed to be positive for growth (Table 2).

Table 2: Results of urinalysis and incidences.

Finding	Number	Percentage
Normal	175	73
Leukocyturia	24	10
Hematuria	6	2.5
Crystals	35	14.5
Growing microorganism		
E.coli	45	76
Klebsiella spp	14	24

Spot urine calcium/creatinine (UCA/Cr) was analysed in 201 infants. Mean spot urine Ca/Cr was found to be 0.30±0.19. Hypercalciuria was found in 111 cases with an accepted cut-off of hypercalciuria as 0.21. Urinary hypercalciuria was found to be 0.77 in the 95th percentile and the UCa/Cr ratio was found to be high in 10 cases (Table 3).

Table 3: UCa/Cr value and percentile.

UCa/Cr	Number	Percentage
Over 0.21	111	55.2
Over 95 p	10	4.9

The mean spot UCa/Cr was compared between the genders. There was no significant difference in mean UCa/Cr between the males (0.29±0.17) and the females (0.31±0.21), (p=0.66). Spot UCa/Cr averages were compared between those who were breastfed alone and who received breastfeeding and formula or formula alone. Urine UCa/Cr averages were significantly lower in those who were breastfed alone (p=0.005).

No statistically significant difference was found between the mean UCa/Cr spot urine in infants with and without UTI (p=0.53). Urinary USG was performed in 108 of the infants in the study group. Vesicoureteral reflux (VUR), ureteropelvic stenosis, hydronephrosis, cystitis and calcium stones were observed in 2, 2, 1, 6 and 9 infants, respectively. Mean urine calcium to creatinine ratio was significantly higher in patients who had positive findings revealed by an imaging method compared to patients with negative findings by an imaging method (p=0.01).

Blood calcium and creatinine levels were measured in 70 of the infants. Creatinine level was normal in all infants. Blood calcium levels were elevated in 11 infants. Mean urinary UCa/Cr was found to be significantly higher in babies with hypercalcemia compared to babies with a normal blood calcium level (p<0.01). Correlation analysis showed a significant correlation between urinary calcium and blood calcium (r:0.38, p<0.001).

4. Discussion

As restlessness and crying are common symptoms in infancy, obtaining a good anamnesis from the parents is the first and most important step in the diagnosis and approach to the infant. Another important step in diagnosis is a detailed physical examination of the infant and evaluation of his/her growth and development. In addition, laboratory and radiological examinations are needed in infants with a good weight gain and normal physical examination. There are studies suggesting that urine analysis might be the only useful laboratory test especially in a baby crying a lot with a normal history and physical examination. (8)

In our study, only infants with the complaint of restlessness were included in the study. Babies with any findings in their examinations or interpreted in favor of infantile colic were excluded from the study, and 240 asymptomatic babies were examined. As indicated by Freedman et al. (8), complete urine analysis and urine culture were requested from all infants. Although leukocyturia was observed in 24 babies, Urine culture of about 1 in 4 babies were positive. Positive urine culture samples were repeated using a urinary catheter and half of them were found to have a positive growth. The rate of false positivity of the urine culture obtained using a bag in the neonatal period was demonstrated to be high (9). In this present we also found this false positive rate to be high. This shows that the urine cultures obtained using a bag should be considered hesitantly and if necessary, urine cultures should be repeated with urinary catheters or suprapubic aspiration.

Urinary infection is more common in males in the newborn period compared to females (10, 11). In our study, 24.6% of the infants had a positive urine culture and urine culture positivity was found to be higher in males compared to females. The urine of the infants with positive urine cultures was positive mostly for *E.coli*. *E. coli* has been reported to be the most frequently isolated pathogen in UTI in many studies (12-14).

Hypercalciuria is one of the most important risk factors for stone disease in children and adults. Most patients, especially younger children, are asymptomatic (15). Young patients present with complaints of restlessness, UTI, vomiting or fever rather than abdominal and flank pain. In this present study, urinary stone and hypercalciuria were found in 8.3% and 4.9%, respectively of infants presenting with restlessness. In the study conducted by Melek et al., the most common reason for presentation in children less than 5 years of age with urinary system stones was reported as restlessness (16). Also, in a similar study by Baysal et

al. 29 patients diagnosed at the first two years of age were reported to be presenting with restlessness as the most common cause (17). In the study of Altincik (18), the mean UCa/Cr of the patients with complaints of restlessness was significantly higher compared to those without complaints.

In this present study, no difference was found between the mean urinary Ca/Cr between male and female infants. Similarly, in the studies of Sonmez et al. (19) and Donmez et al. (6), no association was found between gender and mean urinary Ca/Cr.

In the literature, there are some studies showing that feeding with formula has an effect on urinary stone and hypercalciuria formation (20, 21). Similar to our study, in the study of Erol et al. it was reported that the mean urine Ca/Cr was significantly lower in breastfed infants (22).

In our study, no statistically significant difference was found between the mean spot urine UCa/Cr in infants with and without UTI. It is stated that there is no significant relationship between UTI and urinary calcium excretion (18). Vachvanichsanong et al. reported that the quantitative urinary calcium excretion in children with UTI is not different from those without UTI (23).

In many studies (24-26), urinary calcium excretion was found to be higher in patients with urinary stone detected on USG. Similarly, in our study, it was found that infants with urinary stones had a significantly higher rate of hypercalciuria.

The amount of calcium filtered from the glomeruli varies directly with the concentration of calcium in the serum and glomerular filtrate. The serum concentration of calcium and filtered calcium increase, the amount of calcium excreted in the urine also increases (27). In this present study, it was observed that there was a significant increase in urinary calcium as the blood calcium level of infants increased.

5. Conclusions

As a result, although no definite cause could be found in most of the babies brought for restlessness or they are considered to have infantile colic, urine analysis should be performed and urolithiasis should be excluded in infants who have complaints of restlessness. In patients with hypercalciuria, imaging methods should be used for urinary system stone disease.

Conflict of interest statement

The authors declare that they have no conflicts of interest.

References

1. Hiscock H. The crying baby. *Aust Fam Physician Vol* **2006**; 35: 680-684.
2. Karabel M, Karabel D, Tayman C, Tonbul A, Tatli MM. Evaluation of Risk Factors and Pharmacological Treatment Approaches in Infantile Colic. *Turkish J Pediatr Dis* **2010**; 4(1): 12-17.
3. Wessel MA, Cobb JC, Jackson EB, Harrıs GS Jr, Detwiler AC. Paroxysmal fussing in infancy, sometimes called colic. *Pediatrics* **1954**; 14(5): 421-35.
4. Neu M1, Robinson J. Infants with colic: their childhood characteristics. *J Pediatr Nurs.* **2003**; 18(1): 12-20.
5. Milliner DS. Urolithiasis. In: Avner ED, Harmon WE, Niaudet P, (eds). Pediatric Nephrology. Philadelphia: Lippincott Williams&Wilkins, **2004**: 1094-5.
6. Donmez O, Yuce N, Ilcol YO, Ediz B, Durmaz O, Kilicbay I. Urinary calcium excretion in healthy children. *Turkish Ped Arc* **2009**; 44: 131-4
7. Stanley FL. Reference Intervals for Laboratory Tests and Procedures. In: Kliegman RM, Stanton BF, Schor NF, Geme JW, Behrman RE (eds). Nelson Text Book of Pediatrics. United States of America, Elsevier Saunders, **2011**; 19: 2466-2485.
8. Freedman SB, Al-Harthy N, Thull-Freedman J. The crying infant: Diagnosis testing and frequency of serious underlying disease. *Pediatrics* **2009**; 123: 841-848.
9. Turkmen M, Ozkan P, Aydogdu SA. Yenidoğanlarda torba ve suprpubik yöntemle alınan idrar kültr sonuçlarının karşılaştırılması. *Çocuk Sağlığı ve Hastalıkları Dergisi* **2008**; 51: 193-198.
10. Kanellopoulos TA, Salakos C, Spiliopoulou I, et al. First urinary tract infection in neonates, infants and young children: a comparative study. *Pediatr Nephrol* **2006**; 21: 1131-1137.
11. Gorgen O. An Overview: Childhood Urinary Tract Infection. *Nephrology Nursing Journal* **2016**; 2: 50-64.
12. Gurgoze MK, Dogan Y, Kizirgil A, Toraman Z, Aygun D, Susceptibility of bacteria isolated from children with urinary tract infection to various antibiotics, *Firat Med J* **2002**; 7: 828-832.
13. Cetin H, Oktem F, Ormeci AR, Yorgancigil B, Yayli G, Escherichia coli and antibiotic resistance in childhood urinary tract infections, *Med J SDU* **2006**; 13: 12-16.
14. Yasar KK, Pehlivanoglu F, Şengoz G, Distribution of gram negative microorganisms and antibiotic resistance in urinary tract infections in pediatric age group, *Medical Bulletin of Zeynep Kamil* **2010**; 41: 137-41.
15. VanDervoot K, Wiesen J, Frank R, et al. Urolithiasis in pediatric patients: a single center study of incidence, clinical presentation and outcome. *J Urol* **2007**; 177: 2300-5.
16. Melek E, Gulleroglu KS, Bayrakci US, Aygun C, Baskin E. Clinical and Metabolic Characteristics of Pediatric Patients with Urinary Stone. *Turkish J Pediatr Dis* **2016**; 1: 40-45.
17. Baysal YE, Koyun M, Akman S, Guven AG, Guntekin E. Urolithiasis in children: 10 years of experience in Antalya. *Çocuk Sağlığı ve Hastalıkları Dergisi* **2004**; 47: 254-259.

18. Altincik A. Relationship Between Urinary Tract Infection and Idiopathic Hypercalciuria in Children. Adnan Menderes University, Faculty of Medicine, Department of Pediatrics. Speciality Thesis. Aydin-**2008**.
19. Sonmez F, Akcanal B, Altincik A, Yenisey C. Urinary calcium excretion in healthy Turkish children. *Int Urol Nephrol* **2007**; 39: 917–922.
20. Bastuğ F. Urinary Stone Disease in Infants: Etiology and Treatment. *Bull Endourol* **2013**; 6: 143-151.
21. Alpay H, Gokce I, Ozen A, Biyikli N. Urinary stone disease in the first year of life: is it dangerous? *Pediatr Surg Int* **2013**; 29:311–316.
22. Erol I, Buyan N, Ozkaya O, Sahin F, Beyazova U, Soylemezoglu O. Reference values for urinary calcium, sodium and potassium in healthy newborns, infants and children. *Turkish J Pediatr* **2009**; 51: 6-13.
23. Vachvanichsanong P, Malagon M, Moore ES. Urinary tract infection in children associated with idiopathic hypercalciuria. *Scand J Urol Nephrol* **2001**; 35: 112-116.
24. MH Alemzadeh-Ansari Valavi E, Ahmadzadeh A. Predisposing Factors for Infantile Urinary Calculus in South- West of Iran. *Iran J Kidney Dis* **2014**; 8: 53-57.
25. Bilge I, Yilmaz A, Kayiran SM et al. Clinical importance of renal calyceal microlithiasis in children. *Pediatr Int* **2013**; 55: 731-736.
26. Dursun I, Poyrazoglu HM, Dusunsel R et al. Pediatric urolithiasis: an 8-year experience of single centre. *Int Urol Nephrol* **2008**; 40(1): 3-9.
27. Langman CB. Disorders of phosphorus, calcium, and vitamin D. In: Avner ED, Harmon WE, Niaudet P (eds) Pediatric Nephrology, 5th edition, Philadelphia, Lipincott Williams & Wilkins. **2004**: 237-255.

Authors' ORCID
İsmail Topal
http://orcid.org/0000-0002-2331-7196
Sara Salcan
https://orcid.org/0000-0001-5049-1838

https://dergipark.org.tr/tr/pub/ntms

ISSN: 2717-8161 RESEARCH ARTICLE

New Trend Med Sci 2020; 1(2): 123-131. https://dergipark.org.tr/tr/pub/ntms

18ß-Glycyrrhetinic Acid Reduces Vasospasm After Aneurysmal Subarachnoid Hemorrhage in an Experimental Model

Ahmet Yardım[1*], Ramazan Paşahan[2], Mustafa Namık Öztanır[3], Osman Çiftçi[4], Aslı Çetin[5], Mehmet Arif Aladağ[2], Mehmet Akif Durak[2]

[1]Department of Neurosurgery, Private Buhara Hospital, Erzurum, Turkey
[2]Department of Neurosurgery, Faculty of Medicine, İnönü University, Malatya, Turkey
[3]Department of Neurosurgery, Faculty of Medicine, Bezmi Âlem University, İstanbul, Turkey
[4]Department of Medical Pharmacology, Faculty of Medicine, Pamukkale University, Denizli, Turkey
[5]Department of Histology and Embryology, Faculty of Medicine, İnönü University, Malatya, Turkey

Article History
Received 04 Sep 2020
Accepted 24 Sep 2020
Published Online 30 Sep 2020

[*]***Corresponding Author***
Dr Ahmet Yardım
Private Buhara Hospital,
Erzurum, 25240, Turkey,
Phone: +90505 246 86 65,
E-mail: drahmetyardim01@gmail.com
ORCID: https://orcid.org/0000-0003-1134-6050

Abstract: This study investigated that the beneficial effects of 18ß-Glycyrrhetinic acid (GA) on cerebral vasospasm in subarachnoid hemorrhage (SAH). A total of 28 Spraque-Dawley adult rats were used. Group 1 (Control) (n=7), Group 2 (SAH) (n=7), Group 3 (SAH+GA 50) (n=7), and Group 4 (SAH+GA 100) (n=7). GA performed through gavages in the 30th minute, 12th hour and 24th hour starting from SAH process. The animals sacrificed under intraperitoneal injection anesthesia by taking biochemical and histopathologic samples at the end of 48th hour. TBARS, SOD, CAT, GSH and GPx values were examined in biochemical studies. Brain tissue and basilar arteries were evaluated in histopathological examination. The averages of lumen cross section in histopathologic, morphometric terms and the biochemical values in both groups receiving GA were found different at meaningful levels compare, the biochemical values were found different meaningfully especially in high dose GA group compared to those groups not receiving GA statistically. The results were defined as Mean±Standard Deviation, and $p<0.05$ values were accepted as meaningful statistically. Based on our results, high dose GA found useful in experimental medical treatment of cerebral vasospasm due to SAH. ©2020 NTMS.
Keywords: Subarachnoid Hemorrhage (SAH), Serebral Vasospasm, 18ß Glycyrrhetinic Acid.

1. Introduction

In cranial or spinal region, in the subarachnoid space containing the cerebrospinal fluid between piamater and arachnoid membrane, hemorrhage that occur due to various reasons are called subarachnoid hemorrhage (SAH) (1-3).

Most frequent cause of SAH is traumas. Any SAH with etiologies other than trauma are called primer SAH or spontaneous SAH; and spontaneous SAH may occur because of many different etiologies. Most frequent cause of spontaneous SAH is aneurism ruptures (4). Consensus is not available about its incidence because of different life style, genetic structure, and various risk factors in different populations. Rebleeding and vasospasm in patients with SAH form most significant

Cite this article as: Yardım A, Paşahan R, Öztanır MN, Çiftçi O, Çetin A, Aladağ MA and Durak MA. 18ß-Glycyrrhetinic Acid Reduces Vasospasm After Aneurysmal Subarachnoid Hemorrhage in an Experimental Model, *New Trend Med Sci* **2020**; 1(2): 123-131.

reasons for high mortality and morbidity. Recently, there has been a decrease in the rates of mortality and morbidity based on rebleeding due to early surgical treatment to SAH patients by neurosurgery clinics. In line with such developments, protection, and treatment of vasospasm, being the other most significant cause of mortality and morbidity in SAH patients, gained importance.

Cerebral vasospasm is pathologic stenosis that occurs in cerebral arteries following SAH. Cerebral vasospasm may be diagnosed by the observation of ischemia that occurs in some part of brain following SAH clinically, neurological deterioration that develops in connection with infarcts and stenosis in cerebral artery lumen by radiological means. Cerebral vasospasm is a clinic diagnosis and radiological observation does not make diagnosis alone. It only supports the clinical diagnosis.

Although physiopathology of cerebral vasospasm has been the subject of many studies, it could not been clarified fully. There have been different hypotheses about physiopathology. One of those hypotheses suggested and accepted is the formation of oxyhaemoglobin with deterioration of erythrocytes at subarachnoid distance and that such oxyhaemoglobin is the main spasmogenic responsible in cerebral vasospasm (5-7). Furthermore, it is known that, in cerebral vasospasm, there is reduction in brain perfusion in the distal of artery narrowing in connection with pathologic vasoconstriction and that, as a result, there is oxidative stress in brain tissue due to ischemia/reperfusion. Free oxygen radicals that occur on hypoxic ground are considered as the primary responsible for brain tissue damage during oxidative stress. Antioxidants prevent vasoconstriction making effect of free oxygen radicals that occur during the transition of oxyhaemoglobin into methaemoglobin, which is one of the accepted pathophysiology hypotheses of cerebral vasospasm (5-8).

18β-Glycrrhetinic acid (GA) as we use in our study is a hydrolyzed metabolite of glycyrrhizin. GA is a material known as licorice root extract contained in Glycyrrhiza glabra (licorice) plant that has a wide area of use in traditional Chinese and Japanese alternative medicine (9). Recent studies have shown that GA has strong anticancer, anti-inflammatory, and antioxidant properties (10, 11).

We aimed in this study to determine that GA, having the property of inducing antioxidant defense mechanisms, may prevent cerebral vasospasm in SAH patients and determine how the dose dependent results of its effect reducing the brain tissue damage in connection with ischemia/reperfusion in cerebral vasospasm may be.

2. Material and Methods

2.1. Animals and experimental protocol

The present study was approved by the Ethics Committee on Animal Research of İnönü University and carried out in accordance with The Guidelines for Animal Research from the National Institutes of Health (NIH). Spraque-Dawley male rats weighing 230-250 g were supplied by the İnönü University Laboratory Animals Research Center (Malatya, Turkey), housed in sterilized polypropylene cages, and given an ad libitum diet of standard commercial food pellets and water. All rats were kept under a 12:12 hours light: dark cycle at 22±1 °C ambient temperature and 55±5% humidity.

In this study, the groups were arranged as Group 1 (Control) (n=7) was the one without any processes, Group 2 (SAH) (n=7) that did not receive any treatment following SAH process, Group 3 (SAH+GA 50) (n=7) that received GA, dissolved in corn oil at an amount of 0.5 ml/12.5 mg on the 30th minute, 12th hour and 24th hour starting from SAH process through gavages, and Group 4 (SAH+GA 100) (n=7) that received 1 ml/25 mg GA dissolved in corn oil through gavages in the 30th minute, 12th hour and 24th our starting from SAH process. Totally 28 Spraque-Dawley adult rats were used. The animals in all groups were sacrificed under intraperitoneal injection anesthesia by taking biochemical and histopathologic samples at the end of 48th hour. GA (Sigma-Aldrich, Product No: G10105) was used in our study. GA was prepared by dissolving in corn oil as 25 mg in 1 ml.

2.2. Subarachnoidal hemorrhage model

Following anesthesia, all the rats were shaved between inion and atlas. After cleaning the field with Batticon, approximately 2 cm of skin region was prepared between inion and atlas. Afterwards, the rats in all groups other than the control group were brought to supine position. Abdominal region was cleaned with Batticon; and following skin incision, abdominal aorta was revealed. Abdominal aorta was catheterized and 0.3 ml nonheparinized arterial blood was taken. Then the rats were brought back to prone position. Head was brought to hyperflexion and cisterna magna was entered using PPD injection at the distance of atlanto-occipinal. Cerebrospinal fluid (CSF) of all the rats other than the control group was drained at equal amounts (0.2 ml). Then with the same rats, non-heparinized blood taken from abdominal aorta was injected slowly at equal amounts (0.2 ml). Following this, the rats were kept in trendelenburg position for 15 minutes on the table prepared before to ensure distribution of blood to prepontine cistern. The rats were taken to their cages after waking up.

2.3. Sacrification

Anesthesia was performed on all rats at the end of 48 hours through intraperitoneal injection of the mixture of Ketamine Hydrochloride (60 mg/kg) (Ketalar, Parke Davis) and Xylazine Hydrochloride (10 mg/kg) (Rompun 2% Bayer) by spontaneous respiration. Thoracotomy was applied to all rats following anesthesia. Following thoracotomy, blood drawing started. Left ventricle was entered and 6 cc of blood in

average was drawn from all subjects. Following blood drawing, intracardiac serum physiologic was applied for 5 minutes and tissue perfusion was performed. Thus, brain tissue was mad free of blood elements. Then all subjects were subjected to bilateral frontoparietooccipital craniectomy. The cerebrum, cerebellum and brain stem remaining on the foramen magnum were removed totally by protecting the anatomic integrity.

Macroscopically, subarachnoid hemorrhage was observed prevalently around the vertebral artery and basilar artery on the basal surface of brain stem in all subjects subjected to SAH. Cross sections of brain tissue involving the basilar artery were taken. Those cross sections were fixed by placing in 10% formaldehyde. The samples taken for the purpose of preparing tissue homogenates were stored inside aluminum foil at -30 °C.

The tissues were weighted and placed in glass tubes. 1.15% of potassium chloride was added thereon as dilution at a rate of 1/10 (g/h) and then they were homogenized for 3 minutes at 16.000 cycles/minute in homogenizers of glass-teflon deepfreeze by maintaining their coolness. Tissue protein determinations were performed on such homogenates prepared. The remaining homogenate was centrifuged at 3500 rpm for 45 minutes at +4 °C and supernatant was obtained.

Glutathione (GSH) and protein levels as well as glutation peroxidase (GSH-Px) and catalase (CAT) enzyme activities were measured in those supernatants. The reagent formed of the mixture of chloroform/ethanol (3/5, h/h) was added to the remaining supernatant at a rate of 1/1 (h/h) and was mixed using vortex. Then, it was centrifuged at 3500 rpm for 45 minutes. Tissue superoxide dismutase (SOD) enzyme activity and protein measurements were performed again at the chloroform/ethanol phase on top.

2.4. Biochemical examinations

SOD activity measurement was done based on the method specified by Sun et al. (12). GSH-Px activity determination was done based on the method specified by Beutler (13). CAT enzyme activity determination was done based on the method specified by Aebi. (14). In reduced GSH measurement, the activity was determined based on the method identified by Ellman as dithionitrobenzoic acid recycling method (15). In Tissue Protein Measurement (TBARS), the determination of protein quantity in homogenate and supernatants were done based on the method defined by Lowry at al. (16).

2.5. Histological examinations

The tissue samples were determined for 48 hours inside 10% formaldehyde. Following the determination, histological tissue tracking procedure was applied on the tissue samples and embeded in paraffin blocks. Cross sections of 5µm thickness were taken from paraffin blocks with the help of microtome. Those cross sections were dyed by using Hematoxylin-Eosin dyeing method and were examined and photographed by using Leica DFC 280 light microscope and Leica Q Win Image Analysis System (Leica Microsystems Imaging Solutions, Cambridge, UK).

Transverse sections of basilar arteries in the histological cross sections dyed with Hematoxylin-Eosin were evaluated in histopathologic terms by light microscope. The diameter of basilar arteries, lumen diameter of basilar arteries, and vein wall thickness were measured by using Leica Q Win Image Analysis System.

2.6. Statistical Analysis

Statistical evaluations were performed by using "SPSS for Windows 12.0" package program. Since the data following normality test were in conformity with non-parametric test assumptions, Kruskal-Wallis H variance analysis was used in the comparison of groups. Significances were evaluated by making paired comparisons through Mann-Whitney U test. The results were defined as Mean±Standard Deviation and $p<0.05$ values were accepted as meaningful statistically.

3. Results

3.1. Biochemical findings

The values of TBARS, SOD, CAT, GSH and GPx levels are shown in Table I. As a result of the evaluations, it was determined that the TBARS level, being the indicator of oxidative damage in rats with SAH, increased meaningfully in statistical terms compared to the control and all other groups. Furthermore, it was determined that it caused significant degree of decrease statistically in GSH, SOD, GPx and CAT levels being antioxidant defense system elements in connection with the formation of SAH in the same trial group.

Furthermore, it was determined that there was meaningful level of decrease statistically in the increase of TBARS caused by SAH in GA treatment and that such decrease was shaped in connection with the dosage to the extent that the decrease in TBARS level and the reversal of effects of SAH were more apparent in the group treated with a dosage of 100 mg/kg compared to the group treated with a dosage of 50 mg/kg. It was observed that the TBARS value in the group of high GA dose approached the value of control group and that there was no more a difference between the two groups statistically. In addition, it was determined that GA treatment partially reversed the changes caused by SAH in antioxidant defense systems again in connection with the dosage. It was determined that low dose GA treatment caused meaningful levels of parameters approach normal in GSH, SOD and GPx levels compared to SAH group; however, that there was not any improvement with low dose GA at only CAT level. It was observed that in high dose GA treatment, there were meaningful statistical increases in all parameters compared to SAH group and the values ap-

proached the control group as a result of such increases. It was determined that the changes that occurred when high dose and low dose GA groups were compared changed in all parameters in connection with the dose; and that there were meaningful differences statistically in the groups of high treatment compared to the groups with low dose GA.

3.2. Histopathologic findings:

Brain tissue in the control group was observed with normal histological appearance. In the brain tissue samples of SAH group dyed with Hematoxylin-Eosin, the congestion and cell infiltration (Figure 1A), vascular congestion (Figure 1B), cell infiltration (Figure 1B, 1C, 1D, 1F) and hemorrhage (Figure 1E, 1F) were observed in piamater layer. However, it was determined that 18β-GA application reduced the histopathologic damage in the group of SAH model and remedied such negative effects at meaningful levels. Namely, it was determined that high dose (100 mg/kg) GA application changed the histological damage positively at meaningful level compared to low dose (50 mg/kg) GA application. It was observed that the neurons in brain cortex in the control group had normal histological appearance (Figure 2A). It was determined that, in SAH group (Figure 2B), there were quite a lot degeneration in such neurons; however, 50 mg/kg (Figure 2C) and 100 mg (Figure 2D) GA application caused significant level of decrease in the neuron damage in connection with the dose. In addition to this, it was determined that purkinje cells had normal histological appearance in control group (Figure 3A) when the cerebellum region was examined, and in the group of SAH model (Figure 3B), there were apparent degeneration in purkinje cells.

Again, it was determined that GA meaningfully reversed the cell damage that occurred in 50 mg/kg (Figure 3C) and 100 mg/kg (Figure 3D) doses in connection with the dose.

Basilar artery examination:

It was observed through light microscope examination in control group that basilar artery structure had normal histological appearance. It was observed that intima, media and adventitia layers from the inside out were of normal histological structure. Single layer of flat endothelial cells, circular course smooth muscle cells, and the connective tissue surrounding such formations had normal histological appearance. It was determined that there was meaningful decrease in basilar artery and lumen diameter of basilar artery in SAH group; on the other hand, there was increase in vein wall thicknesses. Decrease in the folds of lamina elastica interna and increase in the contraction of smooth muscle cells of media layer was determined. Furthermore, cytoplasmic vacuolization in smooth muscle cells was distinctive. Moreover, it was determined that GA applications reversed the changes that occurred in basilar artery and caused by SAH meaningfully in connection with the dose (Figure 4).

It was observed through light microscope that the increase in vein wall thicknesses regressed and there was increase in basilar artery diameter and lumen diameter (Table 2). Furthermore, GA application caused minimal contraction in smooth muscle cells and significant decrease in cytoplasmic vacuolization.

Table 1: The values of TBARS, SOD, CAT, GSH and GPx levels in the brain tissue of rats(n=7), (Mean±Standard Deviation).

	Group 1	**Group 2**	**Group 3**	**Group 4**
TBARS nmol/g tissue	8.62 ± 0.46^{a}	18.2 ± 0.93^{b}	14.1 ± 1.21^{c}	9.3 ± 0.96^{d}
GSH nmol/ml	219.8 ± 6.7^{a}	113.9 ± 8.1^{b}	158.8 ± 11^{c}	201.1 ± 9.1^{d}
CAT k/mg protein	0.024 ± 0.001^{a}	0.011 ± 0.001^{b}	0.012 ± 0.001^{c}	0.018 ± 0.001^{d}
SOD U/mg protein	32.60 ± 1.23^{a}	17.16 ± 1.91^{b}	23.81 ± 1.86^{c}	28.15 ± 2.19^{d}
GPx U/mg protein	280.6 ± 12^{a}	165.4 ± 11^{b}	203.6 ± 19^{c}	255.4 ± 17^{d}

Letters a,b,c, and d on the same column show the statistical difference between the groups ($p\leq0.01$).

Table 2: Basilar artery dimension, basilar artery lumen diameter and basilar artery wall thickness values in groups applied with SAH and GA (n=7), (Mean±Standard Deviation).

	Group 1	Group 2	Group 3	Group 4
Diameter of basilar artery	172.98±35.00[a]	106.57±11.66[b]	120.57±10.91[c]	143.48±3.81[d]
Lumen diameter of basilar artery	102.32±23.45[a]	57.65±7.76[b]	65.69±2.08[c]	71.10±9.84[d]
Wall thickness of basilar artery	25.01±1.50[a]	39.95±9.67[b]	38.40±4.34[c]	36.84±3.87[d]

Letters a,b,c, and d on the same column show the statistical difference between the groups (p≤0.01).

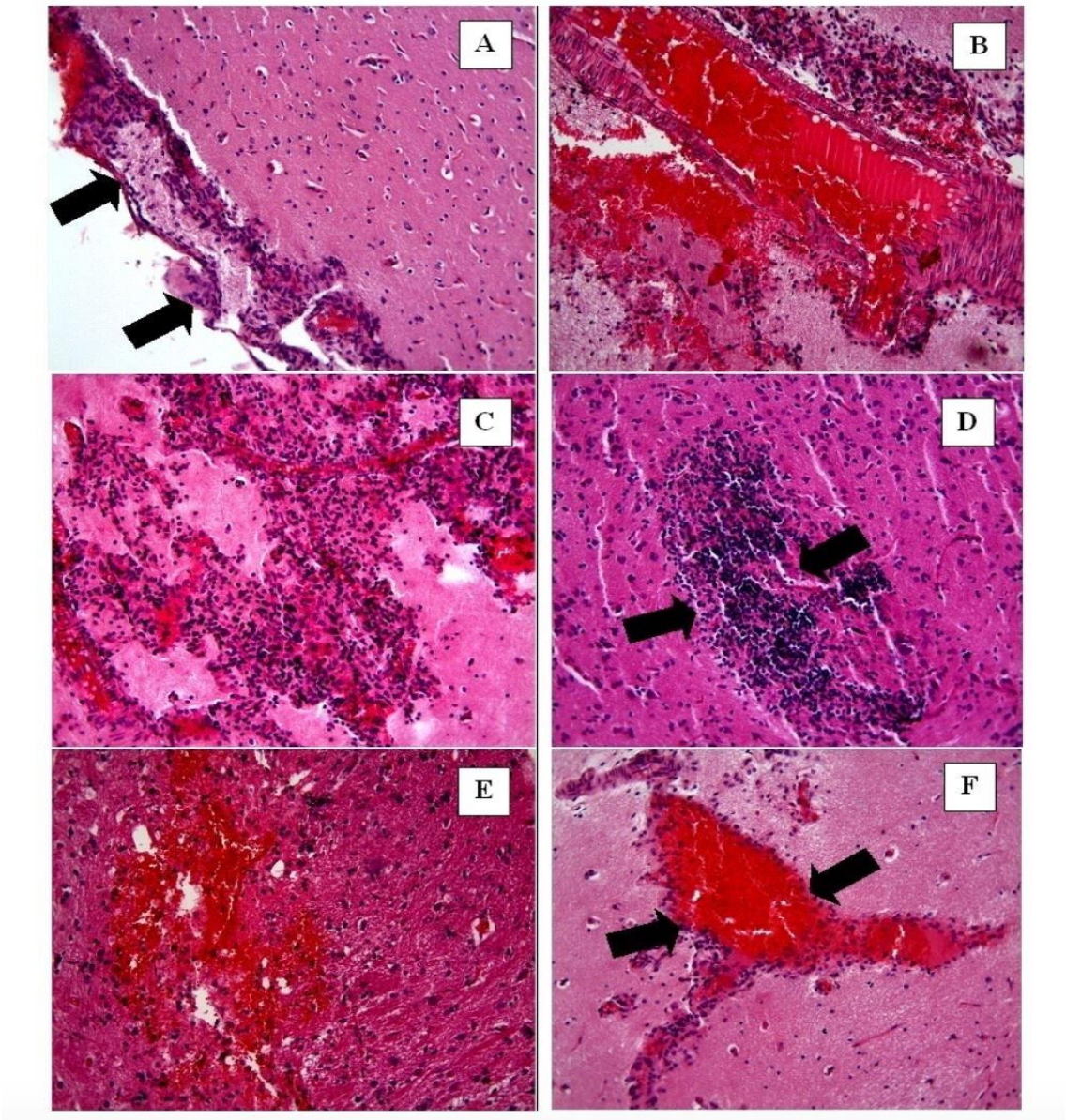

Figure 1: Group 1; In piamater layer, cell infiltration and congestion (arrows) (A), in brain tissue, vascular congestion (B) and cell infiltration (B, C, D, F), hemorrhage (E, F). A, B, C, E, F: H- E; x20, D: Hematoxylin Eosin; x40.

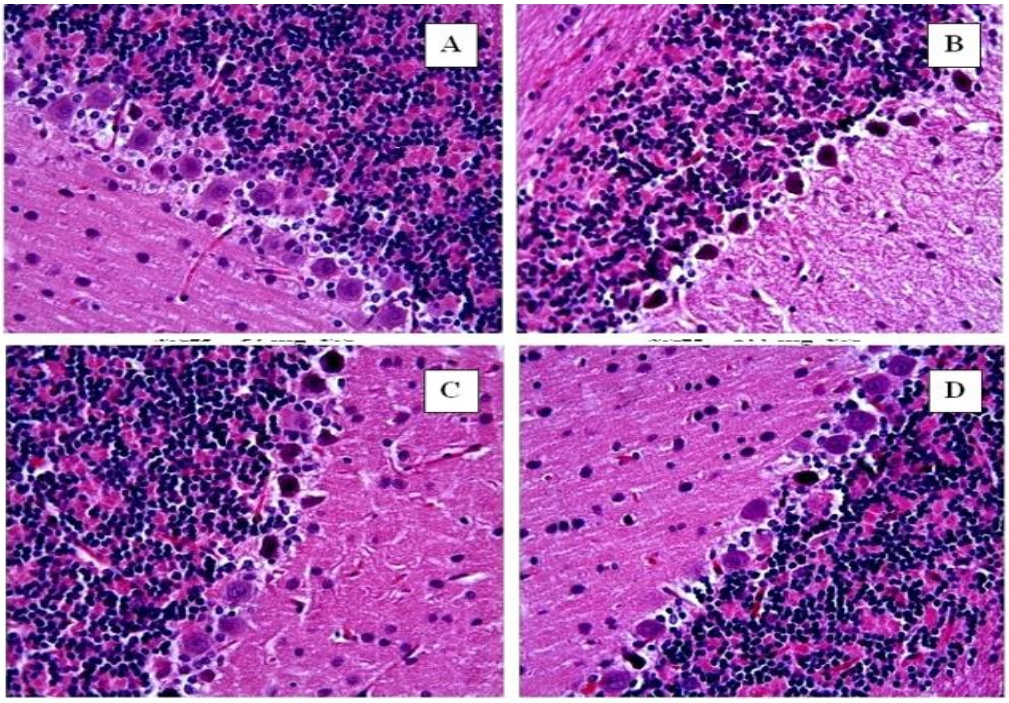

Figure 2: Group 1; (A) Purkinje cells with normal histological appearance. Group 2; (B) degenerated purkinje cells, group 3 (C) and group 4 (D); decrease in degenerated cells. A, B, C, D: H-E; x40.

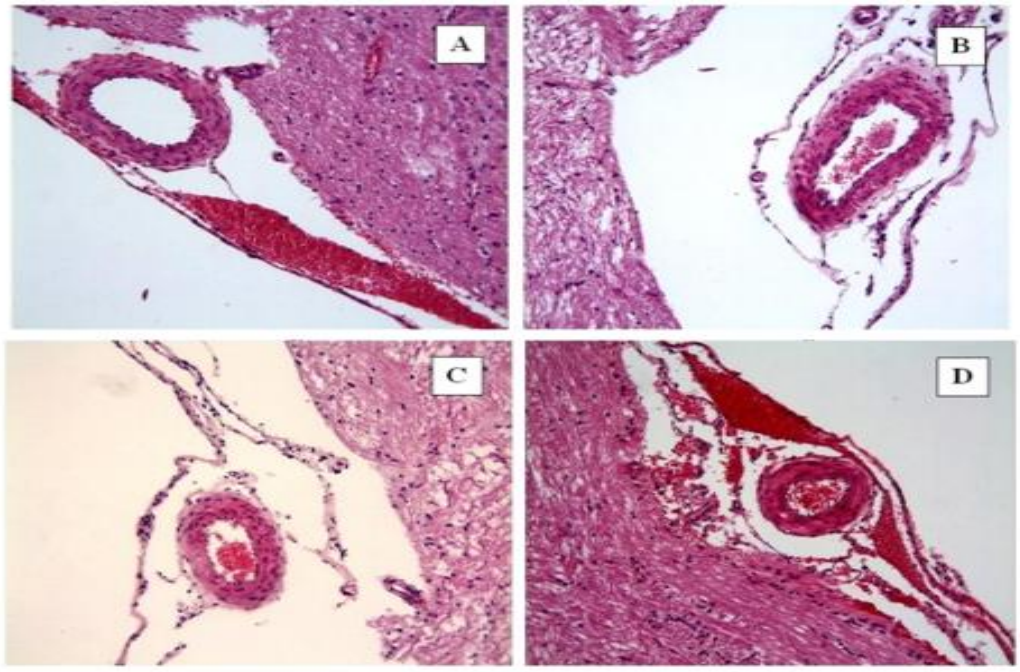

Figure 3: Basilar artery cross sections in group 1 (A), group 2 (B), group 3 (C), group 4 (D) groups. H-E; x20.

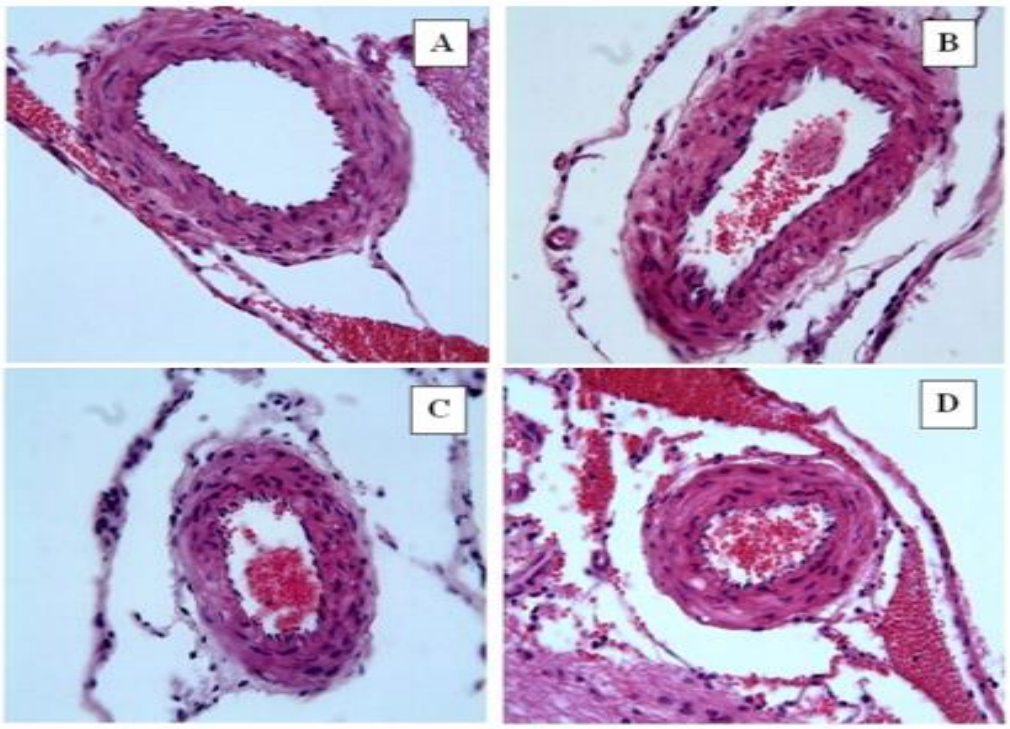

Figure 4: Basilar artery cross sections in group 1(A), group 2 (B), group 3 (C), group 4 (D) groups. Hematoxylin-Eosin; x40.

In addition, it was determined that there was endothelial structure of normal appearance and minimal vacuolization in smooth muscle cells in the group provided with 100 mg/kg GA.

4. Discussion

Cerebral vasospasm is late term recyclable pathological stenosis of large diameter arteries in brain basis. Such pathologic stenosis causes perfusion decrease in brain tissue in the distal of artery of stenosis and consequently ischemic brain damage. Cerebral vasospasm that develops following the subarachnoid hemorrhage in connection with the aneurism rupture is responsible at first degree of late ischemic neurological deficit in aneurism patients and it is the most importance cause of mortality and morbidity (17-19).

The existence of cerebral vasospasm in the first two week following SAH increases mortality from 1.5 times up to 3 times (20). Vasospasm is observed in 70% of aneurismal subarachnoid hemorrhage patients and symptomatic cerebral vasospasm and ischemia is seen in 30-40% of the same. It was notified in joint aneurism study that angiographic vasospasm incidence was in more than 50% of patients and symptomatic vasospasm was in 32% of the patients (17, 20, 21).

Since cerebral vasospasm is considered as the primary responsible of mortality and morbidity in SAH patients that develop in connection with the aneurism rupture, the pathophysiology and treatment of cerebral vasospasm has been the subject of many researches from the description of angiographic vasospasm until today.

Although many studies were performed, the physiopathology and medical treatment of cerebral vasospasm has not been revealed fully yet because of being multifactorial etiology. Clinical and experimental studies are still continued because it can not be revealed. This experimental study was planned for the purpose of developing a pharmacological treatment alternative for vasospasm.

The studies are performed on animal models because of the impossibility to make experimental study on cerebral arteries in human. Ideal subject should be resistant against the efficiency and toxicity of the treatment applied. The applied SAH model should be realized close to the subarachnoid hemorrhage that develops following the aneurism rupture in human. Rats are ideal choice for SAH models that are inexpensive and much easy to use compared to large laboratory animals.

Solomon et al. compared cerebral blood flow before and after SAH in rats and they noted that rates are a potential experimental model for SAH studies. Again according to the same study, they informed that the vasospasm in basilar artery following SAH showed same characteristics with the vasospasm in humans (22). Rats were preferred in this study because of finding them easily, because they are inexpensive, they are easy to maintain, and they are still a current model. Acute vasospasm in rats reach maximum in hour 48. Therefore, the rats were sacrificed in 48th hour in our study. It is reached in 7th day maximum in humans. The rate of neurological deficit in connection with vasospasm is low in rats compared to humans. This is because of the collateral circulation in rat brains.

There are three main methods as experimental SAH

development technique. The technique in which congestion is enabled around by perforating a basilar artery or a large artery; the technique in which the artery is dissected surgically and autologous blood taken from another artery is placed around the artery; the technique in which autologous arterial blood is injected to the subarachnoid space form the three main techniques (23). On the basis of these techniques, many different methods were developed. The SAH formation technique in which the autologous blood is injected to subarachnoid space is the most frequently used techniques in the studies. Our study also developed SAH using this technique.

Previously in our study, the method used by Yu-shu Dong et al., in which medication was performed in 30th minute, 12th hour, 24th hour and sacrification was performed on 48th hour following the development of SAH, was used (24).

It was determined in our experimental examination that GA application reduced the histopathologic damage in the group of SAH model and that remedied the negative effects meaningfully. It was determined that high dose (100 mg/kg) GA application changed the histological damage at more meaningful level and positively compared to low dose (50 mg/kg) GA application. In our study, it was determined through the light microscopic examination that GA application reversed the changes, which occurred in basilar artery and caused by SAH, meaningfully in connection with the dose.

Free oxygen radicals are developed in connection with oxidative stress in brain tissue in biochemical terms in cerebral vasospasm. It is known that, with those free oxygen radicals, lipid peroxidation developed and tissue TBARS level increased, causing decrease in antioxidant defense system elements such as SOD, CAT, GPx and GSH (25).

Based on the results obtained in our study, TBARS level, being the indication of oxidative damage in rats with SAH, was increased meaningfully in statistical terms compared to control and all other groups. Furthermore, it caused significant level of decrease statistically in levels of GSH, SOD, GPx and CAT, being antioxidant defense system elements, in connection with the development of SAH in the same test group. It was determined that GA treatment decreased meaningfully in statistical terms in the increase of TBARS caused by SAH and that such decrease was shaped in connection with the dose. The decrease in TBARS level and the reversal of effects of SAH were more apparent in the group treated with a dosage of 100 mg/kg compared to the group treated with a dosage of 50 mg/kg. It was observed that the TBARS value in the group of high GA dose approached the value of control group and that there was no more a difference between the two groups statistically. In addition, it was determined that GA treatment partially reversed the changes caused by SAH in antioxidant defense systems again in connection with the dosage. It was determined that low dose GA treatment caused meaningful levels of parameters approach normal in GSH, SOD and GPx levels compared to SAH group; however, that there was not any improvement with low dose GA at only CAT level. It was observed that in high dose GA treatment, there were meaningful statistical increases in all parameters compared to SAH group and the values approached the control group as a result of such increases.

Moreover, it was determined that the changes that occurred when high dose and low dose GA groups were compared changed in all parameters in connection with the dose; and that there were meaningful differences statistically in the groups of high treatment compared to the groups with low dose GA.

In our study, we wished to examine whether GA, being an antioxidant, had an effect to settle vasospasm and to reduce brain tissue damage in connection with vasospasm. The averages of lumen cross section in histopathologic and morphometric terms in both groups receiving GA were found different at meaningful levels compared to other groups. Likewise, the biochemical values were found different meaningfully especially in high dose GA group compared to those groups not receiving GA statistically. Based on our results, GA was found beneficial in the experimental medical treatment of cerebral vasospasm.

5. Conclusions

Although there have been many studies performed on this issue, medical treatment of cerebral vasospasm has not been revealed fully yet because of having multifactorial etiology. GA has an effect to reduce brain tissue damage in connection with the ischemia/reperfusion that develops in cerebral vasospasm through the induction of antioxidant defense system and to prevent the development of vasoconstriction. Therefore, we consider that GA may be tried as an alternative agent against a situation of high mortality and morbidity such as vasospasm.

Conflict of interest statement

All authors declared that there is no conflict of interest.

Financial Support

None

Compliance with ethical standards

The study was carried out in accordance with ethical standards in all aspects.

References

1. Weir B, Macdonald RL. Intracraial aneurysms and subarachnoid hemorrhage. An overview. In: Wilkins DH, Regechary SS, (editors). Neurosurgery. 2 nd ed. New York, USA: **1996**. pp. 91- 211.
2. Linn FH, Rinkel GJ, Algra A, van Gijn J. Incidence of subarachnoid hemorrhage: role of region, year, and rate of computed tomography: a meta-analysis.

Stroke **1996**; 27: 625-629.
3. Pfohman M, Criddle LM. Epidemiology of intra cranial aneurysm and subarachnoid hemorrhage. *J Neurologic Surg* **2001**; 33: 39-40.
4. Juul R, Fredriksen TA, Ringkjob R. Prognosis in subarachnoid hemorrhage of unknown etiology. *J Neurosurg* **1986**; 64: 359-62
5. Weir BKA, McDonald RL, Stoodley M: Etiology of cerebral vasospasm. *Acta Neurochir (Wien)* **1999**; 72: 27-46.
6. Pluta RM, Afshar JK, Boock RJ, Oldfield EH. Temporal changes in perivascular concentrations of oxyhemoglobin, deoxyhemoglobin and methemoglobin after subarachnoid hemorrhage. *J Neurosurg* **1998**; 88: 557-561.
7. Macdonald RL: Pathophysiology and molecular genetics of vasospasm. *Acta Neurochir Suppl (Wien)* **2001**; 77: 7-11.
8. Takao Asano1, 2 and Toru Matsui1 Antioxidant Therapy Against Cerebral Vasospasm Following Aneurysmal Subarachnoid Hemorrhage. *Cel Mol Neurobiol* **1999**; 19: (31-44).
9. Kim YJ, Lee CS. Glycyrrhizin attenuates MPTP neurotoxicity in mouse and MPP-induced cell death in PC12 cells. *Korean J Physiol Pharmacol* **2008**; 12: 65–71.
10. Matsui S, Matsumoto H, Sonoda Y, Ando K, Aizu-Yokota E, Sato T, Kasahara T. Glycyrrhizin and related compoundsdown-regulate production of inflammatory chemokines IL-8 and eo- taxin 1 in a human lung fibroblast cell line. *Int Immunopharmacol* **2004**; 4: 1633–1644.
11. Agarwal MK, Iqbal M, Athar M. Inhibitory effect of 18 betaglycyrrhetinic acid on 12-Otetradecanoyl phorbol-13 acetate-induced cutaneous oxidative stress and tumor promotion in mice. *Redox Rep* **2005**; 10: 151–157.
12. Sun Y, Oberley LW, Li Y. A simple method for clinical assay of superoxide dismutase. *Clin Chem* **1988**; 34: 497-500.
13. Beutler E. Red cell metabolism. In: A Manual of Biochemical Methods. *New York: Grune Strottan* **1975**; 67-69.
14. Aebi H. Catalase in vitro assay methods. Methods *Enzymol* **1984**; 105: 121-126.
15. Ellman G. Tissue sulphydryl groups. *Arch Biochem Biophys* **1959**; 82: 70-77.
16. Lowry OH, Rosebrough NJ, Farr AL, Randall RJ. Protein measurement with pholinphenol reagent. *J Biol Chem* **1951**; 193: 265-275.
17. Liu-Deryke X, Rhoney DH. Cerebral vasospasm after aneurysmal subarachnoid hemorrhage: an overview of pharmacologic management. *Pharmacother* **2006**; 26(2); 182-203.
18. Bederson JB, Levy AL, Ding WH, Kahn R, DiPerna CA, Jenkins AL. Acute vasoconstruction after subarachnoid hemorrhage. *Neurosurgery* **1998**; 42: 352-360.
19. Keyrouz SG, Diringer MN Clinical review: Prevention and therapy of vasospasm in subarachnoid hemorrhage. *Crit Care* **2007**; 11(4): 220
20. Reggiari-Venzi MM, Suter PM, Romand JA. Review of medical prevention of vasospasm after aneurysmal subarachnoid hemorrhage: a problem of neurointensive care. *Neurosurg* **2001**; 48: 249-262.
21. Adams HP Jr, Kassell NF, Torner JC, Haley EC Jr. Predicting cerebral ischemia after aneurysmal subarachnoid hemorrhage: influences of clinical condition, CT results, and antifibrinolytic therapy: a report of the Cooperative Aneurysm Study. *Neurology* **1987**; 37: 1586-1591i
22. Solomon RA, Antunes JL, Chen RY, Bland L, Chien S. Decrease in cerebral blood flow in rats after experimental subarachnoid hemorrhage: a new animal model. *Stroke* **1985**; 16(1): 58-64
23. Lynch JR, Wang H, McGirt MJ. Simvastatin reduces vasospasm after aneurysmal subarachnoid hemorrhage: results of a pilot randomizedlinical trial. *Stroke* **2005**; 36: 2024-2026.
24. Yu-shu Dong, Ju-lei Wang, Da-yun Feng. Protective Effect of Quercetin against Oxidative Stress and Brain Edema in an Experimental Rat Model of Subarachnoid Hemorrhage. *Int J Med Sci* **2014**, 11(3): 282-290.
25. Wang JJ, Cui P. Neohesperidin attenuates cerebral ischemia-reperfusion injury via inhibiting the apoptotic pathway and activating the Akt/Nrf2/HO-1 pathway. *J Asian Nat* **2013**; 15(9); 1023-1037.

Authors' ORCID
Ahmet Yardım
http://orcid.org/0000-0003-1134-6050
Ramazan Paşahan
https://orcid.org/0000-0002-3221-1422
Mustafa Namık Öztanır
https://orcid.org/0000-0001-5709-1757
Osman Çiftçi
https://orcid.org/0000-0001-5755-3560
Aslı Çetin
http://orcid.org/0000-0003-3902-3210
Mehmet Arif Aladağ
http://orcid.org/0000-0003-3872-3741
Mehmet Akif Durak
http://orcid.org/0000-0003-0827-2708

https://dergipark.org.tr/tr/pub/ntms

ISSN: 2717-8161 CASE REPORT

New Trend Med Sci 2020; 1(2): 132-136. https://dergipark.org.tr/tr/pub/ntms

Acute Myelitis Secondary to COVID-19 in an Adolescent: Causality or Coincidence?

Muhammet Akif Guler[1]*, Filiz Keskin[2], Hüseyin Tan[2]

[1]Department of Pediatrics, Faculty of Medicine, Atatürk University, Erzurum, Turkey
[2]Department of Pediatric Neurology, Faculty of Medicine, Atatürk University, Erzurum, Turkey

Article History
Received 18 Aug 2020
Accepted 10 Sep 2020
Published Online 30 Sep 2020

****Corresponding Author***
Dr Muhammet Akif Guler
Department of Pediatrics,
Faculty of Medicine,
Atatürk Univeristy, 25240, Erzurum, Turkey,
Phone: +904423449685
E-mail: akif2532@gmail.com
ORCID: https://orcid.org//0000-0002-3147-6429

Abstract: Coronavirus disease 2019 (COVID-19) first emerged in Wuhan, China in December 2019. Headache, dizziness, attenuated taste/smell, stroke, acute disseminated encephalomyelitis, encephalitis, Guillain-Barré syndrome, and myelitis are rare neurological symptoms and complications reported in adults. A 14-year-old girl presented with sudden-onset loss of strength in her right arm and leg. A nasopharyngeal swab was collected because the patient had a history of suspicious contact with a confirmed COVID-19 patient. SARS-CoV-2 nucleic acid testing of the patient's nasopharyngeal swab was positive. Her clinical presentation suggested transverse myelitis. On spinal MRI, a contrast-enhancing lesion causing expansion at the C2-C5 level was observed. On day 5 of pulse methylprednisolone treatment, the patient had 3/5 muscle strength in her right upper extremity and 5/5 muscle strength in her right lower extremity. This case emphasizes that during the pandemic, SARS-CoV-2 must be considered as the etiology in children presenting with neurological involvement if there is a history of contact.
Keywords: Acute Myelitis, COVID-19, Child.

1. Introduction

In December 2019, a large outbreak of pneumonia was reported in Wuhan, China (1). The disease, caused by the novel coronavirus SARS-CoV-2, was named Coronavirus disease 2019 (COVID-19) by the World Health Organization (WHO). On March 11, 2020, after the disease spread to dozens of countries, WHO declared COVID-19 a pandemic (2). The first case in Turkey was detected on March 10, 2020 (3).

COVID-19 is highly contagious and its clinical spectrum varies from asymptomatic infection to deadly pneumonia (2).

However, in series of suspected or confirmed COVID-19 pediatric patients, it has been reported that 13 to 27% of children positive for the virus had asymptomatic infection (4).

Coronaviruses damage the central nervous system (CNS) by directly infecting the CNS via the olfactory nerve, peripheral nervous system, and circulation or via the immune response they induce (5).

In such cases, COVID-19 patients exhibit neurological symptoms such as dizziness, headache, altered consciousness, ataxia, epilepsy, muscle involvement, loss of smell and taste, nausea, and vomiting (6,7).

Although cases of encephalopathy, viral encephalitis/meningitis, peripheral neuropathies, and Guillain-Barré syndrome have been reported in adult COVID-19 patients (6-9) there are few studies reporting the neurological involvement of COVID-19 in pediatric patients.

Cite this article as: Guler MA, Keskin F and Tan H. Acute Myelitis Secondary to COVID-19 in an Adolescent: Causality or Coincidence?, *New Trend Med Sci* **2020**; 1(2): 132-136.

In this report, we present the case of an adolescent who developed transverse myelitis presumably caused by SARS-CoV-2.

2. Material and Methods

2.1. Case

A 14-year-old girl presented to Atatürk University Faculty of Medicine on April 12, 2020 with sudden-onset loss of strength in her right arm and leg. Her vital signs were as follows: pulse: 82 beats/min, respiratory rate: 21 breaths/min, blood pressure: 115/83 mmHg, oxygen saturation: >97%, and body temperature: 36.9°C.

Other than right hemiplegia, the results of detailed physical and neurological examination were normal.

A nasopharyngeal swab was collected because the patient had a history of suspicious contact with a confirmed COVID-19 patient. SARS-CoV-2 nucleic acid testing of the patient's nasopharyngeal swab was positive. The patient was admitted to the isolation ward. Her clinical presentation suggested transverse myelitis. Cranial magnetic resonance imaging (MRI) was normal. On spinal MRI, a contrast-enhancing lesion causing expansion at the C2-C5 level was observed (shown in Fig 1, A-D). MR spectroscopy was normal. Routine hematological tests, biochemical tests, acute phase reactants, prothrombin time (PT), partial thromboplastin time (PTT), and international normalized ratio (INR) were normal. The patient's test results are presented in Table 1.

Lumbar puncture was performed. Cerebrospinal fluid (CSF) pressure was 170 mm/H_20, protein: 262 mg/dl, chlorine: 127 mmol/L, glucose: 81 mg/dL (simultaneous blood glucose: 105 mg/dL), and no cells were detected. COVID-19 PCR and COVID-IgM/IgG test of the CSF could not be performed.

Chest X-ray was normal. Venous blood IgM tests were negative for Chlamydia pneumoniae, Epstein–Barr virus (EBV) viral capsid antigen (VCA), Mycoplasma pneumoniae, cytomegalovirus (CMV), rubella, toxoplasma, herpes simplex virus 1 and 2, measles, mumps, parvovirus B19, varicella zoster virus.

Nasopharyngeal swab samples were also negative for influenza A virus, influenza A H1N1, influenza A H3N3, Bordetella pertussis, Bordetella parabronchi, Bordetella holmesii, influenza B virus, adenovirus, parainfluenza virus 1, 2, 3, and 4, rhinovirus, human metapneumonovirus (hMPV), and respiratory syncytial virus A and B. Acid-fast bacilli (AFB) staining of CSF was negative and tuberculosis PCR was also negative. Moreover, tests for Sm/RNP, SS-A, SS-B, dsDNA, ANA, pANCA, and cANCA were negative.

Table 1: Results of Routine Blood and Biochemical Tests.

Indicators (normal range)	**Results**	**Indicators (normal range)**	**Results**
White blood cell (4.5-13.5x10^3 μL)	5.36	Calcium (8.8-10.8 mg/dl)	8.5
Hemoglobin (12-16 g/dl)	14.3	Creatine kinase (50-240 U/L)	92
Platelet count (150-450x10^3 μL)	369	Ferritin (11-306 ng/ml)	20.6
Sedimentation (<20 mm/h)	11	Fibrinogen (220-440 mg/dL)	325
Procalcitonin (0.5-2 ng/mL)	0.02	Albumin (3.5-5.6 g/dL)	3.8
D-dimer (0-500 ng/mL)	356	Lactic dehydrogenase (0-248 U/L)	225
Alanine aminotransferase (5-45 U/L)	55	Glucose (60-100 mg/dL)	81
Aspartate aminotransferase (10-40 U/L)	36	Creatinine (0.5-1 mg/dL)	0.53
Troponin I (0-11.6 ng/L)	4.3	Uric acid (2.6-6 mg/dl)	3.6
C-Reactive Protein (0-5 mg/L)	5.07	Prothrombin time (12-16 s)	14.1
Phosphorus (2.9-5.4 mg/dL)	3.5	International normalized ratio INR (0.9-1.3)	1.04
B12 (180-505 pg/mL)	214	Folate (3.1-19.9 ng/ml)	13.3

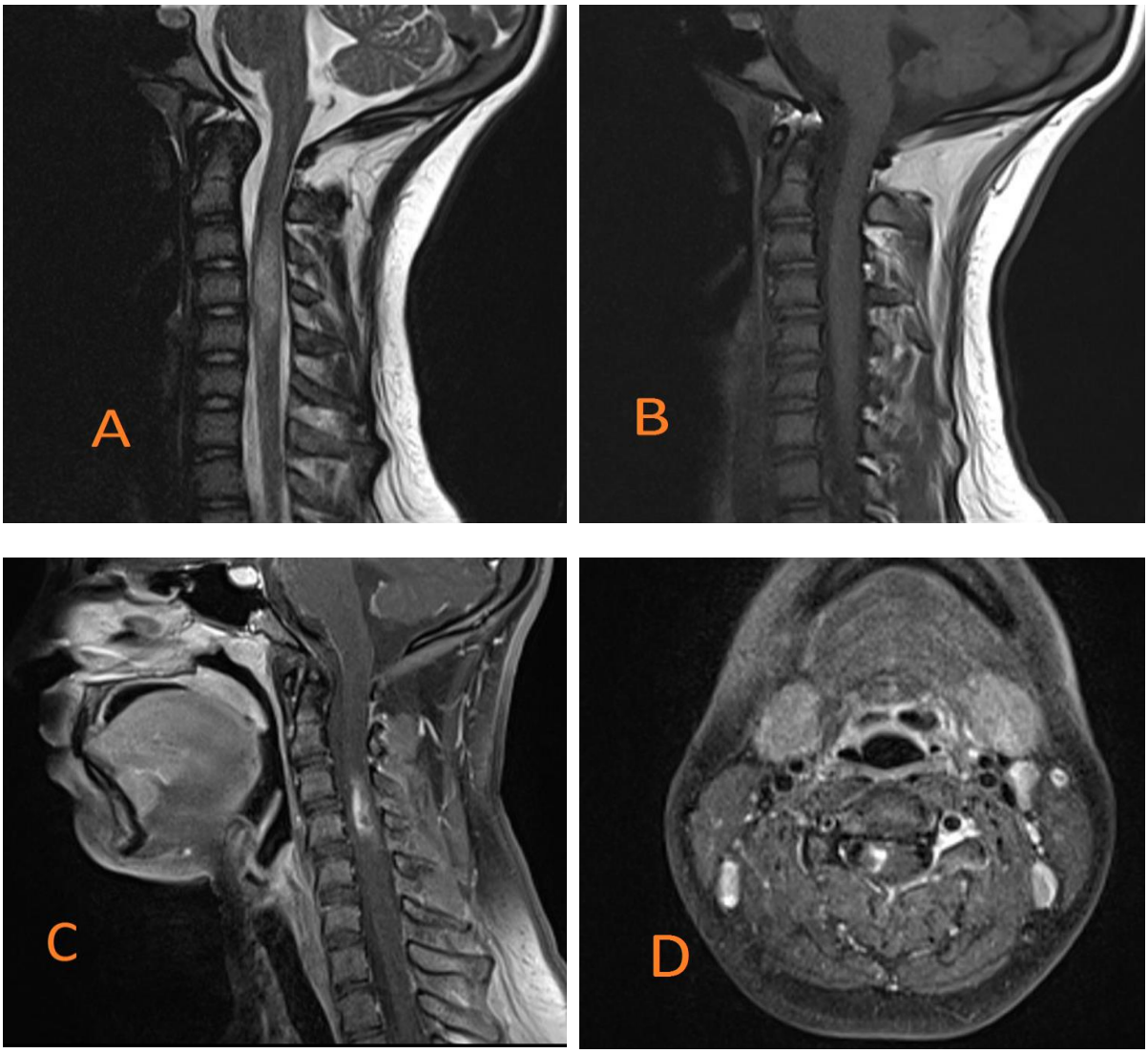

Figure 1: Images of the lesion causing expansion in the medulla spinalis at the C2-C5 level: **A)** Sagittal T2-weighted image showing hyperintense lesion, **B)** Sagittal T1-weighted image showing heterogeneous, iso-hypointense lesion causing medulla spinalis expansion, **C)** Sagittal and **D)** Axial T1-weighted fat-suppressed contrast-enhanced images showing marked irregular contrast enhancement surrounding the lesions.

Transverse myelitis associated with SARS-CoV-2 infection was suspected. Intravenous immunoglobulin (IVIg) was administered at 400 mg/kg/day for 5 days. Fentanyl and gabapentin were initiated for neuropathic pain in the patient's right arm and leg. The patient showed no clinical response to IVIg therapy. Pulse methylprednisolone therapy was given at 30 mg/kg/day for 7 days. On day 5 of steroid treatment, the patient had 3/5 muscle strength in her right upper extremity and 5/5 muscle strength in her right lower extremity.

She exhibited right foot drop, but started to walk unsupported. CSF culture was negative. Serum anti-NMO IgG and CSF oligoclonal band were negative. Serum COVID-19 IgM/IgG test was negative. The patient was recommended home isolation and physical therapy upon discharge 16 days after hospital admission.

3. Discussion

In this report, we present the first pediatric patient with acute transverse myelitis associated with COVID-19. The patient underwent SARS-CoV-2 nucleic acid test due to her history of contact with a confirmed COVID-19 patient and was found to be positive. Moreover, tests for other potential etiologies of acute myelitis were negative. Acute myelitis in this case was either caused by SARS-CoV-2 or occurred coincidentally. However, we believe that the former is more likely.

SARS-CoV-2 enters the human body by binding to ACE2 receptors on cells (10). ACE2 receptors have also been detected on the surfaces of spinal cord neurons (11). Although molecular mimicry is implicated in the pathogenesis of acute myelitis, there may be a relationship between acute myelitis and spinal cord ACE2 receptors. Furthermore, as the liver, bile

ducts, and proximal renal tubules are sites with high ACE2 receptor density like the lungs, COVID-19 can manifest with multiorgan failure in addition to respiratory system signs and symptoms (10).

Many factors play a role in the etiology of postinfectious acute myelitis. The probable pathogenesis of acute myelitis induced by infectious or parainfectious diseases can be explained by the molecular mimicry theory. According to this theory, antigenic structures in the cell walls of pathogenetic microorganisms show antigenic similarity to the surface structures of host neurons. As a result, immune activation against these microorganismic antigens causes cross-reactivity with the antigenic structures on the neuronal surface. This reaction leads to neuronal damage. However, it is not clear why the activated immune system is unable to recognize the host's own cells and tissues (12). Molecular mimic can induce the formation of antibodies that cross-react with self-antigens, leading to immune complex formation and complement-mediated or cell-mediated damage in self tissue (13,14). These autoantibodies may function as an agonist to cellular receptors, altering cellular signaling, metabolism or activity (14). Inflammatory changes were detected in the tissue samples of all patients with a diagnosis of transverse myelitis. These pathologic abnormalities included focal infiltration by monocytes and lymphocytes into segments of the spinal cord and perivascular spaces. Superantigens are peptides capable of stimulating lymphocytes more effectively than conventional antigens. Transverse myelitis may be the fulminant activation of lymphocytes by microbial superantigens. Stimulation of large numbers of lymphocytes can trigger autoimmune disease. Additionally, patients with a diagnosis of transverse myelitis have significantly higher levels of interleukin -6 and nitric oxide in the spinal fluid (15). M. pneumoniae, EBV, CMV, rhinoviruses, and measles are the microorganisms most commonly reported in the etiology (10-12,16).

COVID-19 typically leads to pneumonia characterized by cough, fever, and respiratory distress (1). Neurological involvement in COVID-19 patients is usually reported in adult case studies and manifests with headache, dizziness, and hypogeusia, stroke, coma, and muscle injury (5,6).

Microbiological diagnosis of viral encephalitis is made based on virus isolation, specific IgM positivity, and PCR analysis of the CSF. However, since SARS-CoV-2 titers are very low in the CSF of COVID-19 patients, virus isolation is difficult (17). If we had been able to demonstrate the presence of SARS-CoV-2 in CSF using PCR or specific IgM assay, we could say with more confidence that this case was associated with COVID-19. However, we were unable to perform these tests. Yeh et al. reported a 15-year-old boy with acute disseminated encephalomyelitis in whom human coronavirus (hCoV) was detected in both CSF and nasopharyngeal samples by PCR (18).

Kang Zhao et al. recently reported an adult patient with acute myelitis associated with COVID-19. In their case, acute myelitis was observed together with the typical clinical signs of COVID-19 such as fever, cough, and respiratory distress (10). Moriguchi et al. reported a case of viral encephalitis caused by SARS-CoV-2 in a 24-year-old man. In this case, presence of SARS-CoV-2 in CSF was confirmed via genome sequencing, thus demonstrating that COVID-19 can cause nervous system damage (7). Similarly, among adult COVID-19 patients there are reported cases of Miller Fisher syndrome, polyneuritis cranialis (ageusia, bilateral abducens palsy, areflexia), Guillain-Barré syndrome, encephalopathy, encephalitis, anosmia, acute cerebrovascular disease and stroke (8-10,19).

4. Conclusions

In this report we present the first case of a pediatric patient developing transverse myelitis following SARS-CoV-2 infection and asymptomatic COVID-19. Especially during the pandemic, SARS-CoV-2 should be considered as the etiology in children presenting with neurological involvement if they have a history of risky contact.

Conflict of interest statement

The authors declare that they have no conflict of interest.

References

1. Zhu N, Zhang D, Wang W, et al. A novel coronavirus from patients with pneumonia in China, 2019. *N Engl J Med* **2020**; 382: 727-733.
2. Park SE. Epidemiology, virology, and clinical features of severe acute respiratory syndrome - coronavirus-2 (SARS-CoV-2; Coronavirus Disease-19). *Clin Exp Pediatr* 2020; 63: 119-124.
3. Mehmet Şahin. Impact of weather on COVID-19 pandemic in Turkey. *Sci Total Environ* **2020**; 728: 138810.
4. Bialek S, Gierke R, Hughes M, et al. Coronavirus Disease 2019 in Children United States, February 12–April 2, 2020. *MMWR Morb Mortal Wkly Rep* **2020**; 69: 422-426.
5. YeshunWu, Xiaolin Xu, Zijun Chen, et al. Nervous system involvement after infection with COVID-19 and other coronaviruses. *Brain Behav Immun* **2020**.
6. Werner C, Scullen T, Mathkour M, et al. Neurological Impact of Coronavirus Disease (COVID-19): Practical Considerations for the Neuroscience Community. *World Neurosurg* **2020**; 139: 344-354.
7. Moriguchi T, Harii N, Goto J, et al. A first case of meningitis/encephalitis associated with SARS-Coronavirus-2. *Int J Infect Dis* **2020**; 94: 55-58
8. Consuelo Gutiérrez-Ortiz, Antonio Méndez, Sara Rodrigo-Rey, et al. Miller Fisher Syndrome and polyneuritis cranialis in COVID-19. *Neurology* **2020.**

9. Zhao H, Shen D, Zhou H, et al. Guillain-Barré syndrome associated with SARS-CoV-2 infection: causality or coincidence? *Lancet Neurol* **2020**; S1474-4422(20)30109-5.

10. Zhao K, Huang J, Dai D, Feng Y, et al. Acute myelitis after SARS-CoV-2 infection: a case report. *Med Rxiv* **2020**.

11. Y. Ogata, W. Nemoto, R. Yamagata. Anti-Hypersensitive Effect of Angiotensin (1-7) on Streptozotocin-Induced Diabetic Neuropathic Pain in Mice. *Eur J Pain* **2019**; 23: 739-749.

12. Varina L. Wolf, Pamela J. Lupo, Timothy E. Lotze. Pediatric Acute Transverse Myelitis Overview and Differential Diagnosis. *J Child Neurol* **2012**; 27: 1426-1436.

13. Levin M.C, Lee S.M, Kalume F, et al. Autoimmunity due to molecular mimicry as a cause of neurological disease. *Nat Med* **2002**; 8(5): 509-513

14. DeGiorgio LA, Konstantinov KN, Lee SC, et al. A subset of lupus anti-DNA antibodies cross-reacts with the NR2 glutamate receptor in systemic lupus erythematosus. *Nat Med* **2001**; 7(11): 1189-1193.

15. Krishnan C, Kaplin AI, Deshpande DM, et al. Transverse myelitis: pathogenesis, diagnosis and treatment. *Front Biosci* **2004**; 9: 1483-1499

16. T.W. West, C. Hess, B.A. Cree. Acute Transverse Myelitis: Demyelinating, Inflammatory, and Infectious Myelopathies. *Semin Neurol* **2012**; 32: 97-113

17. Ye M, Ren Y, Lv T. Encephalitis as a clinical manifestation of COVID-19. *Brain Behav Immun* **2020**; S0889-1591(20): 30465-7.

18. Yeh EA, Collins A, Cohen ME, et al. Detection of coronavirus in the central nervous system of a child with acute disseminated encephalomyelitis. *Pediatrics* **2004**; 113(1 Pt 1): 73-76.

19. Ellul M, Benjamin L, Singh B, Lant S, Michael BD, Easton A, et al. Neurological Associations of COVID-19. *Lancet Neurol* **2020**, S1474-4422(20)30221-0.

Authors' ORCID

Muhammet Akif Guler
http://orcid.org/0000-0002-3147-6429
Filiz Keskin
https://orcid.org/0000-0001-8166-5773
Hüseyin Tan
http://orcid.org/0000-0003-3331-1828

https://dergipark.org.tr/tr/pub/ntms

ISSN: 2717-8161 REVIEW ARTICLE

New Trend Med Sci 2020; 1(2): 137-145. https://dergipark.org.tr/tr/pub/ntms

Use of Immun Checkpoint Inhibitor Ipilimumab in Renal Transplant Patients with Advanced Cancer: Is Risk/Benefıt Ratio Dilemma?

Merve Anapalı[1*], Eda Balkan[1]

[1]Department of Medical Biology, Faculty of Medicine, Atatürk University, Erzurum, Turkey

Article History
Received 12 Aug 2020
Accepted 21 Sep 2020
Published Online 30 Sep 2020

[*]***Corresponding Author***
Merve Anapalı
Department of Medical Biology,
Faculty of Medicine,
Atatürk Univeristy, Erzurum, Turkey,
Phone: +90 536 935 1569
E-mail merveanapali@atauni.edu.tr
ORCID: https://orcid.org//0000-0003-0212-3760

Abstract: End stage kidney disease is one of the most common diseases seen worldwide with high morbidity and mortality rate. Given current renal replacement therapies, the most effective method is renal transplantation compared to dialysis. Renal transplantation improves the patient's quality of life and complications related to dialysis are minimized. Long-term immunosuppressant therapy is applied to transplantation patients to ensure organ continuity by reducing the risk of acute rejection. Survival time after renal transplantation and increased use of immunosuppressive drugs increase the risk of developing metastatic tumors in these patients. It is predicted that immune checkpoint inhibitors applied to cancer patients can be used in patients with cancer development after transplantation. Ipilimumab is a cytotoxic T-lymhocyte-associated antigen 4 (CTLA-4) inhibitor developed specifically for use in metastatic melanoma patients and approved by the FDA in 2011. The effect of ipilimumab on allograft survival has been reported compared to other immune checkpoint inhibitors. Based on these data, we examined the renal case reports available in the literature to evaluate the relationship between cancer outcome and graft rejection.
Keywords: CTLA-4, ipilimumab, melanoma, PD-1, rejection, transplantation.

1. Introduction

Renal transplantation is an effective treatment method for late kidney patients. With transplantation, the patient's quality of life improves and the risk of mortality due to complications caused by dialysis is reduced. Renal transplantation is alive or cadaveric depending on the source of the donor organ. These patients use long-term immunosuppressants to reduce the risk of acute rejection, maintain the transplanted organ and increase renal function. Survival time after renal transplantation and increased use of immunosuppressive drugs increase the risk of developing metastatic tumors in these patients (1, 2). Although the effect of immune checkpoint inhibitors has been shown in more than 20 types of cancer (3) this treatment protocol has not been applied to organ transplant patients (4). However, the critical effect of CTLA-4 antibody preventing solid organ rejection (5) and maintaining allograft tolerance of PD-1/PD-L1 interaction in peripheral tissues has been reported (6, 7). Therefore, available data have suggested the idea that immune checkpoint inhibitors can be used in patients with cancer development after transplantation. Ipilimumab is a CTLA-4 inhibitor developed specifically for use in metastatic melanoma patients and approved by the FDA in 2011. It has been reported in the literature that ipilimumab use is more effective on allograft survival compared to other immune checkpoint inhibitors (8).

Cite this article as: Anapalı M. and Balkan E. Use of Immun Checkpoint Inhibitor Ipilimumab in Renal Transplant Patients with Advanced Cancer: Is Risk/Benefit Ratio Dilemma?, *New Trend Med Sci* **2020**; 1(2): 137-145.

Although the alternatives used for the treatment of cancers in renal transplant patients are limited, we examined the renal case reports available in the literature to evaluate the relationship between cancer outcome and graft rejection.

1.1. Renal Transplant Rejection

The definition of rejection was first described as "biocompatibility" by Alexis Carrell in the early 1900s (9). Rejection is an immunological reaction to donor antigens recognized by the recipient's immune system. Renal transplantation is an effective remedy for patients with end-stage renal disease. The first successful renal transplantation was carried out between identical twins in the United States in 1954 (9). Regression risk is one of the most important problems in long-term allograft survival despite developing surgical techniques and immunosuppressive drugs (10). Pathological changes detected in the late 1960s have been reported to be associated with acute and chronic renal allograft rejection (11, 12). Rejection pathology can be seen in 4 different components of the kidney-glomeruli, tubules, interstitium and vessels either separately or with a combination of these regions (13). In the most common rejection cases, renal allograft biopsies show morphological damage resulting in cellular or antibody-related mechanisms. This damage is classified as acute or chronic due to graft survival and rejection activity after transplantation (13).

1.2. Rejection Types

Rejection is the adaptive immune response seen through T cell and humoral immune mechanisms. It is characterized by delay and disruption in early graft function. There are 3 major rejection forms: hyperacute, acute and chronic. Biochemical changes such as fever, malaise, tenderness on graft, graft enlargement, low urine, and increased serum creatinine and decreased glomerular filtration rate are associated with acute rejection. Acute rejection usually develops in the first month after transplantation, but it can be seen later. Chronic rejection, also known as chronic allograft nephropathy, is characterized by slow decline in graft function, often associated with hypertension and proteinuria. Biopsies performed on the first day following the transplantation to patients whose previous graft functions were delayed and then repeated at regular intervals were the diagnostic procedure for rejection. However, the expansion (enlargement) of histological lesions and subjectivity in interpretation of their severity was insufficient in establishing the diagnosis of rejection. For this reason, Banff Scheme was created to standardize renal biopsy interpretations. With this scheme, the lesions were classified for the diagnosis of acute and chronic rejection, and the types of histological findings were classified and the lesions were exacerbated (14-17).

When acute and chronic rejection is evaluated from an etiopathogenic point of view, it is seen that it is mediated by T cells and antibodies (14, 16). T cell mediated rejection is the most common early rejection type with its major features such as tubulitis and vasculitis (15). In chronic active T cell-mediated rejection, inflammatory cells in fibrotic intima and elasticity are impaired (15, 16). Alloantibodies against HLA class I, II and other antigens can be caused by both acute and chronic humoral rejection (18, 19). Although acute and chronic rejection is characterized by Cd4 accumulation in peritubular capillaries, at least 3 of 4 findings must be present for diagnosis: arterial intimal fibrosis, interstitial fibrosis / tubular atrophy, duplication of the glomerular basement membrane and lamination of peritubular capillary basement membranes (20-23).

1.3. Immun Checkpoınt Inhibitors

The life of the T cell begins in the thymus, where a large TCR repertoire is created and the immature cells undergo proliferation through the combination of T cell receptor (TCR) gene segments. T cells that bind strongly to their own peptides are eliminated in the thymus to prevent autoimmunity (24). While T cells that are insufficient to bind to MHC undergo apoptosis, T cells that are poorly attached to MHC and their peptides are released into the spleen, blood and lymphatic organs as naive cells. Some T cell receptors (TCR) may have cross-reactive specificity with their antigens. To prevent autoimmunity, many immune checkpoint pathways regulate the activation of T cells throughout the immune response called peripheral tolerance (24, 25). These pathways are cytotoxic T lymphocyte-associated antigen 4 (CTLA-4) pathway and programmed cell death protein-1 (PD-1) pathway (25). Immune checkpoint therapies targeting these pathways provide clinical advantage for patients with malignant diseases (26).

1.4. CTLA-4 Pathway

T cell activation is a complex process that requires multiple stimulating signals. A T cell receptor (TCR) that binds to MHC provides specificity for T cell activation. However, activation mostly requires the presence of co-stimulatory signals. CD28 molecules in T cells cause the signal in T cells together with B7-1 and B7-2 molecules on antigen presenting cells (APC). Adequate level of CD28: B7-1/2 binding causes proliferation in T cells, increasing survival and differentiation of T cells through the production of cytokines such as IL-2 (27). CTLA-4 is a CD28 homologue with a high binding affinity to B7 (28). However, unlike CD28, CTLA-4 connected to B7 does not generate a stimulating signal. Competition between CD28 and CTLA-4 binding to B7 determines whether T cell will undergo activation or anergia (29).

Some findings show that CTL4-A, which binds to B7, produces inhibitory signals that inactivate stimulating signals in relation to TCR: MHC and CD28: B7 binding (30). Mechanisms associated with inhibitory signals are associated with these reasons, which are seen as a result of a decrease in the ability to interact with APCs due to direct inhibition of the TCR immune synapse, CD28 or inhibition of the associated signal pathway or increased mobility of T cells (31, 32). CTLA-4 is localized in intracellular space in naive T cells at rest (33). With the stimulating signals that result in both TCR and CD28: B7 binding, an increase in the regulation of CTLA-4 is observed on the cell surface with exocytosis of vesicles containing CTLA-4 (33). Activation of T cells is prevented by negative signal that occurs by CTLA-4:B7 binding (34). Regulatory T cells (Treg) control the functions of effector T cells. For this reason, Treg cells play a key role in maintaining peripheral tolerance. Unlike effector cells, Treg cells express CTLA-4, which explains the suppressive functions of Treg cells (35). In animal models, genetic CTLA-4 deficiency in Treg cells has been reported to impair suppressive functions (35, 36). The mechanism that suggests that Tregs control effector cells is associated with a decrease in the regulation of B7 ligands on APCs, which causes decreased CD28 co-stimulation (36, 37).

1.5. PD-1 Pathway

Programmed cell death protein-1 (PD-1) is a member of the B7/CD28 family. It regulates T cell activation by binding to programmed cell death ligands 1 and 2 (PD-L1/2) (38). Similar to the CTLA-4 signal, activation of the PD-1 signal pathway reduces T cell proliferation and T cell survival. In addition, it inhibits interferon gamma (IFN-γ), tumor necrosis factor-alpha (TNF-α) and IL-2 production (38). When TCR and PD-1 binding is seen in a T cell, the signals produced by PD-1 cause a decrease in the activation of T cells (39, 40). PD-1 expression is one of the most important distinguishing features of exhausted T cells (41). This fatigue seen during chronic infection and cancer is characterized by T cell dysfunction resulting in inadequate control of infection and tumor. Both CTLA-4 and PD-1 binding have a negative effect on T cell activation. However, the timing of downregulation, responsible signaling mechanisms, and anatomical locations distinguish these two immune checkpoint inhibitors. Unlike CTLA-4, PD-1 is mostly expressed in active T cells, B cells and myeloid cells (25, 38). While CTLA-4 functions in the priming phase of T cell activation, PD-1 functions in the effector phase (38).). B7 ligands for CTLA-4 are typically expressed by lymph nodes or professional APCs located in the spleen (25). However, PD-L1 is expressed in leukocytes, non-hematopoietic cells, non-lymphoid tissues. PD-L1 can also be induced in parenchymal cells by IFN-γ or tumorigenic signal pathways (42). PD-L1 expression has been found in many different types of tumors and is associated with an increased amount of tumor-infiltrating lymphocytes (TILs) (43-45). PD-L2 is expressed in dentritic cells and monocytes, but can be induced in other immune and non-immune cells depending on the local microenvironment (46). Inhibition of PD-L2 binding causes increased TH2 activation (47) but binding of PD-L1 to CD80 has been shown to inhibit the T cell response (48). It has been reported that PD-L1 helps transformation of naive CD4+T cells into Treg cells and inhibits T cell response by stimulating the maintenance of Treg cells (49).

1.6. Solid Organ Transplant Rejection Associated with Immune-Checkpoint Inhibitors

In solid organ transplantations, the survival rate of graft has increased recently. Patients undergoing organ transplantation should use long-term immunosuppressants to balance side effects such as the risk of allograft rejection and infection. Acute rejection risk generally decreases with the time elapsed after transplantation. In this process, transplant patients need less immunosuppressor than the dose they originally used. The required level of immunosuppressant varies according to the different type of organ transplant. The general procedure applied is the combination of 2 or 3 drugs. Thus, dose-dependent side effects are minimized (50).

In the post-operative process, many patients are treated with corticosteroids. Due to the side effects of chronic steroid use, it is either gradually reduced in the first months or a permanent low (maintenance) dose is administered. Calcineurin inhibitors (CNI) such as cyclosporine and tacrolimus block T cell activation signal-2. These agents form the basis of immunosuppressants in almost all protocols. Agents affecting the cell cycle, such as mycophenolate mofetil, are often added to the treatment protocol. Because of the nephrotoxicity associated with calcineurin inhibitors, agents that interact with the mTOR pathway such as sirolimus and everolimus are used (51). However, chronic immunosuppressive treatments applied to organ transplant patients have been reported to be associated with malignancies which involve increased de novo non-melanoma skin cancer, malignant melanoma, lymphoma, kidney, head and neck cancer, choleratal cancer and lung cancer (52-55). The use of immune checkpoint inhibitor antibodies such as CTLA-4 and PD-1 in small cell lung cancer, melanoma and renal cell cancer has been reported to provide long-term stabilization and tumor regression effects (56, 57). However, it is thought that the use of these inhibitors may be associated with increased graft rejection. Blocking CTLA-4 and PD-1 increases the activation of T cells. Activation of T cells is not only against malignant cells but also against other cells expressing foreign antigens such as kidney allograft donor antigens. This T cell activation can cause acute cellular rejection, and active CD4+T cells can stimulate the proliferation and activation of B cells through co-stimulatory ligands such as CD40 and cytokines such as IL-4, IL-21, and IFN-γ that cause antibody-mediated rejection (58). If there is a decrease in

immunosuppressive drugs or transplanted organ sensitization, B cells can act directly on memory B cells expressing PD-1. Management of melanoma in kidney transplant patients includes aggressive reduction in immunosuppressant medications, which are tailored based on the patient's age, HLA compliance, time after transplantation, and a history of rejection (53). In studies, it has been reported that the time to start applying the immune checkpoint inhibitor therapy for cancers seen after transplantation is average 12.5 years (51). While melanoma patients with a history of allograft rejection take prednisone only, patients without a history of rejection complete their treatment with immunosuppressants such as tacrolimus, mycophenolate mofetil or cyclosporine (59-62).

1.7. Use of Ipilimumab for Renal Transplant Patients with Advanced Cancer

Ipilimumab: It is a fully humanized monoclonal antibody that acts directly against CTLA-4, a member of the CD28-B7 superfamily. CTLA-4 activation reduces CD4+T helper cell activity and induces immune tolerance by increasing the function of CD4+T regulatory cells (Treg) (63). Ipilimumab blocks the inhibitory T cell signal by binding to CTLA-4. It was approved by the FDA in 2011 for use in the treatment of patients with metastatic melanoma that cannot be surgically removed. It resulted in durable clinical response in patients with metastatic malignant melanoma (64). Phase III studies have reported that ipilimumab increases the survival rate compared to dacarbazine or peptide vaccine control (64, 65). Since Ipilimumab blocks CTLA-4, the activity of T cells against donor antigens expressed by cancer cells and allografts of solid organ transplantation patients increases. The primary event in acute kidney transplantation rejection is the recognition of donor antigens by T cells. Full activation of T cells is completed by the interaction of co-stimulator molecules that bind to CD28 and its ligands (33). The risk/benefit ratio of ipilimumab in transplant patients makes the use of immune checkpoint inhibitors in transplant patients therapeutic dilemma.

Ipilimumab+PD-1 inhibitors: While CTLA-4, predominantly found in lymphoid tissues, plays a critical role in early immune response, PD-1 regulated after T cell activation in peripheral tissues plays a role in late immune response (66). The positive effect of PD-1 and ligand PD-L1 on survival with its anti-cancer activity and regulatory effect has been shown in metastatic melanoma, non-small cell lung cancer and renal cell carcinoma (56, 57). Blocking these pathways with anti-CTLA-4, anti-PD-1 and anti-PD-L1 antibodies help maintain the anti-tumor properties of T cells (57, 64, 66). PD-1 inhibitors such as nivolumab and pembrozulimab have been shown to have a far greater effect than ipilimumab in metastatic melanoma. However, due to similar therapeutic mechanisms, both nivolumab and pembrolizumab applications can result in allograft rejection. It has been reported that the risk of rejection posed by PD-1 inhibitors after transplantation is higher than CTLA-4 antagonists (67). Blocking PD-1-PD-L1 interaction in kidney tubular cells may impair FoxP3+regulatory T cell-mediated graft tolerance (68). In some studies, it has been reported that glucocorticosteroid administration may impair the anti-tumor response of immune checkpoint inhibitors (69). It is recommended to use anti-CTLA-4 agents in solid organ transplantation patients compared to PD-1 because CTLA-4 receptors are non-peripheral tissue-specific mechanism and the risk of acute rejection of allograft is lower. Ong et al. (60) suggested that patients with high rejection risk can be classified by characterizing PD-L1 expression on the renal allograft before applying the anti-PD-1 agent. Although there is no study on this subject, it has been reported that T cells expressing PD-1 may be a marker for the risk of renal transplant rejection (70). There are ideas that PD-1 inhibitors are beginning to replace ipilimumab monotherapy due to the increased risk/benefit ratio. Therefore, the combination of both is considered as an alternative treatment method (71).

2. Discussion

Allogeneic kidney transplantation is a good option for end-stage kidney patients in relation to increased quality of life and survival. These patients use long-term immunesuppressants to reduce the risk of acute rejection, maintain the transplanted organ and increase renal function. The development of immunosuppressive drugs plays a key role in suppressing allograft rejection. With its increasing immunosuppressive activity, acute rejection incidence decreases significantly. However, increased immunosuppressive effect brings with it increased infection and malignancies after transplantation. The risk of cancer developing after transplantation is 3-5 times higher when compared to the general population (72).

Developments in cancer therapy are increasing day by day. One of them is immunotherapy. The use of immunotherapy in cancer treatment brings different side effects. Immune checkpoint inhibitors act by modulating the co-inhibitor T cell signal (73). Immune checkpoint inhibitors targeting CTLA-4 and PD-1 have been used in many types of cancer. The CTLA-4 pathway plays a key role in suppressing the immune response and tolerating itself (74). CTLA-4 blockade has been reported to increase the anti-tumor response with the study in the mouse model (75). Tivol ve ark (76) reported that CTLA-4 deficient mice are susceptible to autoimmune infiltration and organ damage. In addition, antibodies used against CTLA-4 receptors in mouse cardiac transplant patients have been reported to accelerate acute cellular rejection and graft loss (77, 78). CTLA-4 antagonists have the

potential to trigger rejection events in transplant patients (79). Based on all these data, the high risk of graft rejection due to chronically used immunosuppressors in organ transplant patients limits the use of immune checkpoint inhibitors.

Ipilimumab is a fully humanized monoclonal antibody that acts directly against CTLA-4. Ipilimumab blocks the inhibitory T cell signal by binding to CTLA-4. It was approved by the FDA in 2011 for use in the treatment of patients with metastatic melanoma that cannot be surgically removed. CTLA-4 activation reduces CD4+T helper cell activity and induces immune tolerance by enhancing the function of CD4+T regulatory cells (Treg) (63). CD28-B7 (CD80) interaction which is blocked by using CTLA-4-Ig in mice has been reported to reduce IgA accumulation, mesengial proliferation and proteinuria level. These studies provide evidence that the reduction or exacerbation of IgA nephropathy is a potential complication of ipilimumab therapy (80).

In the literature, it has been reported that the ratio between ipilimumab monotherapy applied to organ transplant patients and organ rejection is low (23%, 3/13 patients) but not insignificant (8, 81-84). The risk/benefit ratio of ipilimumab during treatment in these patients is controversial.

Since it has little effect on the control of oncological diseases, it is believed that the dose of immunosuppressant should not be reduced before the use of an immuno-checkpoint inhibitor to minimize the risk of renal transplant rejection (85). Immune checkpoint inhibitor deficiency is thought to be effective rather than immunosuppressant deficiency in the progression of melanoma (85). However, it is believed that the effect of ipilimumab used with an immunosuppressive agent such as rapamycin to prevent graft rejection during treatment may vary depending on the immunosuppressive and dose used (81). Similarly, Alhamad et al. (61) reported that ipilimumab, which was applied for the treatment of metastatic melanoma seen in the renal transplant patient after transplantation, improved kidney function, but the patient resulted in hemodialysis. Conversion of tacrolimus's rapamycin inhibitors to mammalian target and increased dose of prednisone are thought to be an alternative solution for preventing rejection.

Lipson et al. (8) reported that ipilimumab treatment which is used for post-transplant melanoma in renal transplant patients treated with ipilimumab did not cause graft rejection and graft functions continue normally. It is thought that rejection is not seen due to the fact that the treatment is performed many years after the transplant, these patients need low dose prednisone to maintain their renal function and the body accepts graft after all. The activation and expression of donor antigens may vary in patients. The balance between Treg and effector T cells may differ between different anatomical compartments such as peripheral blood, tumor and allograft. This variation is another way of explaining that allograft function is not impaired despite the use of ipilimumab in 2 patients (86). Based on all this, Lipson et al. (8) suggested that ipilimumab can be a safe option for the treatment of post-transplant melanoma in patients who had solid organ transplantation. Similarly, Ranganath et al. (83) reported that graft rejection was not observed in the patient who underwent liver transplantation with ipilimumab treatment for malignant melanoma seen after transplantation.

In the case reports, Zehou et al. (85) reported that only one of the patients had acute graft rejection after the first ipilimumab injection in the case of reduced immunosuppressants. Therefore, each factor causing rejection could not be clearly defined. Current immune checkpoint inhibitor strategies are based on anti-PD-1 alone or in combination with ipilimumab. Considering the risk of organ rejection, ipilimumab has been reported to be safer than anti-PD-1. However, the immune checkpoint inhibitor combinations planned to be applied in the evaluation of the tolerance to the transplanted organ need to be well documented (85).

Spain et al. (59) reported that the PD-1 inhibitor nivolumab used in the treatment of malignancy developed after transplantation in renal transplant patients, besides ipilimumab, showed graft loss due to secondary acute rejection in the patient. It is believed that these agents are applied consecutively in a short time leads to an increase in T cell activation beyond induced by ipilimumab alone, and the risk of toxicity associated with immunity may be increased.

PD-1 inhibitor nivolumab, used for the treatment of invasive melanoma after renal transplantation, has been reported to cause impaired renal allograft functions and results in hemodialysis. The immune checkpoint blockade applied to solid organ transplant patients is considered to be more dangerous than non-renal transplant patients (60).

The use of mTOR inhibitors for immunosuppression has been shown to further reduce the risk of malignancy compared to calcineurin inhibitor-based regimens (87). However, most renal transplant patients with intact graft integrity are applied treatments combined with immunosuppressive drugs or mTOR inhibitors. It is thought that low dose steroids and mTOR inhibitors given during anti-PD-1 inhibitors, which are used for anti-tumor treatment in renal transplant patients, prevent graft rejection (88). Barnett et al. (89) administered PD-1 inhibitor nivolumab for use in the treatment of metastatic adenocarcinoma after transplantation in a renal transplant patient. It is thought that glucocorticoid and sirolimus (a mammalian target of rapamycin [mTOR] inhibitor) applied to the patient during the treatment prevent the adverse effect of nivolumab and sirolimus may have synergistic antitumor effect in addition to being an immunosuppressive agent.

Local immunomodulatory strategies theoretically increase the anticancer response without affecting the risk of rejection. The immune-modulating effect of radiotherapy as well as the use of immune checkpoint

inhibitors has been demonstrated in many preclinical and clinical studies. Radiation can trigger the release of antigens from the tumor by inducing antitumor immune response (90). Many studies have shown that immunotherapy can increase this effect (91-93), and recent phase I studies have reported that the combination of radiotherapy and immunomodulator has different clinical outcomes (94). If synergy between radiotherapy and checkpoint inhibitors is approved for many malignancies, it may be an alternative option for use in transplant patients with cancer development.

Although allograft kidney transplantation is a good option for end-stage kidney patients, immunosuppressants, which are used chronically to prevent graft rejection, can cause various malignancies in the long term. Today, different protocols are applied to these patients with many alternative treatment methods. Although the use of immune checkpoint inhibitor is one of these methods, the risk/benefit ratio is controversial.

3. Conclusion

The immune checkpoint inhibitor treatment protocol applied according to the duration after the transplant in the treatment process, the improvement in kidney functions, the level of donor antigens' expression, the immunosuppressants used and malignancy, affects the renal survival rate. Although the exact solution cannot be fully provided, new treatment protocols and combinations need to be developed.

Conflict of interest statement

The authors declare that they have no conflict of interest.

References

1. Hart A, Smith JM, Skeans MA, et al. OPTN/SRTR 2016 Annual Data Report: Kidney. *Am J Transplant* **2018**; 18(1): 18-113.
2. Kim WR, Lake JR, Smith JM, et al. OPTN/SRTR 2016 Annual Data Report: Liver. *Am J Transplant* **2018**; 18(1): 172-253.
3. Tsiatas M, Mountzios G, Curigliano G. Future perspectives in cancer immunotherapy. *Ann Transl Med* **2016**; 4(14): 273.
4. Munker S, De Toni EN. Use of checkpoint inhibitors in liver transplant recipients. *United European Gastroenterol J.* **2018**; 6(7): 970-973.
5. Grinyo JM, Del Carmen Rial M, Alberu J, et al. Safety and Efficacy Outcomes 3 Years After Switching to Belatacept From a Calcineurin Inhibitor in Kidney Transplant Recipients: Results From a Phase 2 Randomized Trial. *Am J Kidney Dis* **2017**; 69(5): 587-94.
6. Tanaka K, Albin MJ, Yuan X, et al. PDL1 is required for peripheral transplantation tolerance and protection from chronic allograft rejection. *J Immunol **2007***; 179(8): 5204-5210.
7. Riella LV, Watanabe T, Sage PT, et al. Essential role of PDL1 expression on nonhematopoietic donor cells in acquired tolerance to vascularized cardiac allografts. *Am J Transplant* **2011**; 11(4): 832-840.
8. Lipson EJ, Bodell MA, Kraus ES, Sharfman WH. Successful administration of ipilimumab to two kidney transplantation patients with metastatic melanoma. *J Clin Oncol* **2014**; 32(19): 69-71.
9. Doyle AM, Lechler RI, Turka LA. Organ transplantation: halfway through the first century. *J Am Soc Nephrol* **2004**; 15(12): 2965-71.
10. Sellares J, de Freitas DG, Mengel M, et al. Understanding the causes of kidney transplant failure: the dominant role of antibody-mediated rejection and nonadherence. *Am J Transplant* **2012**; 12(2): 388-99.
11. Lindquist RR, Guttmann RD, Merrill JP, Dammin GJ. Human renal allografts. Interpretation of morphologic and immunohistochemical observations. *Am J Pathol* **1968**; 53(5): 851-81.
12. Kincaid-Smith P. Histological diagnosis of rejection of renal homografts in man. *Lancet* **1967**; 2(7521): 849-52.
13. Jeong HJ. Diagnosis of renal transplant rejection: Banff classification and beyond. *Kidney Res Clin Pract* **2020**; 39(1): 17-31.
14. Solez K, Colvin RB, Racusen LC, et al. Banff 07 classification of renal allograft pathology: updates and future directions. *Am J Transplant* **2008**; 8(4): 753-60.
15. Racusen LC, Solez K, Colvin RB, et al. The Banff 97 working classification of renal allograft pathology. *Kidney Int* **1999**; 55(2): 713-23.
16. Solez K, Colvin RB, Racusen LC, et al. Banff '05 Meeting Report: differential diagnosis of chronic allograft injury and elimination of chronic allograft nephropathy ('CAN'). *Am J Transplant* **2007**; 7(3): 518-26.
17. Solez K, Axelsen RA, Benediktsson H, et al. International standardization of criteria for the histologic diagnosis of renal allograft rejection: the Banff working classification of kidney transplant pathology. *Kidney Int* **1993**:44(2): 411-22.
18. Scornik JC, Guerra G, Schold JD, Srinivas TR, Dragun D, Meier-Kriesche HU. Value of posttransplant antibody tests in the evaluation of patients with renal graft dysfunction. *Am J Transplant* **2007**; 7(7): 1808-14.
19. Terasaki PI. Humoral theory of transplantation. *Am J Transplant* **2003**; 3(6): 665-73.
20. Takemoto SK, Zeevi A, Feng S, et al. National conference to assess antibody-mediated rejection in solid organ transplantation. *Am J Transplant* **2004**; 4(7): 1033-41.
21. Racusen LC, Haas M. Antibody-mediated rejection in renal allografts: lessons from pathology. *Clin J Am Soc Nephrol* **2006**; 1(3): 415-20.

22. Colvin RB. Antibody-mediated renal allograft rejection: diagnosis and pathogenesis. *J Am Soc Nephrol* **2007**; 18(4): 1046-56.

23. Gloor J, Cosio F, Lager DJ, Stegall MD. The spectrum of antibody-mediated renal allograft injury: implications for treatment. *Am J Transplant* **2008**; 8(7): 1367-73.

24. Goldrath AW, Bevan MJ. Selecting and maintaining a diverse T-cell repertoire. *Nature* **1999**; 402(6759): 255-62.

25. Fife BT, Bluestone JA. Control of peripheral T-cell tolerance and autoimmunity via the CTLA-4 and PD-1 pathways. *Immunol Rev* **2008**; 224: 166-82.

26. Sharma P, Allison JP. The future of immune checkpoint therapy. *Science* **2015**; 348(6230): 56-61.

27. Buchbinder EI, Desai A. CTLA-4 and PD-1 Pathways: Similarities, Differences, and Implications of Their Inhibition. *Am J Clin Oncol* **2016**; 39(1): 98-106.

28. Chambers CA, Kuhns MS, Egen JG, Allison JP. CTLA-4-mediated inhibition in regulation of T cell responses: mechanisms and manipulation in tumor immunotherapy. *Annu Rev Immunol* **2001**; 19: 565-94.

29. Krummel MF, Allison JP. CD28 and CTLA-4 have opposing effects on the response of T cells to stimulation. *J Exp Med* **1995**; 182(2): 459-65.

30. Fallarino F, Fields PE, Gajewski TF. B7-1 engagement of cytotoxic T lymphocyte antigen 4 inhibits T cell activation in the absence of CD28. *J Exp Med* **1998**; 188(1): 205-210.

31. Egen JG, Kuhns MS, Allison JP. CTLA-4: new insights into its biological function and use in tumor immunotherapy. *Nat Immunol* **2002**; 3(7): 611-8.

32. Schneider H, Downey J, Smith A, et al. Reversal of the TCR stop signal by CTLA-4. *Science* **2006**; 313(5795): 1972-5.

33. Linsey PS BJ, Greene J, et al. Intracellular trafficking of CTLA-4 and focal localization towards sites of TCR engagement. *Immunity* **1996**; 4: 535-43.

34. Krummel MF, Allison JP. CTLA-4 engagement inhibits IL-2 accumulation and cell cycle progression upon activation of resting T cells. *J Exp Med* **1996**; 183(6): 2533-40.

35. Takahashi T, Tagami T, Yamazaki S, et al. Immunologic self-tolerance maintained by CD25(+) CD4(+) regulatory T cells constitutively expressing cytotoxic T lymphocyte-associated antigen 4. *J Exp Med* **2000**; 192(2): 303-310.

36. Wing K, Onishi Y, Prieto-Martin P, et al. CTLA-4 control over Foxp3+ regulatory T cell function. *Science* **2008**; 322(5899): 271-275.

37. Qureshi OS, Zheng Y, Nakamura K, et al. Trans-endocytosis of CD80 and CD86: a molecular basis for the cell-extrinsic function of CTLA-4. *Science*. **2011**; 332(6029): 600-603.

38. Keir ME, Butte MJ, Freeman GJ, Sharpe AH. PD-1 and its ligands in tolerance and immunity. *Annu Rev Immunol* **2008**; 26: 677-704.

39. Parry RV, Chemnitz JM, Frauwirth KA, et al. CTLA-4 and PD-1 receptors inhibit T-cell activation by distinct mechanisms. *Mol Cell Biol* **2005**; 25(21): 9543-53.

40. Bennett F, Luxenberg D, Ling V, et al. Program death-1 engagement upon TCR activation has distinct effects on costimulation and cytokine-driven proliferation: attenuation of ICOS, IL-4, and IL-21, but not CD28, IL-7, and IL-15 responses. *J Immunol* **2003**; 170(2): 711-718.

41. Wherry EJ. T cell exhaustion. *Nat Immunol* **2011**; 12(6): 492-499.

42. Chen L. Co-inhibitory molecules of the B7-CD28 family in the control of T-cell immunity. *Nat Rev Immunol* **2004**; 4(5): 336-347.

43. Hino R, Kabashima K, Kato Y, et al. Tumor cell expression of programmed cell death-1 ligand 1 is a prognostic factor for malignant melanoma. *Cancer* **2010**; 116(7): 1757-66.

44. Taube JM, Klein A, Brahmer JR, et al. Association of PD-1, PD-1 ligands, and other features of the tumor immune microenvironment with response to anti-PD-1 therapy. *Clin Cancer Res* **2014**; 20(19): 5064-74.

45. Zou W, Chen L. Inhibitory B7-family molecules in the tumour microenvironment. *Nat Rev Immunol* **2008**; 8(6): 467-77.

46. Rozali EN, Hato SV, Robinson BW, Lake RA, Lesterhuis WJ. Programmed death ligand 2 in cancer-induced immune suppression. *Clin Dev Immunol* **2012**; 2012: 656340.

47. Huber S, Hoffmann R, Muskens F, Voehringer D. Alternatively activated macrophages inhibit T-cell proliferation by Stat6-dependent expression of PD-L2. *Blood* **2010**; 116(17): 3311-20.

48. Butte MJ, Keir ME, Phamduy TB, Sharpe AH, Freeman GJ. Programmed death-1 ligand 1 interacts specifically with the B7-1 costimulatory molecule to inhibit T cell responses. *Immunity* **2007**; 27(1): 111-22.

49. Francisco LM, Salinas VH, Brown KE, et al. PD-L1 regulates the development, maintenance, and function of induced regulatory T cells. *J Exp Med* **2009**; 206(13): 3015-29.

50. Moini M, Schilsky ML, Tichy EM. Review on immunosuppression in liver transplantation. *World J Hepatol* **2015**; 7(10): 1355-68.

51. Smedman TM, Line PD, Guren TK, Dueland S. Graft rejection after immune checkpoint inhibitor therapy in solid organ transplant recipients. *Acta Oncol* **2018**; 57(10): 1414-8.

52. Piselli P, Serraino D, Segoloni GP, et al. Risk of de novo cancers after transplantation: results from a cohort of 7217 kidney transplant recipients, Italy 1997-2009. *Eur J Cancer* **2013**; 49(2): 336-44.

53. Zwald FO, Christenson LJ, Billingsley EM, et al. Melanoma in solid organ transplant recipients. *Am J Transplant* **2010**; 10(5): 1297-304.

54. Sint Nicolaas J, de Jonge V, Steyerberg EW, Kuipers EJ, van Leerdam ME, Veldhuyzen-van Zanten SJ. Risk of colorectal carcinoma in post-liver transplant patients: a systematic review and meta-analysis. *Am J Transplant* **2010**; 10(4): 868-876.

55. Verran DJ, Mulhearn MH, Dilworth PJ, et al. Nature and outcomes of the increased incidence of colorectal malignancy after liver transplantation in Australasia. *Med J Aust* **2013**; 199(9): 610-612.

56. Motzer RJ, Escudier B, McDermott DF, George S, Hammers HJ, Srinivas S, et al. Nivolumab versus Everolimus in Advanced Renal-Cell Carcinoma. *N Engl J Med* **2015**; 373(19): 1803-13.

57. Topalian SL, Hodi FS, Brahmer JR, et al. Safety, activity, and immune correlates of anti-PD-1 antibody in cancer. *N Engl J Med* **2012**; 366(26): 2443-54.

58. Hoffman W, Lakkis FG, Chalasani G. B Cells, Antibodies, and More. *Clin J Am Soc Nephrol* **2016**; 11(1): 137-154.

59. Spain L, Higgins R, Gopalakrishnan K, Turajlic S, Gore M, Larkin J. Acute renal allograft rejection after immune checkpoint inhibitor therapy for metastatic melanoma. *Ann Oncol* **2016**; 27(6): 1135-7.

60. Ong M, Ibrahim AM, Bourassa-Blanchette S, Canil C, Fairhead T, Knoll G. Antitumor activity of nivolumab on hemodialysis after renal allograft rejection. *J Immunother Cancer* **2016**; 4: 64.

61. Alhamad T, Venkatachalam K, Linette GP, Brennan DC. Checkpoint Inhibitors in Kidney Transplant Recipients and the Potential Risk of Rejection. *Am J Transplant* **2016**; 16(4): 1332-3.

62. Herz S, Hofer T, Papapanagiotou M, et al. Checkpoint inhibitors in chronic kidney failure and an organ transplant recipient. *Eur J Cancer* **2016**; 67: 66-72.

63. Peggs KS, Quezada SA, Chambers CA, Korman AJ, Allison JP. Blockade of CTLA-4 on both effector and regulatory T cell compartments contributes to the antitumor activity of anti-CTLA-4 antibodies. *J Exp Med* **2009**; 206(8): 1717-25.

64. Hodi FS, O'Day SJ, McDermott DF, al. Improved survival with ipilimumab in patients with metastatic melanoma. *N Engl J Med* **2010**; 363(8): 711-723.

65. Robert C, Thomas L, Bondarenko I, et al. Ipilimumab plus dacarbazine for previously untreated metastatic melanoma. *N Engl J Med* **2011**; 364(26): 2517-26.

66. Ribas A. Tumor immunotherapy directed at PD-1. *N Engl J Med* **2012**; 366(26): 2517-9.

67. Lipson EJ, Bagnasco SM, Moore J, Jr. et al. Tumor Regression and Allograft Rejection after Administration of Anti-PD-1. *N Engl J Med* **2016**; 374(9): 896-898.

68. Riella LV, Paterson AM, Sharpe AH, Chandraker A. Role of the PD-1 pathway in the immune response. *Am J Transplant* **2012**; 12(10): 2575-87.

69. Margolin K, Ernstoff MS, Hamid O, et al. Ipilimumab in patients with melanoma and brain metastases: an open-label, phase 2 trial. *Lancet Oncol* **2012**; 13(5): 459-465.

70. Pike R, Thomas N, Workman S, et al. PD1-Expressing T Cell Subsets Modify the Rejection Risk in Renal Transplant Patients. *Front Immunol* **2016**; 7: 126.

71. Winkler JK, Gutzmer R, Bender C, et al. Safe Administration of An Anti-PD-1 Antibody to Kidney-transplant Patients: 2 Clinical Cases and Review of the Literature. *J Immunother* **2017**; 40(9): 341-344.

72. Acuna SA. Etiology of increased cancer incidence after solid organ transplantation. *Transplant Rev (Orlando)* **2018**; 32(4): 218-224.

73. Ventola CL. Cancer Immunotherapy, Part 1: Current Strategies and Agents. *PT* **2017**; 42(6): 375-383.

74. McCoy KD, Le Gros G. The role of CTLA-4 in the regulation of T cell immune responses. *Immunol Cell Biol* **1999**; 77(1): 1-10.

75. Leach DR, Krummel MF, Allison JP. Enhancement of antitumor immunity by CTLA-4 blockade. *Science* **1996**; 271(5256): 1734-6.

76. Tivol EA, Borriello F, Schweitzer AN, Lynch WP, Bluestone JA, Sharpe AH. Loss of CTLA-4 leads to massive lymphoproliferation and fatal multiorgan tissue destruction, revealing a critical negative regulatory role of CTLA-4. *Immunity* **1995**; 3(5): 541-547.

77. Zhang T, Fresnay S, Welty E, et al. Selective CD28 blockade attenuates acute and chronic rejection of murine cardiac allografts in a CTLA-4-dependent manner. *Am J Transplant* **2011**; 11(8): 1599-609.

78. Lin H, Rathmell JC, Gray GS, Thompson CB, Leiden JM, Alegre ML. Cytotoxic T lymphocyte antigen 4 (CTLA4) blockade accelerates the acute rejection of cardiac allografts in CD28-deficient mice: CTLA4 can function independently of CD28. *J Exp Med* **1998**; 188(1): 199-204.

79. Jose A, Yiannoullou P, Bhutani S, et al. Renal Allograft Failure After Ipilimumab Therapy for Metastatic Melanoma: A Case Report and Review of the Literature. *Transplant Proc* **2016**; 48(9): 3137-41.

80. Okano K NK, Horita S, et al. Effect of soluble form CTLA-4 on spontaneous IgA nephropathy in ddY mice. *Nephrology* **2001**; 6(1):A3-A3.

81. Morales RE, Shoushtari AN, Walsh MM, Grewal P, Lipson EJ, Carvajal RD. Safety and efficacy of ipilimumab to treat advanced melanoma in the

setting of liver transplantation. *J Immunother Cancer* **2015**; 3: 22.
82. Qin R, Salama AK. Report of ipilimumab in a heart transplant patient with metastatic melanoma on tacrolimus. *Melanoma Manag* **2015**; 2(4): 311-314.
83. Ranganath HA, Panella TJ. Administration of ipilimumab to a liver transplant recipient with unresectable metastatic melanoma. *J Immunother* **2015**; 38(5): 211.
84. Matin RN, Mesher D, Proby CM, et al. Melanoma in organ transplant recipients: clinicopathological features and outcome in 100 cases. *Am J Transplant* **2008**; 8(9): 1891-900.
85. Zehou O, Leibler C, Arnault JP, et al. Ipilimumab for the treatment of advanced melanoma in six kidney transplant patients. *Am J Transplant* **2018**; 18(12): 3065-71.
86. Curiel TJ. Tregs and rethinking cancer immunotherapy. *J Clin Invest* **2007**; 117(5): 1167-74.
87. Geissler EK. Post-transplantation malignancies: here today, gone tomorrow? *Nat Rev Clin Oncol* **2015**; 12(12): 705-717.
88. Lai HC, Lin JF, Hwang TIS, Liu YF, Yang AH, Wu CK. Programmed Cell Death 1 (PD-1) Inhibitors in Renal Transplant Patients with Advanced Cancer: A Double-Edged Sword? *Int J Mol Sci* **2019**; 20(9).
89. Barnett R, Barta VS, Jhaveri KD. Preserved Renal-Allograft Function and the PD-1 Pathway Inhibitor Nivolumab. *N Engl J Med* **2017**; 376(2): 191-192.
90. Kang J, Demaria S, Formenti S. Current clinical trials testing the combination of immunotherapy with radiotherapy. *J Immunother Cancer* **2016**; 4: 51.
91. Hiniker SM, Reddy SA, Maecker HT, et al. A Prospective Clinical Trial Combining Radiation Therapy With Systemic Immunotherapy in Metastatic Melanoma. *Int J Radiat Oncol Biol Phys* **2016**; 96(3): 578-88.
92. Reynders K, Illidge T, Siva S, Chang JY, De Ruysscher D. The abscopal effect of local radiotherapy: using immunotherapy to make a rare event clinically relevant. *Cancer Treat Rev* **2015**; 41(6): 503-510.
93. Vanpouille-Box C, Formenti SC. Dual Transforming Growth Factor-beta and Programmed Death-1 Blockade: A Strategy for Immune-Excluded Tumors? *Trends Immunol* **2018**; 39(6): 435-437.
94. Luke JJ, Lemons JM, Karrison TG, et al. Safety and Clinical Activity of Pembrolizumab and Multisite Stereotactic Body Radiotherapy in Patients With Advanced Solid Tumors. *J Clin Oncol* **2018**; 36(16): 1611-8.

Authors' ORCID
Merve Anapalı
http://orcid.org/0000-0003-0212-3760
Eda Balkan
https://orcid.org/0000-0002-7065-8161

https://dergipark.org.tr/tr/pub/ntms